M 2015

U.PORTO
FEUP FACULDADE DE ENGENHARIA
UNIVERSIDADE DO PORTO

BIOMECHANICAL CHARACTERISATION OF KNEE LIGAMENTS: NEW APPROACH FOR MECHANICAL TESTING AND COMPUTER MODELLING

JOANA MARISA ARANTES SILVA

DISSERTAÇÃO DE MESTRADO APRESENTADA
À FACULDADE DE ENGENHARIA DA UNIVERSIDADE DO PORTO EM
ENGENHARIA BIOMÉDICA

U.PORTO
FEUP FACULDADE DE ENGENHARIA UNIVERSIDADE DO PORTO

MEB - MESTRADO EM ENGENHARIA BIOMÉDICA | **2014/2015**

A Dissertação intitulada

"Biomechanical Characterisation of Knee Ligaments: New Approach for Mechanical Testing and Computer Modelling"

foi aprovada em provas realizadas em 14-07-2015

o júri

Presidente Professor Doutor João Manuel Ribeiro da Silva Tavares
Professor Associado c/ Agregação do Departamento de Engenharia Mecânica da Faculdade de Engenharia da U. Porto

Professor Doutor António Manuel Godinho Completo
Professor Auxiliar c/ Agregação do Departamento de Engenharia Mecânica da Universidade de Aveiro

Professor Doutor Rui Jorge Sousa Costa de Miranda Guedes
Professor Associado do Departamento de Engenharia Mecânica da Faculdade de Engenharia da U. Porto

O autor declara que a presente dissertação (ou relatório de projeto) é da sua exclusiva autoria e foi escrita sem qualquer apoio externo não explicitamente autorizado. Os resultados, ideias, parágrafos, ou outros extratos tomados de ou inspirados em trabalhos de outros autores, e demais referências bibliográficas usadas, são corretamente citados.

Joana Arantes Silva

Autor - Joana Marisa Arantes Silva

Faculdade de Engenharia da Universidade do Porto

Joana Arantes Silva

Pós-graduação em Micro e Nano Tecnologias pela Universidade do Minho (2014)

Licenciatura em Engenharia Biomédica pela Universidade Católica Portuguesa – Escola de Biotecnologia (2013)

Thesis under supervision of:

Prof. Doutor Rui Jorge Sousa Costa de Miranda Guedes

Professor Associado do Departamento de Engenharia Mecânica

Faculdade de Engenharia da Universidade do Porto

Dr. Miguel Marta

Assistente Hospitalar Graduado de Ortopedia e Traumatologia

Thesis partners

Laboratório de Biomecânica do Porto

LOME

inegi Instituto de Engenharia Mecânica e Gestão Industrial

São João Hospital

Porto, 2015

[This page was intentionally left in blank]

"Do what you can, with what you have, where you are."
Theodore Roosevelt.

[This page was intentionally left in blank]

ACKNOWLEDGMENTS

Ao **Professor Doutor Rui Miranda Guedes** por todo o acompanhamento, assim como ao **Dr. Miguel Marta** por todo o apoio demonstrado durante a realização desta tese.

Ao **Professor Doutor Marco Parente** por toda a paciência e pelas diretrizes para a realização de todo o trabalho da parte da simulação.

Ao **Professor Doutor Mário Vaz** por toda a motivação para a realização e o sucesso deste trabalho.

À **Engenheira Viviana Correia Pinto** pela sua amizade, por toda a dedicação, disponibilidade e acompanhamento durante o trabalho desenvolvido.

Ao **Engenheiro Nuno Viriato** por toda a simpatia e apoio durante a conceção da amarra e dos ensaios mecânicos, pois não teria sido possível sem a sua ajuda.

Ao **Professor Doutor José Carlos Noronha** por me ter possibilitado a oportunidade de assistir a duas ligamentoplastias diferentes do ligamento cruzado anterior.

Ao **Dr. João Duarte**, médico ortopedista no Hospital São João, pela disponibilidade para a dissecação dos ligamentos.

Ao **Engenheiro Joaquim Fonseca** pela disponibilidade no apoio da construção da amarra.

Ao **Senhor José**, chefe das oficinas de mecânica, pela construção das amarras.

À **Engenheira Célia Novo** pela escolha e cedência do revestimento ideal para as amarras.

Ao **Jonas de Andrade Nobre** por todas as sugestões e revisões que me possibilitou também evoluir e pela palavra amiga sempre cheia de força.

Às minhas colegas de grupo **Joana Machado e Diane Carvalho** pela amizade, sorrisos e por toda a motivação para continuar.

À **Diva Felix, Inês Lopes e Teresa Carvalho** por serem as melhores, e que sem vocês teria sido mais difícil. E a todos os **meus amigos da UCP e do MEB** que me apoiaram e incentivaram para que este trabalho fosse realizado.

Aos **meus pais e irmã** por todo o apoio, carinho e paciência sempre demonstrados.

E, por último, ao **Diogo,** que é o meu porto seguro. Obrigada pela paciência, ajuda e carinho. Esteve sempre comigo nos maus e bons momentos, sendo que, nos maus conseguiu sempre fazer com que tudo melhorasse.

A todos, o meu sincero obrigado.

[This page was intentionally left in blank]

PUBLICATIONS

J. A. Silva, R. M. Guedes, and M. Marta, "Biomechanical Characterisation of Human Knee Ligaments : New Approach for Finite Element Analysis," in 1st Doctoral Congress in Engineering, 2015, p. 2.

J. A. Silva, R. M. Guedes, N. Viriato, M. Marta, and M. A. P. Vaz, "Methods Used in Clamping Soft Tissues Specimen : Review and New Approach," in 1st Doctoral Congress in Engineering, 2015, p. 2.

[This page was intentionally left in blank]

ABSTRACT

The ligaments are the main object of study of this thesis, whose primary aim is to contribute to the mechanical characterization of the ligaments by means of experimental tests as well as the finite element method (FEM). These two parts assist in the acquisition of information that can eventually be applied as a tool to support medical decision in orthopaedics.

As far as the experimental tests are concerned, a new clamp for the bone - ligament - bone complex was developed, in order to be used in uniaxial tensile testing. Thus, this new customized clamp, combined with the use of bone cement, was created and tested in the TIRAtest machine with porcine knee ligaments. The results proved to be consistent with literature. Nonetheless, the achieved rupture tensions were higher than those found in literature. This step allowed the setup validation and the study of the behaviour of the ligaments under tensile, creep and relaxation.

As for the FEM study, the OpenKnee Project, a knee model available online was used by the group members, inserted in LABIOMEP activities, so as to study and improve each knee structure. The available model lacks validation and verification, consequently this becomes one of the main objectives of the knee group. In this particular case, the focus was on the ligaments, thus the menisci and cartilages were disregarded. Four constitutive models, two isotropic and two anisotropic, were studied to define the behaviour of the ligaments. The neo-Hookean with fibres model exhibited the best results, owing to the fact that it revealed the most realistic stress distribution and that the maximum stress obtained, in a simulation of a common walk, was the smallest in comparison to other models. After the constitutive model selection, five mechanisms of injury of each main knee ligament were investigated. Each one of these mechanisms revealed consistency in terms of stress distribution. However, there are only a few studies of these mechanisms, which made the quantitative validation more difficult. The outcomes analysis indicated that several kinematic and kinetic aspects are satisfactorily reproduced. Therefore, the variation in the constitutive models shows how important its role is in the ligaments behaviour, since analysing the results there is a wide quantitative and qualitative variation.

Key Words: Biomechanical properties, clamps, computer modelling, constitutive models, finite element, knee joint, knee ligaments, ligament's clamping, mechanical tests, mechanisms of injury, uniaxial tensile tests.

RESUMO

A tese aqui apresentada foca-se unicamente no estudo dos ligamentos de joelho, tendo como objetivo primordial contribuir para a caracterização mecânica dos ligamentos tanto por ensaios experimentais como pelo método de elementos finitos (MEF). Estas duas partes permitem adquirir informações que futuramente podem ser aplicadas como ferramentas de apoio à decisão médica em ortopedia.

Relativamente aos ensaios experimentais, foi desenvolvido um novo dispositivo de amarração do complexo osso – ligamento – osso de forma a ser utilizado em testes de tração uniaxiais. Esta nova amarra, aliada à utilização de cimento ósseo, foi criada e testada na TIRA*test* com ligamentos de joelho de suíno. Os resultados mostraram-se coerentes com a literatura, tendo no entanto alcançado tensões de rutura superiores às encontradas na pesquisa bibliográfica. Esta etapa permitiu a validação do *setup* e o estudo do comportamento dos ligamentos sob ensaios de tração, fluência e relaxação.

Em relação ao estudo por MEF, o *OpenKnee project*, um modelo do joelho disponível *online* foi utilizado por todos os elementos do grupo inserido nas atividades do LABIOMEP, de forma a estudar e desenvolver cada estrutura do joelho. O modelo disponível carece de validação e verificação, logo este torna-se um dos objetivos principais do grupo do joelho. Neste trabalho em particular, como o foco principal são os ligamentos, as cartilagens e meniscos foram desconsideradas. Assim, quatro modelos constitutivos, que definem o comportamento dos ligamentos, foram estudados: dois isotrópicos e dois anisotrópicos. O modelo que revelou melhores resultados foi o neo-Hookean com fibras uma vez que apresentava uma distribuição de tensões mais realística e a tensão máxima obtida para uma simulação de caminhada era a menor comparada com os restantes modelos. Posteriormente a esta seleção, cinco mecanismos de lesões de cada um dos principais ligamentos do joelho foram analisados. Cada um destes mecanismos demonstrou coerência em termos de distribuição de tensões. No entanto, não existem muitos resultados de estudos destes tipos de mecanismos de forma a fazer uma comparação quantitativa direta.

A análise de resultados permitiu observar que vários aspetos cinemáticos e cinéticos são satisfatoriamente reproduzidos. A variação de modelos constitutivos dos ligamentos mostra-se assim relevante, pois, analisando os resultados obtidos há uma grande variação quantitativa e qualitativa.

Palavras-chave: Amarras, agarramento de ligamentos, articulação do joelho, elementos finitos, ligamentos do joelho, mecanismos de lesão, modelos constitutivos, modelação computacional, propriedades mecânicas, testes de tração uniaxial.

CONTENTS

Part II - Mechanical Tests

Part III- Computer Modelling

[This page was intentionally left in blank]

LIST OF FIGURES

[This page was intentionally left in blank]

LIST OF TABLES

LIST OF

I. ABBREVIATIONS

ACL	Anterior Cruciate Ligament
AM	Anteromedial
AL	Anterolateral
BLJ	Bone Ligament Junction
CAD	Computer-aided design
CT	Computed tomography
D	Distally
e.g.	Exempli gratia
FEM	Finite Element Modelling
HGO	Holzapfel, Gasser and Ogden
i.e.	Id est
INEGI	Instituto de Ciência e Inovação em Engenharia Mecânica e Engenharia Industrial
SD	Standard Deviation
SI	International System of Units
LCL	Lateral Collateral Ligament
M	Mean
MCL	Medial Collateral Ligament
MRI	Magnetic Resonance Imaging
MS	Mid-Substance
P	Proximally
PB	Posterior Bundles
PCL	Posterior Cruciate Ligament

PL	Posterolateral
PM	Posteromedial
PMMA	Poly (methyl methacrylate)
PBS	Phosphate- Buffered Saline
QLV	Quasi-linear viscoelastic
SI	International System of Units
SIFS	Single integral finite strain
UFS	Universal Force Sensor
UTS	Ultimate Tensile Strength
3D	Three Dimensional

II. SYMBOLS

A	Area
cm	Centimetres
K	Degree of Heterogeneity
°	Degrees
$\boldsymbol{F}$	Deformation Gradient Tensor
$\boldsymbol{J^{el}}$	Elastic Volume Ratio
F	Force
L	Final Length
$\bar{I}_1$	First Strain Invariant
C1	Material constant
m	Meters
M	Molar
mm	Millimetres
ms	Milliseconds
MPa	Mega Pascal
N	Newton
σ	Normal Stress
$\mathbf{L_0}$	Original Length
Pa	Pascal
%	Percentage
®	Officially registered
s	Seconds
σ	Standard deviation

ε	Strain
τ	Shear stress
λ	Stretch
w	Width
T	Tesla
t	Thickness
t	Time
E	Young's Modulus (elastic modulus)

III. SOFTWARE

ABAQUS®

FEMAP®

SOLIDWORKS®

[This page was intentionally left in blank]

1 INTRODUCTION

The knee articulation is one of the most complex structures of the human body constituted by a well-organized bone architecture and by the soft tissue stakeholders, which allow the correct functioning. Being the most mechanically requested articulation of our skeletal system and due to the large number of injuries associated to it, an investigation group of the knee was created, integrated as part of the LABIOMEP activities. An overall main goal is to understand each stakeholder of the knee and, in this thesis in particular, the ligaments. Thus, the primary objective is to investigate the ligaments as a material, whose exceptional properties lead to different traumatic patterns. Consequently, the reconstruction methods do not fulfil all the requirements for a lifelong stable solution. Evaluation of the influence of loading rates on patterns of injury (e.g. [1]) and even testing under normal conditions (fatigue injuries) are examples of sources of biomechanical knowledge of the knee ligaments' properties. Moreover, combining the knowledge acquired from the mechanical tests, the computer modelling relies an important base for the mechanical, or even medical predictions. Therefore, this knowledge is used for the selection, design and evaluation of ligament reconstruction techniques.

In a large number of cases, engineers find it difficult to conduct medical research owing to the shortage of knees from human corpses. Furthermore, complex issues arise about the biomechanical properties of each knee ligament (mainly as a result of the high variance between each individual ligament), mechanisms of injury (questions about how injuries happen, how they affect lower limb biomechanics and the other tissues) and about the reconstruction procedures' efficacy (there is no standard ligament reconstruction method). For this reason, the effectiveness of a proposed surgical procedure or the introduction of a new biomaterial to replace or reconstruct any tissue of the human body can be studied in the first line by computer modelling based previously on *ex vivo* experiments.

Computational modelling of the knee joint using the finite element method has been dealing with the constant challenge to achieve a knee joint simulation as real as possible. In addition, the model's validation must be done through experimental studies. The biomechanical properties of

the knee ligaments are usually measured by a set of tensile *ex vivo* tests, in which the bone-ligament-bone complex is fixed relative to the axis of pull. Hence, the ligament study is possible and the results of a study may confirm the accuracy of one another [2]. Overall, the main goal of these finite element models is to allow a deeper study of this complex articulation and to make a contribution for the improvement of reconstruction methods used in medical service.

1.1 STRUCTURE

This thesis is divided into three major parts. The first part is dedicated to providing the essential information required to a full understanding of the present work. It concerns the anatomy of the knee and each of its major ligaments, as well as, its kinematics and biomechanical properties. Finally, for the record, there is also a chapter on ligament injuries and methods for reconstruction

The second part is focused on the biomechanical tests. It includes an overall description about the state of the art on the characterisation of the ligament's mechanical properties, its results and conclusions. Herein, there is an explanation of the experimental work, including the clamp's approach description. Moreover, the protocol of the mechanical tests performed with porcine knee ligaments is described in detail. The results of the tensile, creep and stress-relaxation tests are also presented and discussed.

The third part is directed for computational modelling, describing the state of the art and the fundamental concepts on the finite element method. Some important and recent studies in this field are also reported. Furthermore, four constitutive models, two isotropic and two anisotropic, were investigated and the results compared. The isotropic models are the neo-Hookean and the polynomial hyperelastic, while the anisotropic models are the neo-Hookean with reinforcing fibres and the Holzapfel-Gasser-Ogden model. Furthermore, with the more suitable model, five mechanisms of injury of the main knee ligaments were studied.

Finally, a chapter is reserved for a summary, with the most important highlights of this thesis. The overall conclusions and discussions of the two previous parts are described and analysed. In addition, future work is proposed and recommended as a follow-up of this thesis.

1.2 OBJECTIVES

The overall goal is to make a contribution to the study and progression of the knee ligaments for the preventive and reconstructive methods. In order to do this, to overcome problems during the mechanical tests, a new approach of ligaments' clamping should be proposed. The clamp design

should be tested and the most suitable geometry and material should be chosen. Thus, through *ex vivo* mechanical testing in porcine knee ligaments the new customized clamps will be validated. On the other hand, using a three-dimensional (3D) human knee finite element model, four constitutive models that define the ligaments' behaviour will be studied to analyse the effect of the variation in the stress distributions and joint kinematics. Furthermore, with the most suitable model, mechanisms of injury were simulated in order to investigate the type and location of the ligament rupture.

This thesis also intends to provide important background, with the necessary theoretical foundations for the current and future study. It is divided into different chapters, containing the necessary information, including a summary of the current studies both *ex vivo* in mechanical testing and in numerical modelling. The information provided is important for the performed investigation in this thesis, where mechanical tests and computer modelling were conducted.

[This page was intentionally left in blank]

PART I

FROM ANATOMY TO INJURY

ANATOMICAL NOMENCLATURE

THE KNEE

THE KNEE LIGAMENTS

LIGAMENT INJURIES

[This page was intentionally left in blank]

2 NOMENCLATURE

2.1 BODY PLANS AND AXES OF MOVEMENT

In order to obtain a consensus on body studies and research, Kinesiology (or human kinematics, the scientific study of human movement) considers the human body as a coordinate system with its origin in the centre of the body. Based on this system, three major plans were defined which allow an easier space orientation of the human body (Figure 2-1).

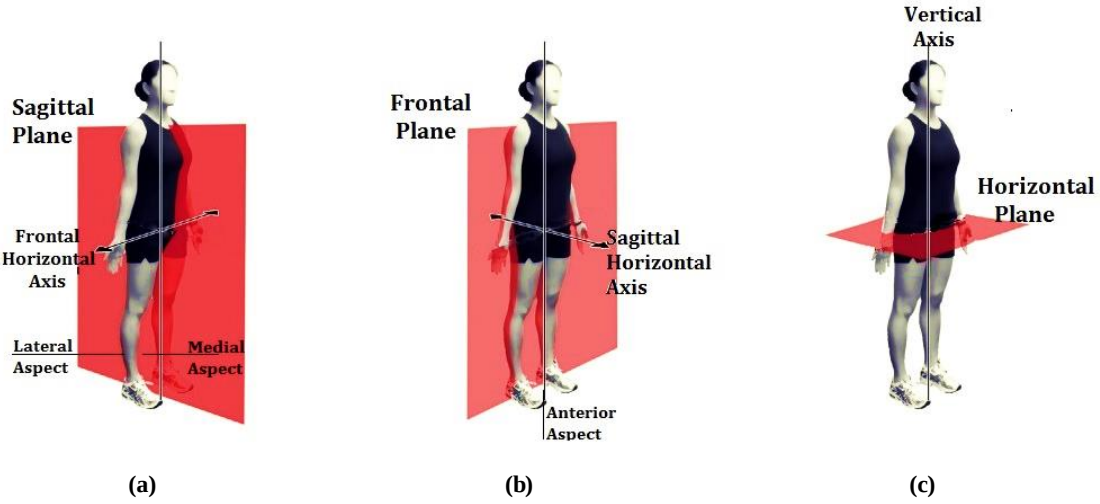

Figure 2-1 *- Planes of motion and axes of rotation.* ***(a)*** *Sagittal plane in relation to the frontal axis;* ***(b)*** *Frontal plane in relation to the sagittal axis and* ***(c)*** *Transverse plane in relation to the vertical axis. Adapted from* [3].

Figure 2-1-(a) depicts the division of the human body into two parts by the sagittal plane (also known as the median plane). Movements in this plane are always paired with the frontal axis, which goes through the lateral, coronal and medialateral parts. Related to this plane are the terms "medial", which means "toward the midline", and "distal" meaning "away from the midline". The frontal plane, also known as the coronal plane (Figure 2-1-b), divides the human body into back and front, and the movements associated to this plane are always paired with the sagittal axis, which goes through the anterior and posterior parts. Therefore, related to this plane are the terms

"anterior" and "posterior" with the first meaning "that which goes before" and the latter meaning "that which follows". Finally, the last main plane is the transverse plane, also known as the axial or the horizontal plane (Figure 2-1 - c), which divides the human body into a superior part and an inferior one. In reference to this plane, the terms "proximal", which means "nearest", and "distal", which means "distant", are introduced. These terms are used to refer to linear structures, in which one end is nearer to another structure, whereas the other one is farther away [4], [5].

Moreover, as the human body is divided into three planes according to motion, the knee also has a coordinate system according to its degrees of freedom. Kinematics relates to the knee by means of three axes (Figure 2-2). According to these axes, six degrees of motion are allowed in a normal knee: three translations and three rotations. The vertical axis going through the tibia is the tibial shaft axis, which allows the internal and external rotation of the distal part of the leg. Furthermore, the rotation related to the epicondylar axis (axis through femur condyles) is the extension and flexion motion. Lastly, the anteroposterior axis allows the varus (adduction) and valgus (abduction) motion. The translations along these axes are referred as proximal-distal, medial-lateral and anteroposterior, respectively [4], [6]–[9].

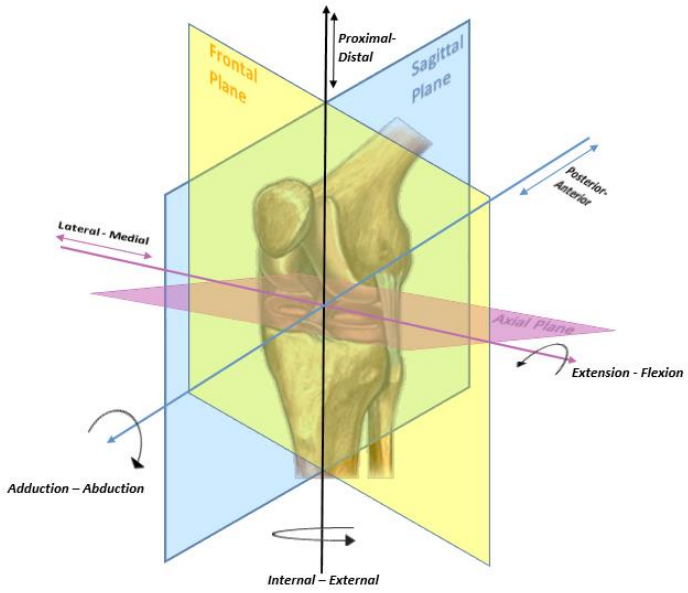

***Figure 2-2**-Schematic representation of the six degrees of motion, according to the plans allowed to the human knee. Adapted from* [10].

This taxonomy regarding the reference axes and planes will be used for joint motion throughout this dissertation.

2.2 MECHANICAL FUNDAMENTALS AND CONCEPTS

The stress in a body is defined as the force per unit of area, in this case, the total tensile load (in the direction of the long axis) per unit by the cross-sectional area of the ligament under analysis

[11]–[14]. Expressed in physical symbols, according to the International System of Units (from French: Système International d'Unités, SI), the stress (σ) is calculated by an external applied force (F) upon a cross-sectional area (A) as it is represented in Equation 2.1.

$$\sigma = \frac{F}{A} \tag{2.1}$$

Force is measured in newton (N), area in square meters (m^2) and, consequently, the stress, like pressure, is measured in Pascal (Pa), where 1 Pa = 1 $N.m^{-2}$. To measure the cross-sectional area, the contact and noncontact methods are used. For the example, callipers are a contact method and are used to measure the width and the thickness of the ligament, assuming a rectangular or elliptical shape. Because of its lack of complexity, this method may introduce large measure errors as a result of its inaccuracy [15]. On the other hand, noncontact methods involve an optical system (either visible or laser light) for measure or an image-reconstruction technique to determine the cross-sectional area and/or full shape [16].

For instance, when stress is applied in a ligament, a ratio of the length change in comparison to the original length is defined as strain (symbolized by the Greek letter ε). It is a dimensionless quantity (or expressed as percentage), expressing the proportional relation between the length changed ($L-L_0$) and the original length (L_0), see Equation 2.2 [11]–[14], [17].

$$Strain\ (\varepsilon) = \frac{L-L_0}{L_0} \tag{2.2}$$

The relation between the stress-strain curves allows the calculation of a mechanical property from the linear slope. This property can be referred as tangent [14], tensile, elastic or Young's modulus (E) and expresses the steepness of the stress-strain curve [11], [17], [18].

$$Young's\ Modulus(E) = \frac{\sigma}{\varepsilon} \tag{2.3}$$

Since strain is dimensionless, the Young's modulus has the dimension of the stress and is measured in units such as $N.mm^2$ or MPa. The Young's modulus represents a linear and proportional relationship between load and deformation or stress and strain (Equation 2.3), i.e. it is a measurement unit for the stiffness of an elastic material. In this case, if a material has a low Young's modulus, it means that a small load will generate a relatively high strain: the material is flexible. In opposition, a high Young's modulus would mean that the material is stiff and rigid, and a large load would be needed to stretch or bent the material. Usually, the ligaments show low Young's modulus due to its flexibility [11], [13], [17], [18].

[This page was intentionally left in blank]

3 THE KNEE

The knee is the largest and the most superficial joint, being one of the most important and commonly injured joints of the human body. Therefore, a thorough knowledge of this complex joint's anatomy and biomechanics is needed so that there is a truthful insight on the knee, allowing combination of engineering with medicine.

3.1 BONE ARCHITECTURE

Concerning the bone architecture, the knee joint is composed of three major bones: distal epiphysis[1] of femur, proximal epiphysis of tibia and patella (Figure 3-1). In the femur epiphysis, there are two round knobs known as femoral condyles, which are articulated with an intercondylar eminence in the centre of the tibial *plateau* (tibia epiphysis). In the anterior view of the knee, the patella, also known as kneecap, sits in front of the joint protecting it and aiding in the support of extension loads [4],[19]. These bones together allow movements as flexion, extension and rotation, but also contribute for stabilisation and control under a large range of loading conditions [4], [20]–[22]. The knee joint consists of three articulations: two tibiofemoral joints and one patellofemoral joint. The anatomical features on femur, tibia and patella, such as sulcus or prominences, provide attachments for muscles and ligaments [4], [11], [21]–[23].

Lastly, in Figure 3-1, although the fibula is articulated with the lateral side of the tibia, it is not considered as part of the knee joint. Fibula plays a significant role in stabilising the ankle and supporting the muscles of the lower leg [4],[19],[24].

[1] An epiphysis is the rounded head part of a long bone, usually playing a role in a joint [4].

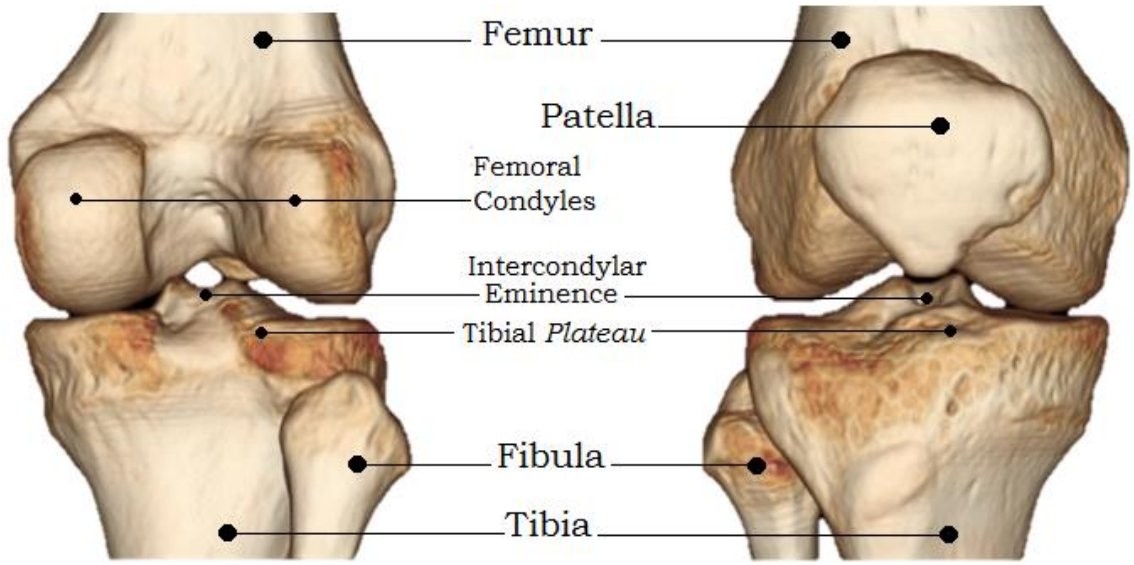

(a) **(b)**

Figure 3-1 *– Bone architecture of the right knee.* ***(a)*** *Posterior and* ***(b)*** *anterior views.*

3.2 SOFT TISSUES

Soft tissues are the tissues with the function of connection, supporting, or surrounding other structures and organs of the body. The knee's soft tissues include the ligaments, the cartilages and the menisci. The ligaments are included in the connective tissues, whereas the menisci and cartilages are inserted in the supportive and connective tissues category [4].

The knee is a hinge type synovial joint, which means that it is bathed in synovial fluid in order to lubricate and reduce friction between the articular cartilage-bones [4]. The cartilage, defined as connective tissue, is not rigid as bone, and it is also less flexible than muscle. There are known three types of cartilage: fibrous cartilage (present in meniscus), elastic cartilage (present, for instance, in the external ear), and articular or hyaline cartilage. The latter covers the articular surfaces of the patellofemoral and tibiofemoral joints (Figure 3-2). Furthermore, this cartilage has exceptional mechanical properties due to histological features. The articular cartilage is entirely made of fibrocartilage (mixture of fibrous tissue and cartilaginous tissue) conferring it elastic properties. Its main functions are: to allow the distribution of mechanical loads, to absorb shocks, to offer resistance to compressive forces, and ensuring that the joint surfaces easily slide over each other without causing damage to either one of them [20], [21], [25], [26].

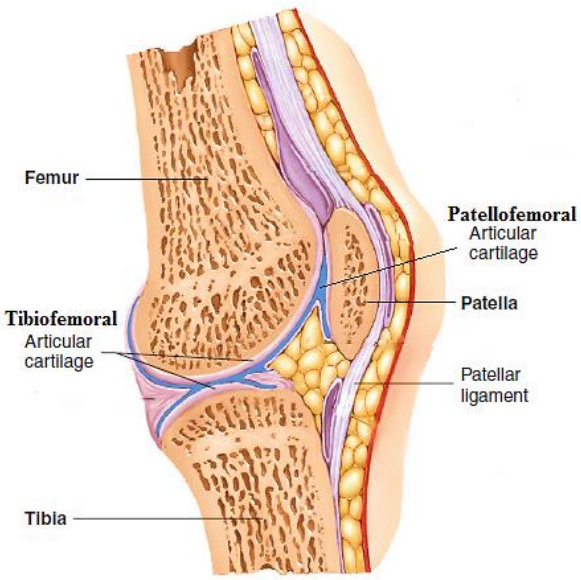

Figure 3-2- *Sagittal section of right knee, with special attention to articular cartilage. Adapted from* [4].

In addition to the articular cartilage, the menisci also play the role of shock absorber, working as dampers, when the knee is subjected to loads. The menisci are in contact with the tibial and femoral articular cartilage. Moreover, not only do the menisci avoid rubbing the femur and the tibia against each other, but they also deepen the articulation, increasing the contact area between the articular surfaces. The knee has two menisci, the medial and lateral meniscus, which can be found between the femur and tibia (Figure 3-3) [4], [19], [21].

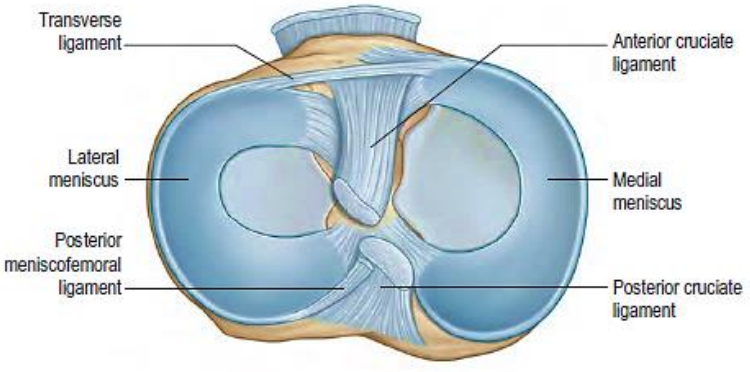

Figure 3-3- *Superior view of the left tibia, with special attention to menisci and cruciate ligament's attachments. Adapted from* [21].

The knee is surrounded by a joint capsule consisting of two thin layers: an external fibrous layer and the internal synovial membrane. As a fragile housing, the joint capsule is strengthened by tendons and ligaments. There are five extra-capsular ligaments: patellar ligament, lateral collateral ligament, medial collateral ligament, oblique popliteal ligament, and arcuate popliteal ligament. Additionally, in order to provide strength inside the articulation, there are the intra-

articular ligaments: the anterior and posterior cruciate ligaments. In Figure 3-4, the spatial position of some knee ligaments, previously mentioned, is depicted.

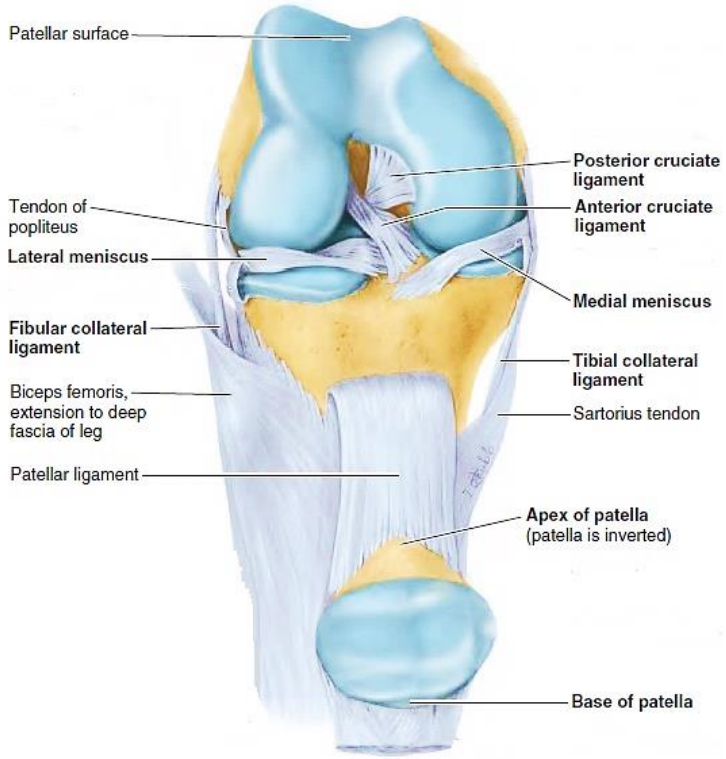

Figure 3-4- *Anterior view of the intra and some extra articular ligaments in a flexed knee. Adapted from* [20].

The ligaments are essential for the musculoskeletal system, guaranteeing the correct function of diarthrodial joints. For this reason, the main knee ligaments, such as the collateral and the cruciate ones, play an important role in the stabilisation, support and guidance of the knee's motion. When a ligament injury occurs, apart from the pain and discomfort it causes, the body's lower limbs' stability is affected and sometimes significant damages in the surrounding tissues arise. The research in knee ligaments is of high importance, since it allows the discovery of new repair solutions and accurate substitutions. This research becomes more crucial when there is still no complete concordance about those methods in the medical community [4], [11], [20]–[22]. In light of these arguments and as the main subject of this dissertation, Chapter 4 is reserved for describe its anatomical and biomechanical features found in literature.

Finally, in a brief reference, the knee has, basically, just one muscle, which exhorts a direct influence in motion: the popliteus muscle (Figure 3-5). It originates from the lateral of the femoral condyle and inserts into the posterior surface of body tibia. Its main function is to assist in flexing the knee itself, unlocking the knee and rotating the leg medially [4], [21].

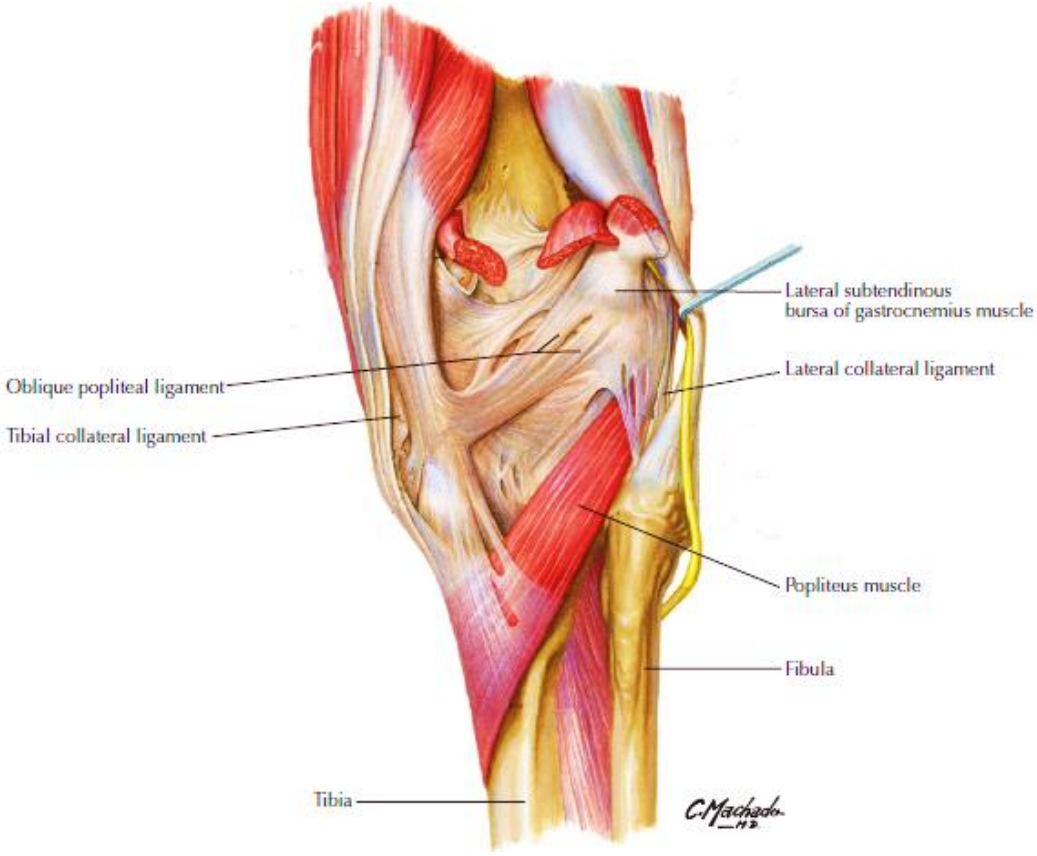

Figure 3-5 *- Posterior view of the right knee with special attention to popliteus muscle. Adapted from* [27].

3.3 KNEE BIOMECHANICS

As already stated in the previous section, the knee joint is one of the most complex articulations, both anatomical and mechanically. Composed of diverse tissues, each one of them has an important role in the knee joint mechanics. The knee joint mechanics has distinct motion patterns and relies on a combination of its passive motion characteristics and the external loads. Consequently, in this section a deep kinematics of the knee is described. The kinematics takes in consideration the segmental movement of the joint (motion characteristics) according to a coordinate system, without reference to forces, moments or mass. On the other hand, kinetics deals with motion of the different structures of the joint under the action of forces and moments, however, it won't be described in this thesis due to the complexity according to different situations. Nonetheless, the understanding of the normal joint kinematics and kinetics is essential for comparison purposes during diagnosis of knee injuries, for the evaluation of rehabilitation or reconstruction success [11].

3.3.1 **Joint Kinematics**

Concerning kinematical issues, besides the incongruent surfaces of this joint, the knee is capable of a six degree motion freedom: back and forth movement (anterior/posterior), up and down (compression/distraction) and left and right shift (medial/lateral). These translations mentioned before, according to the perpendicular axes described in Section 2.1, are combined with rotation allowing very slight movements, such as abduction and adduction, slight internal - external and flexion - extension rotations. All of these translations and rotations mentioned before compose the major movements of the knee.

3.3.1.1 Sagittal plane

The motion of the knee occurs primarily in the sagittal plane and a relatively minor degree of movement occurs in the transverse plane. Thus, in a simple view, the knee may be described as a modified hinge type due to the tibiofemoral joints (see Figure 3-6), which work only in one axis (epicondylar axis) allowing for flexion and extension of the lower limb [4], [19], [28].

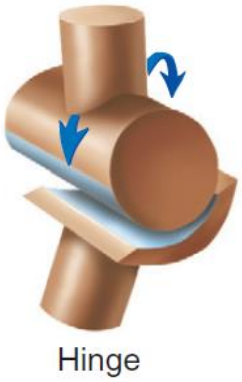

Figure 3-6 *– The knee is usually described as hinge type, allowing flexion, extension and a measure of rotatory motion* [4].

Extension is the anterior movement of the lower limb until it gets in straight alignment with the axes of tibia and femur. Full extension value for humans is taken as reference for flexion measurements, setting an initial value of zero degrees (neutral position) [11], [17], [21], [29], [30]. It is known that the knee is fully extended when it passively "locks" like a "screw-home mechanism" due to the medial rotation of the femoral condyles on the tibial plateau [20], [31]. On the contrary, blocked by the posterior horn of the menisci, at maximum flexion, the medial posterior femoral cortex impacts, limiting flexion [11]. Figure 3-7 depicts the extension and flexion motion of the distal lower limb powered by the knee joint for a better understanding of this kind of motion.

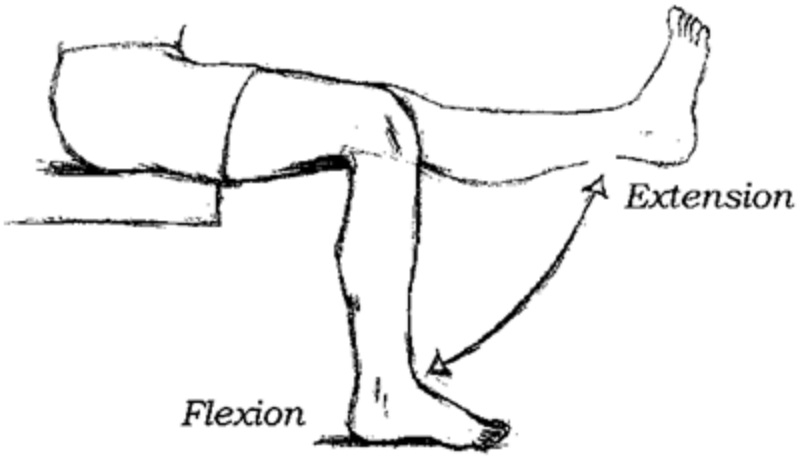

Figure 3-7 - *Range of motion of knee in flexion and extension.*

Due to the anatomical and physiological features, which may vary with age, sex, injuries and even from individual knee to individual knee, there is not a stated value for the range of knee motion in extension and flexion. Instead, there is a range of values for each limit [32]–[34]. The range of motion can be measured grossly by a goniometer or by more specific measurement such as electrogoniometer, roentgenography, stereophotogrammetry, or photographic and video techniques using skeletal pins [11], [17], [33], [35]. According to literature [33], [35]–[37], the normal range of motion for the knee joint presents a standard derivation, this means that there is not a stipulated value for the range of motion. Thus, the limits for range of flexion generally vary from 120 degrees (^{o}) to 160^{o}, depending on the organisation of the anatomical segments. Therefore, the active flexion is between 120^{o}-130^{o} with the hip extended, 140^{o} when the hip is flexed and 160^{o} when aided by a passive element (e.g. sitting on heels).

The range of extension, according to different references [11], [21], [33], [35], goes from 0^{o} to 10^{o} beyond the "straight position" (hyperextension). It is important to take into account the range of extension, once the neutral position in this situation allows the leg to support the body weight like a simple structure when standing still. Hence, if the knee does not reach the normal range of extension (e.g. in an envelope or gait test), then the standing motion is compromised and this will result in adverse consequences. In Table 3-1, values for the range of motion of the tibiofemoral joint in relation to the sagittal plane during common activities are presented. Analysing these data, the activity which requires a higher range of motion occurs when lifting an object from the ground, whereas the activity which requires a lower range of motion is walking. The data are coherent with reality, since, during a walk, the human is up standing and, when lifting an object from the ground, it is necessary to flex the knees: first, until the object is reached and, then, to get it up until a standing position (zero degrees position). Consequently, it is of high importance to consider this information in future computer modelling.

Table 3-1*-Range of tibiofemoral joint motion in the sagittal plane during common activities. Mean for 20-30 subjects. Adapted from* [38]–[40].

Activity	Range of Motion from Knee Extension to Knee Flexion (Degrees)
Walking	0-67
Climbing stairs	0-83
Descending stairs	0-90
Sitting down	0-93
Tying a shoe	0-106
Lifting an object	0-117

Previous anatomical and biomechanical studies [35], [41]–[44], which compared the human knee kinematics with other mammals, indicated there is a high similarity between the human knee and other species. This possibility has revolutionised biomechanical investigation overcoming the difficulty of obtaining human knees for biomechanical tests. For a clearer view regarding these data, the range for human knee motion and five other species is illustrated in Table 3-2. These data allow for a basis of comparison. The pig, goat, sheep and cow subjects are the most suitable species to use in experimental assays, since the range of motion is more similar to humans.

Table 3-2 *- Passive range of motion compared between human and five animal species. Adapted from* [35].

	Range of motion	
	Extension [in degrees ± σ]	Flexion [in degrees ± σ]
Human	2.5 ± 2.9	137.5 ± 9.6
Cow	35 ± 5.8	145 ± 7.1
Sheep	40 ± 5	146.7 ± 2.9
Goat	45 ± 9.1	145.5 ± 8.7
Pig	42 ± 4.5	144 ± 5.5
Rabbit	22 ± 2.7	161 ± 2.2

3.3.1.2 Transverse plane

Despite having a plain mechanics similar to a hinge, internal and external rotations can be noticed during the knee motion. These rotations are adjustable according to the motion regarding the transverse plane. This phenomenon is known by the scientific term laxity [11]. Thus, the angles of rotation at the range of flexion are called internal and external rotational laxity, relatively to the neutral position. As the knee is flexed until a maximum of 30º to 40º, the external tibial rotation is approximately 18º and internal rotation of the femur is approximately 25º, hence, the range of

rotational laxity increases. Beyond 40º of flexion, the internal and external rotational laxity remains constant up until 120º and then decreases again up to full flexion [11], [45]. When an external tibial rotation combined with internal femur rotation is more than the soft tissues can handle (e.g. ligaments), the soft tissues tighten up and can lead to a ligament tear, as Figure 3-8 illustrates.

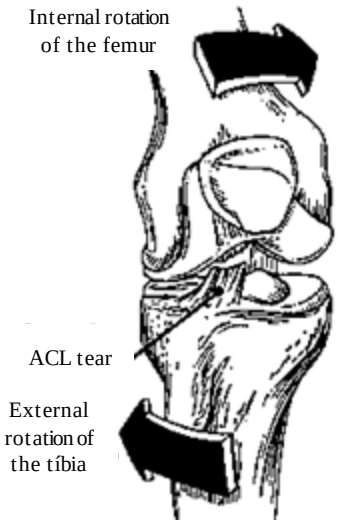

Figure 3-8 *–ACL tearing after crossing the limit of external tibial rotation. Adapted from* [46].

3.3.1.3 Frontal Plane

Rotations like adduction (also known as varus) and abduction (also known as valgus) happen in relation to the frontal plane (see Figure 2-2). Similarly to internal and external rotations, they are also affected by the angles of the joint flexion. With the knee flexed up to 30º passive adduction and abduction reaches a maximum of only a few degrees, whereas beyond 30º the motion in the frontal plane decreases because of the limiting function of the soft tissues. Moreover, as described in the previous chapter, in the laterals of the knee, the collateral ligaments are found to restrict the adduction and abduction rotation. As the stiffness of medial collateral ligament (MCL is higher than the lateral collateral ligament (LCL), the adduction rotation is greater than the abduction [11], [21].

Overall, when the knee flexes, three different movements occur. First, the rotation of the femur on the tibia epiphysis is eminent in relation to sagittal plan. Second, the rolling/gliding motion (medial-lateral translations) of the two epiphysis on occurs each other. Finally, the joint capsule expands by fault of synovial fluid in order to facilitate the gliding motion. According to [21], the conjunct rotation is only 20º, whereas voluntary rotation is 60º-70º. This means that during the passive motion, e.g. knee flexion, slight rotations (conjunct rotation) occur regarding sagittal and frontal planes. Such event is mainly caused by the flexion itself. While in the beginning of the action this means just a rotation of the femoral condyles (sagittal plane), towards

the end, the rotation changes into a gliding action (frontal plane). In addition, voluntary rotation means the intentional abduction - adduction or internal-external rotations, rising the maximum value to almost 70^{o} [21], [47].

4 KNEE LIGAMENTS

4.1 ANATOMY AND MORPHOLOGY

An articulation is composed of several ligaments which provide interoperability among stakeholder bones. The ligaments are bands composed of strong and tough (but flexible) multi-collagenous fibres which provide exceptional mechanical properties. Reinforce the joint capsule and acting as stabilisers against the considerable biomechanical demands that are imposed upon the joint are examples of its functions [21], [22], [48], [49]. As mentioned in Section 3.2, the ligaments can be divided into groups according to their anatomical position. Some ligaments are thickeners of the joint capsule (extracapsular ligaments), whereas others are stabilizing structures (intracapsular ligaments). In either case, all of them have the function of preventing the excessive movement of the joint [22]. Therefore, the knee has five main ligaments that provide support to the knee joint: the posterior cruciate ligament (PCL), the anterior cruciate ligament (ACL), the medial (also known as tibial) collateral ligament (MCL), the lateral (also known as fibular) collateral ligament (LCL) and the patellar ligament (sometimes referred as patellar tendon (e.g. [21])). The cruciate ligaments are located within the joint capsule (intracapsular ligaments), whereas, the last three mentioned ligaments stabilise and strengthen the joint capsule of the knee (extracapsular ligaments).

The ACL is inserted in the posteromedial surface of the lateral femoral condyle and extends until the intercondylar eminences of the tibia, while the PCL extends from the lateral surface of the medial femoral condyle and travels posterolaterally behind the ACL to insert on the sulcus between the two plateaus of the tibia [4], [19], [50], [51]. These ligaments are known as cruciate ligaments because of the crossed arrangement between them within the knee. The cruciate ligaments work together in order to control the posterior and anterior motion of the tibia and stabilise the knee joint during the motion, i.e. they are the primary restraints of the flexion (PCL) and the extension (ACL) [17], [43]. In a study contemplating five hundred knee injuries, the anterior cruciate ligament proved to be the most susceptible to injuries [52].

The cruciate ligament are being referred in literature as composed of fibre bundles with different lengths and orientations [53]. Particularly, the ACL varies from 31 mm to 38 mm of length [50], and it is mainly described in literature as composed of two separate bundles, the anteromedial (AM) one and the posterolateral one (PL) [30]. Each bundle has different lengths, being the PL much shorter than the AM. This can be explained by the oblique insertion on the tibial plateau. Thereby, when the knee is extended, the posteromedial bundle tightens up and becomes more convex, while during flexion the anteromedial bundle is the one to tighten, increasing the biomechanical efficiency of the ligament as a restraint [17], [50]. Similarly to ACL, the PCL is mainly composed of two distinct bundles, the anterolateral (AL) and the posteromedial (PM) bundle [51], [54]. The average length of the PM bundle is bigger than that of the AL bundle, measuring approximately 38.7 mm and 35.5 mm, respectively. The average length, as a whole, for PCL is approximately 38 mm. Unlike the ACL, the PCL has an irregular width. It is narrowed in tibial insertion (average 13 mm, depending on the intercondylar notch), being 20 percent (%) greater than the cross-section area of the ACL, and 50% greater in femoral attachment [19], [50], [53], [55]. Figure 4-1 and Figure 4-2 depict the attachments of the cruciate and collateral ligaments.

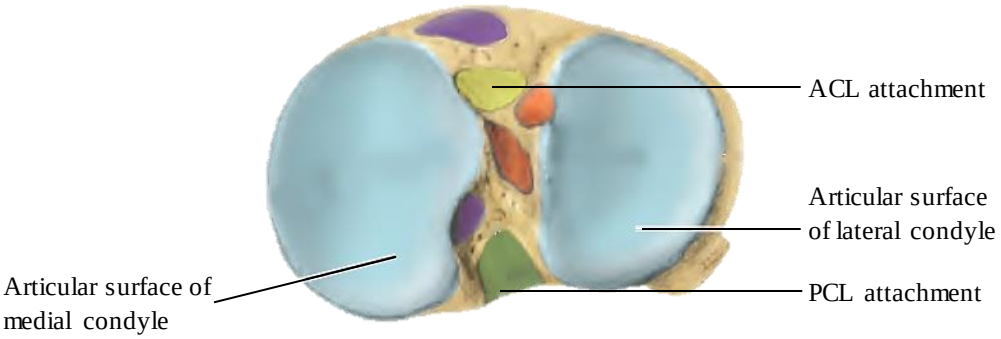

Figure 4-1 *- Superior view of tibia plateau, with special attention to the attachments of the cruciate ligaments. Adapted from* [20] .

Additionally, to prevent the knee from moving too far to either side, caused, for instance, by an external force, there are two ligaments which run along the side of the knee: the MCL and the LCL. The MCL has origin in the medial femoral epicondyle and the posteromedial margin of the medial condyle of the tibia. The LCL connects the femur to the fibula, hence it is attached to lateral epicondyle femoral and passes posterodistally to the top fibular head (see Figure 4-2 for a view on femoral attachments) [4], [19], [48], [51]. According to the referenced literature [52], the LCL is less commonly injured when compared to other knee ligaments, due to its anatomy, function and location. On the other hand, the MCL is the second more susceptible to injuries, mainly due to external forces. The average length of the LCL is within a range of 59 to 72 mm. It is bigger anteroposteriorly (3 to 4 mm) than medial-laterally (1.5 to 3 mm) [56]. The LCL has

been described as having a role in limiting external rotation, whereas the MCL is responsible for limiting internal rotation, during knee flexion [57]. The MCL has a triangular cross-sectional shape with approximately 11 cm in length [19].

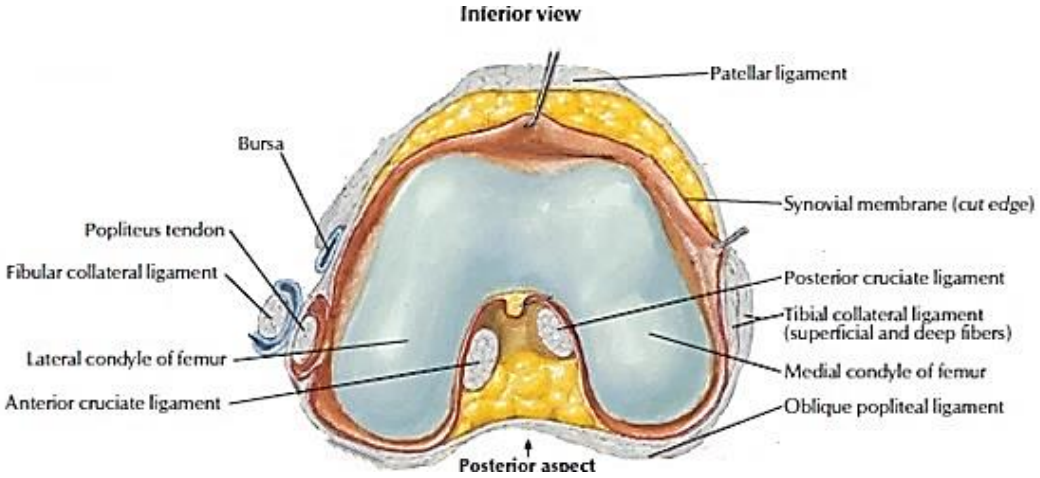

***Figure 4-2**- Inferior view of the femur condyles, where it is visible the correspondent ligament attachments* [27].

The patellar ligament is a thick and heavy central band, located in the anterior part of the knee with 6 to 8 centimetres (cm) long and 2.5 cm wide [21], [23]. This ligament is a continuation of the quadriceps femoris tendon. Consequently, it is attached to the lower part of the posterior surface of the patella to the upper part of the tibial tuberosity. This ligament plays an important role in maintaining the patella aligned relatively to the patellar articular surface of the femur and, moreover, it has the function of conducting force from the contracting quadriceps muscle to the tibia and as a result aids producing movement of the lower limb [20]–[22], [58]. The Table 4-1 presents the range of ligament measurements available in literature.

***Table 4-1**- Range of values of the ligaments' measures from previous studies.*

Human knee ligaments		Length (mm)	Width (mm)	Cross-sectional area (mm^2)
ACL	AM	44.4 [59]	6 – 7 [50]	34 (Proximally) 35 (Mid-substance level) 42 (Distally) [60] Mean: 31.3 [61]
	PL	28.5 [59]	5-6 [50]	
	ACL	22-41 [60]	7-12 [60]	
PCL	AL	35.5 [55]	7.2 [62]	43 [55]
	PM	38.7 [55]	8.08 [62]	10 [55]
	PCL	38 [61]	13 [61]	40.9 [61]
MCL		11 [19] – 15.07 ± 2.46 [63]	3.56 [63]	25 [64]
LCL		59 - 72 [56]	1.5 -3.0 [56]	15 – 30 [56]

4.2 HISTOLOGY

Histologically, the ligaments and tendons are dense connective tissues known by its parallel-fibred collagenous organization. Therefore, they are mainly composed of water and collagen [11], [26]. One of the reasons ligaments are cablelike structures (mechanically) and, consequently, very strong is the orientation of collagen fibres, which are grouped in long, parallel bundles, in one direction [4]. The ligaments are mainly composed of type I collagen fibres, which is the most abundant in our body. Due to this typical composition, the ligaments are structures characterised as viscoelastic materials, i.e., typically made of collagen fibres [4], [21], [51], [65].

Packaging of collagen fibres has many hierarchies as shown in Figure 4-3. The smaller bundle of fibrils is collagen, which assembles with other collagen fibrils creating a microfibril. Several microfibrils assemble into one subfibril and so forth until the last structure is obtained, in this case the ligament.

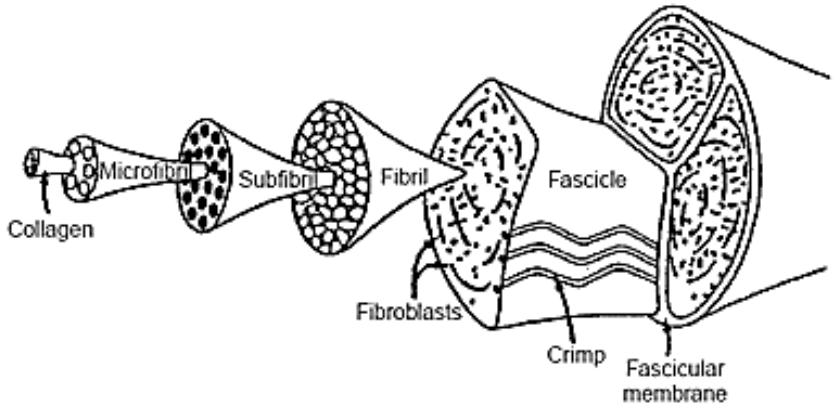

Figure 4-3- *Ligaments are organised hierarchically adopting an assembled structure. Adapted from* [26].

Collagen is a fibrous protein and it is synthesised by fibroblasts (the most common cells of connective tissue in mammals). The structural composition of the ligaments is 20% of fibroblasts (cellular material) and 80% of extracellular matrix in which 60-80% is water and 20-40% is solid matter as ground substance (20-30%), collagen (70-80%) of type I (90%) and type III (10%), and a small amount of elastin. Thus, the type I collagen is the major constituent and is considered to be responsible for the ligament's stiffness and strength [11], [51], [66]. The complexity of interactions between the ligaments' components displays a dependency on time and history of the mechanical properties (Figure 4-4) [51]. Hence, the mechanical behaviour of the ligamentous tissue is considered nonlinear.

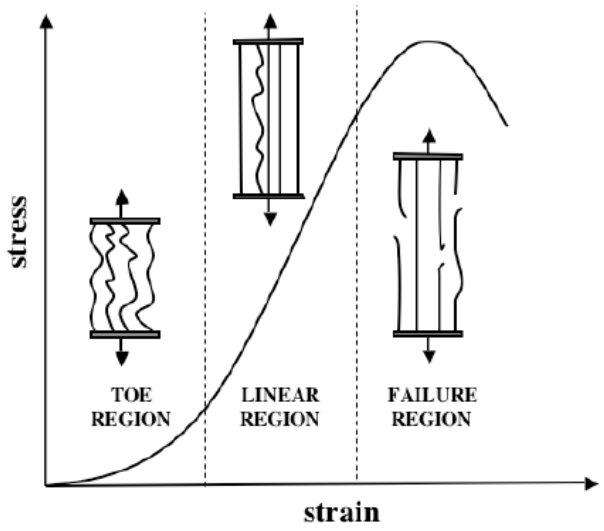

Figure 4-4 *- Typical ligament strain-stress relationship* [67] .

The major difference between tendons and ligaments is the structural orientation of fibres, as it can be visualise in Figure 4-5. The tendons adopt an organised orientation in contrast to ligaments which present a random organisation more like a weaving pattern [11]. Therefore, the ligaments are considered anisotropic structures [2].

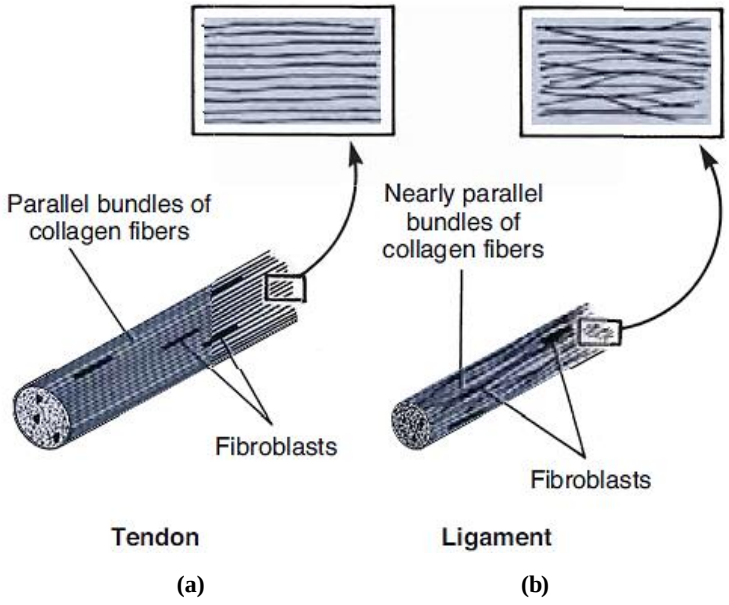

Figure 4-5*- Structural orientation of the fibres in* ***(a)*** *tendon contrasting with* ***(b)*** *ligaments [12].*

The percentages given previously for each basic constituents of the ligaments are represented in ranges due to a diverse array of mechanical behaviours of knee ligaments that are suitable for their respective functions. For instance, it depends on the solicited strength and where it is solicited. Moreover, studies (e.g. in [68]) have shown that mechanical loading regulates the gene

expression of the collagen in ligaments. Thus, the ligament's composition is believed to be directly correlated to its mechanical properties.

4.3 VISCOELASTIC PROPERTIES OF LIGAMENTS

Ligaments are flexible and pliant allowing natural motion of the bones to which they are attached. Nevertheless, they are also inextensible and extremely resistant to pulling forces in order to offer resistance and control of the applied forces by the human weight and motion [4], [11], [51]. The soft tissues category, where the ligaments are included, is mainly characterized by the composition of collagen (main load bearing components of tissues [69]), and is known to have viscoelastic features [11], [51], [70]. Viscoelastic materials exhibit both fluid (measure of resistance to flow) and solid (elasticity) characteristics which are dependent of the type and pattern of the tensile loads, endowing it with unique mechanical properties [13]. This kind of materials exhibits a creep behaviour (i.e. slow continuous increase in strain), when subjected to a constant stress. In contrast, a slow continuous decrease in stress over time, or stress-relaxation, is observed when subjected to a constant strain [51], [69]. Moreover, in response to various tensile solicitations, ligaments exhibit hysteresis, that is, an internal energy dissipation [51].

The stress-strain relation for a viscoelastic material exhibits a time-dependent function. This affects the response on how quickly the load is applied or removed, i.e., the tensile loads in the material are dependent on the strain and strain rate (velocity of deformation) (Figure 4-6) [11], [13].

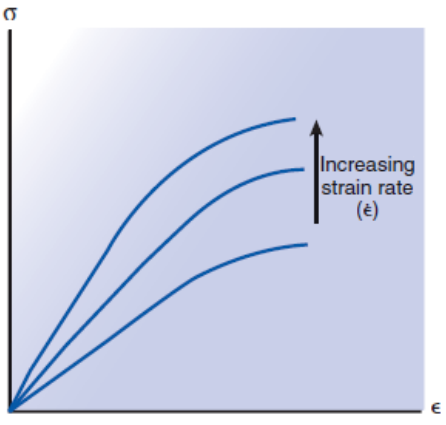

Figure 4-6 *- Stress-strain graphic for viscoelastic materials under different strain rate* [11].

Analysis of the mechanical behaviour and biomechanical properties of ligaments provides important information to the understanding of soft tissues, injuries mechanics and potential solutions for reconstruction.

4.4 LIGAMENTS KINEMATICS

This section's main aim is to explain the ligament's behaviour during knee motion. Every single knee ligament has different kinematics due to their corresponding insertion sites location and area. These factors employ a kinematic pattern that it is also affected by length, width and cross-sectional area of the ligament [50].

Nonetheless, the ACL and the PCL behaviour is often referred to as the four-bar linkage system which represents a functional isometry between femur and tibia [50], [71]. The concept of a four-bar link consists of four bars connected to each other by hinges. Visualising Figure 4-7, it is possible to distinguish two up and lower bars. They represent the femoral and tibial couplers, while the sloping bars are the connections between the attachment areas of the cruciate ligaments function on the sagittal plane [43], [71]. This concept can be used as basis for mathematical models [17].

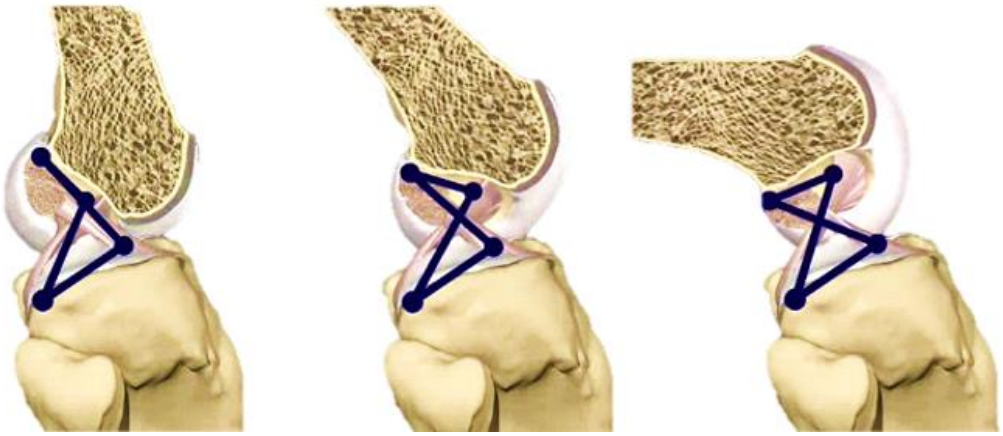

Figure 4-7- *Kinematics of the anterior and posterior cruciate ligaments.* ***(a)*** *Full extension,* ***(b)*** *20-50 º of flexion and* ***(c)*** *full flexion. Adapted from* [72].

The four-bar linkage demonstrates that the centre of joint rotation (ACL and PCL interception) moves posteriorly with knee flexion. This allows for both the sliding and the rolling movements of the femur during flexion and prevents it from rolling off the tibial plateau at extremes of flexion [73].

Concluding, the length and tension of the ACL and the PCL change during the knee motion, owing to their asymmetric insertion sites. Additionally, during the path of the femur in relation to the tibia (in extension), the ACL tightens and the PCL loosens until full extension (see Figure 4-7- a) is reached. On the contrary, in flexion, the PCL tightens (specially the AM bundle) and ACL posterolateral bundle relaxes (see Figure 4-7 –c) in order to provide stability to the knee

joint. In the range of flexion from 20° to 50° (see Figure 4-7 – c), the stability of the knee is more tenuous, once neither ACL or PCL are very taut [50].

The cruciate ligaments are usually represented in multi bundles as explained in Section 5.1. The AM bundle from ACL has higher strength and it is thought to be an important restraint to anteroposterior translation, while PL bundle is considered to be an important restraint to rotational moments of the knee [54]. This is mainly due to the variable relative insertion orientation of the bundles from the respective ligaments [74].

4.5 BIOMECHANICAL PROPERTIES OF LIGAMENTS

Second to muscles, the ligaments are important stabilisers of the knee, divided into internal stabilisers (cruciate ligaments) and external stabilisers (collateral ligaments). During common activities, the ligaments experience loads, stretching and loosing, which may have an influence in their role as stabilisers. Many studies have been performed to determine the biomechanical properties of the four major ligaments (PCL, ACL, MCL and LCL) e.g. [8], [48], [51], [74]–[78]. The biomechanical properties of ligaments can be evaluated either by using a set of bone-ligament-bone specimen [18], [68], [74]–[76], [79], [80] , or through measurements of *in situ* forces (undissected knee) [14], [28], [29], [44], [51], which allow for the understanding of tissue biomechanics [81]. The instrumentation usually used in bone-ligament-bone are creep and stress-rupture systems, as the uniaxial tensile machines, which are mainly Instron ®(Canton, USA) machines [17], [18], [32], [44], [48], [76], [82]–[86]. On the other hand, to measure *in situ* forces, a robotic/universal force-moment sensor (UFS) [28], [29], [51], [87], [88] or finite element modelling (FEM) [1], [2], [89]–[96] can be used, being the UFS a direct measure and the FEM an indirect measure.

Young's modulus and failure characteristics are examples of useful measurements for comparison of different ligaments material properties [48]. These material properties are of high significance not only for the research for a new solution of ligament repair or material replacement, but also as input parameters for computational models of human knee joint. Ligaments have the function to transfer loads from bone to bone along the longitudinal direction. Hence, their properties are commonly studied by means of uniaxial tensile test of bone-ligament-bone complex [51]. Nevertheless, recent study groups have directed their attention to the orientation of the ligament using robotic technologies to simulate the natural motion of the knee e.g. in [28], [74], [87] and focusing on the influence of the strain rate in the ligament's properties e.g. in [48], [75], [83], [84].

Ligaments are known for their viscoelastic behaviour which displays two types of characteristic curves: load-deformation curves and strain-stress curves [97]. Each obtained curve is unique and is found by recording with the appropriate devices the amount of deformation produced by tensile strength. If the cross-sectional area and the original length are not taken into account, a load-elongation curve is reached (Figure 4-8 – a). Consequently, this type of curve is less accurate, and only offers information regarding the tensile capacity of a ligament structure after loading a ligament to failure [11]. From the load-deformation curve between two points of the curvature's slope, the stiffness ($N.mm^{-1}$) of the material is obtained. Besides, it is possible to get the maximum elongation (mm) and the ultimate load (N) of the ligament at failure. Integrating the curve, it is possible to know the energy stored by the ligament at failure ($N.mm^{-1}$) [98]. Furthermore, using the load data along with cross-sectional area and original length measurements of a ligament, stress-strain curves are also generated (Figure 4-8 – b) [14], [98]. The values for stress and strain are calculated[2] and so structural and mechanical properties for ligaments are analysed. In this case, values are obtained from the linear region where stress is linearly proportional to the strain and the slope between two limits of this region in the Young's modulus ($N.mm^{-2}$ or MPa). The ultimate strain (%) is the strain at failure, that is, when the tearing of the ligament occurs. Finally, integrating the stress-train curve, the energy density is obtained.

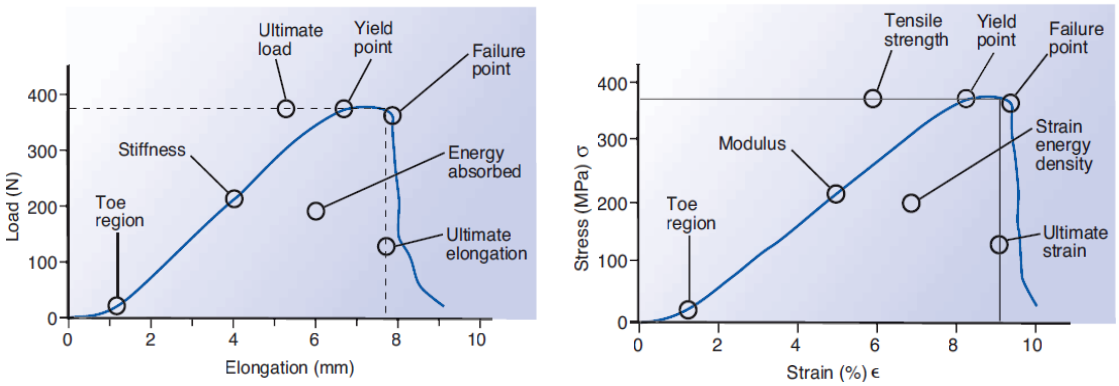

Figure 4-8- (a) *Example of load-elongation curve and* ***(b)*** *stress-strain curve of a tendon or ligament with the correspondent regions of concern until the failure point* [11].

The mechanical response of the ligament depends greatly on the fibre bundle structure, its orientation and length. Thus, they are expected to differ from ligament to ligament within or from donor to donor (according to sex, age and anatomy), consequently, this implies a challenging mechanical standard characterisation [18], [53], [83], [86].

[2] Consult Section 2.2 for information about the calculus.

In computational knee ligaments models and in investigation of materials to obtain a ligament replacement when injured, it is important to define some mechanical parameters which are obtained from the curves previously explained. Quantification of the tensile properties of knee ligaments has received the attention of several researchers in biomechanics. Clearly, the knowledge of Young's modulus, the tensile strength and the ultimate strain are useful measurements to apply in finite element and reconstruction methods. Moreover, these properties are also used to compare the material properties of different ligaments and materials and to use them as input parameters for computational models [48].

The ligament's material behaviour is dependent on the strain rate due to their histological structure and it has been studied [48], [75], [84], [99]. Table 4-2 presents a range of values according to the influence of strain rates.

Table 4-2- *Range of values for mechanical parameters of the human knee ligaments, adapted from Annex II.*

Human knee ligaments and bundles		**Young's modulus (MPa)**	**Failure stress (MPa)**	**Strain rate (% .s^{-1})**
ACL	AM	283.1±114.4	45.7± 19.5	100
	AL	285.1± 140.6	30.6 ± 11.0	100
	PB	154.9 ± 119.5	15.4 ± 9.5	100
	ACL	111- 309,7	24,36 - 63,8	100
PCL	AL	150- 248	35,9 ± 15.2	50
	PM	145 - 294	24,4 ± 10.0	50
	PCL	109 -384.7	26,8 – 38,5	100
MCL		332.2 ± 58.3	38.6±4.8	1
LCL		372 ± 33.9	36.5 ± 6.16	100

5 LIGAMENT INJURIES

Knee ligament injuries occur when a ligament is stretched beyond its normal limits, driving to a partial or complete tear [51], [100], [101]. They can happen from sprains, avulsion fractures, congenital deficiencies and complex structural injuries [101]. More than half of all types of injuries occur associated with damages made in other regions of the knee, most commonly, due to another ligament, articular cartilage or menisci injuries. Moreover, the ligament injuries can lead to further damages to the menisci and chondral surfaces. For the example, in fourteen years an injury can lead to osteoarthritis following ligament injury [102], [103]. Nonetheless, ligament injuries may also happen due to external factors. Some of them are, for instance, in a car accident, when the knees strike strongly on the dashboard of the car [101], when changing direction or stopping suddenly (this happens frequently to handball or football athletes), when slowing down during jogging, if landing incorrectly from a jump or fall (it frequently happens in long jump sports), or getting hit directly during a contact (this may happen in several sports, like football or martial arts) [47], [104].

There are several signs or symptoms of a knee ligament injury. The most common are pain, swelling and instability in the knee. Likewise, other examples are the "popping" noise (probably ACL injured), feeling that the knee is unstable (can be any of the major ligaments), pain on the inside of the knee (MCL), pain on the lateral side of the knee (LCL), inability to move the knee normally or reduced range of motion (probably ACL injured). If some of these symptoms happen, medical advice and proper exams (like computed tomography (CT) and/or magnetic resonance image (MRI)) are advisable for a correct diagnose [51], [101], [104].

Ligament injuries are classified according to grades: I, II, and III depending on the severity:

- •Grade I distension: Pain with minimum ligament injury.
- •Grade II distension: Partial tear of some ligament fibres and small articulation laxity.
- •Grade III distension: Total tearing of the ligament, consequently, the articulation becomes loose or instable. The lateral meniscus injury may be associated.

Grade I distensions are the less aggressive, but the most frequent. The treatment is the plainest one [34]. To the inflammation reduction, it is important to use ice on the articulation, and to take anti-inflammatory or analgesics. Elevating the knee with a pillow under it, also prevents the edema from getting worst. Overall, in these type of cases, the treatment is based on resting and using crutches [101].

Partial tears (Grade II) are rare, but when they happen, if the overall stability of the knee is intact, the doctor may recommend nonsurgical possibilities [34]. Resting the injured knee, wrapping it and use crutches (to avoid putting weight on the leg) or knee rehabilitation are some of the options. Note that the ligaments are not regenerative. Therefore, if nonsurgical management is not possible, the only solution is to reconstruct the ligament, once the ligaments cannot be sutured. The latest accepted procedures and materials approved by the medical community and regularly used in medicine will be discussed next [101].

According to a knee dislocation study, the cruciate ligaments tend to be completely disrupted during a motor vehicle injury and in sports [101],[105], leading to grade III panorama. In the next section, reconstruction solutions are discussed when a ligament is totally disrupted and chirurgical intervention is needed.

5.1 LIGAMENTS' RECONSTRUCTION SOLUTIONS

Ligament reconstruction surgery is based on two established concepts: using a tissue graft with similar biomechanical properties with bone in the ends or doing the fixation of the graft by means of sutures. Both concepts do the fixation in the most rigid form possible and as close as possible to the ligament attachments in the joint [106]. For the reconstruction relying on the biological graft, a large choice of graft sources is available. These might include autografts and allografts (for instance, from patellar tendon, hamstrings tendons and the quadriceps tendon [79], [102], [107], [108]). The most popular biological graft is from the patellar tendon (one third of the central part [101]) for its mechanical resistance, rapid integration, rigid fixation, ease of collection and due to the structural properties similarity to the ACL [79], [102]. Nonetheless, choosing the graft is often done by the surgeon according to the amount of graft available and type of ligament injury [79], [102] and considering the post-operative conditions [51], [79], [107], [109], [110]. Both types of graft reconstruction involve healing at the graft attachment site and also the process of graft revascularization and incorporation [102].

If the graft is boneless, sufficiently strong stiches are needed for suturations (see Figure 5-1), allowing sufficient pressure levels in order to promote graft incorporation conditions in the host bone.

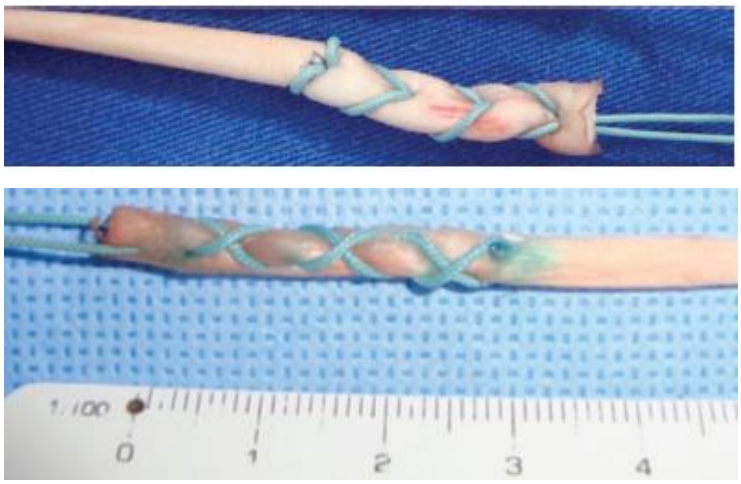

Figure 5-1- *Two different suture configurations in preparation of tendons for knee ligament reconstruction.* ***(a)*** *In point loop and* ***(b)*** *in point X suture* [106].

Soft tissues grafts take longer (eight to twelve weeks) to fully recover into the host bone. On the other hand, the grafts containing bone are more invasive but the recovery time is shorter (within six weeks) [102]. This type of reconstruction involves tunnel positioning, graft tensioning and initial fixation and strength. Allografts reconstructions have become the most used techniques (example of ACL reconstruction by this method in Figure 5-2) , but the reproducibility of tension during the fixation of the graft has been questioned, since most surgeons do this manually and this method can differ considerably from surgeon to surgeon [102], [111].

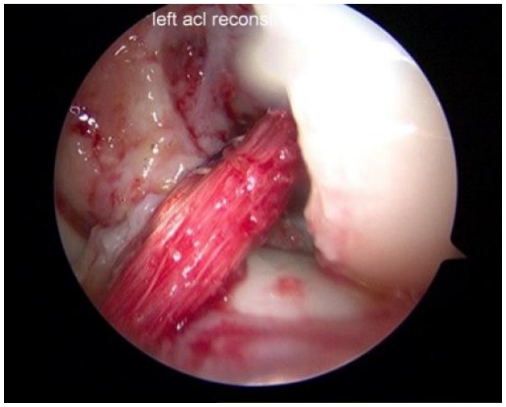

Figure 5-2- *ACL reconstruction by allograft* [102].

Furthermore, the nature of reconstruction is another aspect that should be taken into account. For the reconstruction, one has to decide between single-bundle and double-bundle. In single bundle technique only the stronger bundle is reconstructed, whereas in double bundle technique both of the bundles are reconstructed [102], [112]. In previous chapters, the ACL and the PCL were mentioned as multi-bundle material. Thus, a double bundle should be considered for a more

accurate reconstruction and it proved to me more suitable according to recent studies [102], [112]–[114]. Figure 5-3 is a picture of the tunnel position for double bundle PCL reconstruction.

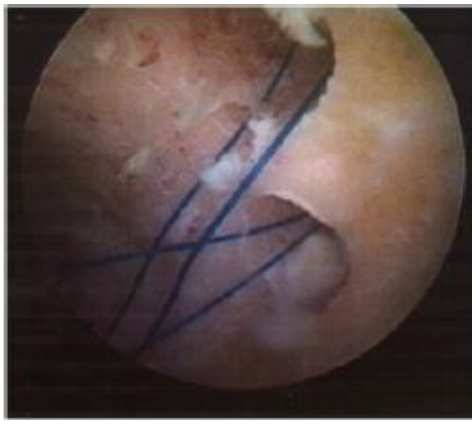

Figure 5-3 *– Two tunnels in femur for double bundle PCL reconstruction* [102].

Further, the ideal graft should offer solid fixation, rapid biologic incorporation and limit donor site morbidity [79]. There are some required characteristics and relations that should be followed to achieve the successful development of a regenerated functional ligament. Figure 5-4 illustrates these requirements and relationships in a schematic diagram.

Recent progressions in this field have been conducted in terms of materials that are usually used for ligament regeneration: natural polymers [115], synthetic degradable polymers, carbon nanomaterials, nano-fibres and porosity in engineered ligament scaffolds, composites for engineered ligament scaffolds [103]. Moreover, Achilles et al., in 2010, developed a ligament repair device to replace the injured ligament, which is grafted into place to hold the knee joint together [116].

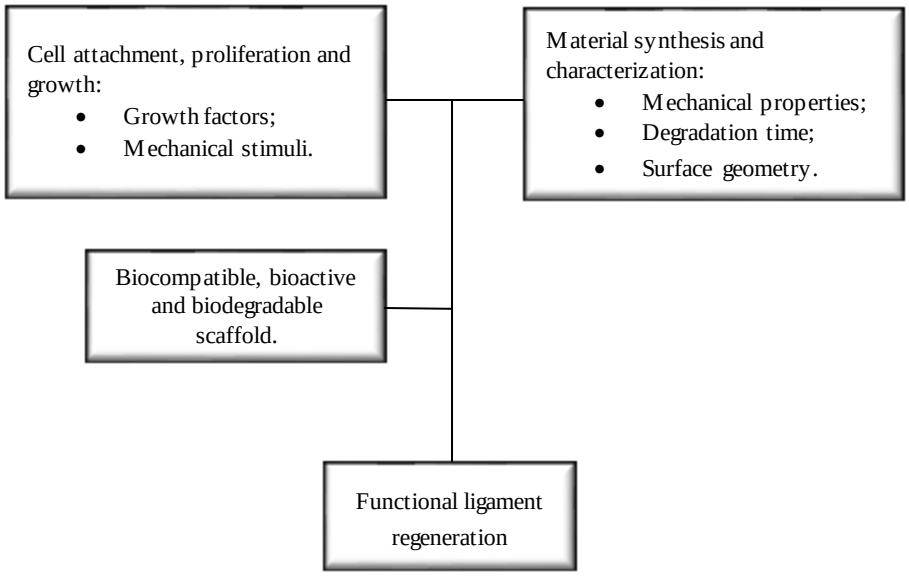

Figure 5-4 *– Schematic diagram indicating the main requirements to the successful ligament regeneration development. Adapted from* [103].

PART II

MECHANICAL TESTS

MECHANICAL PROPERTIES CHARACTERIZATION

STATE OF THE ART

NEW APPROACH FOR MECHANICAL TESTING

EXPERIMENTAL MECHANICAL TESTS

[This page was intentionally left in blank]

6 MECHANICAL PROPERTIES CHARACTERISATION

The biomechanical properties of ligaments are often evaluated by using mounted specimens such as bone-ligament-bone complexes [74], [75], [99]. These complexes are usually tested in a uniaxial tension model [14], [48], [51], [114], [115], [117]–[119] (with some exceptions, e.g. in [28], [87], [89], [120]), since ligaments' main function is according to the fibres orientation and to stabilise the knee, when submitted to tensile efforts [121]. Moreover, different types of tests are used to evaluate different mechanical properties, such as tensile, creep, fatigue [83], [86], shear [122], stress-relaxation and recovery after loading [118], [123]. All of these tests are under stress conditions where the ligament deforms and creates a strain distribution [29], [124].

Numerous experimental studies have been conducted to characterise the mechanical behaviour and properties of knee ligaments. Their performance is challenging because of several factors, either of external biological nature or associated with the experimental methods themselves. Biological factors result from morphological, biomechanical and biochemical changes in the knee, due to its location, aging, physical activity and the adaptation which is forced upon it from motion and load requests [11], [121].

In *ex vivo* condition, some factors should be taken into account. Ligaments are soft and moisty tissues with viscoelastic properties, which can difficult the clamping of samples. In order to solve this problem, not only different types of clamping have been developed but also some methods to hold the specimens [18], [48], [74], [76], [83]–[86], [88], [115], [119], [123], [125]. Another difficulty is the measurement of the cross-sectional area, as the geometry of the ligament is very irregular. This affects the measurement of the instantaneous elongation and the calculation for real stress [121]. Among other factors which require attention, strain rate [48], [75], [77], [84], [99] and the orientation of insertions [74], [126] should be carefully considered and also how it influences the results.

6.1 EXPERIMENTAL METHODS – STATE OF THE ART

The protocol for the experimental procedures should be defined and followed strictly due to the sensitivity of the organic tissues. According to studies found in literature, the sample collection, storage and thawing conditions, methods used in clamping, test conditions including the load speed and strain rate, are important parameters that should be well-defined. Nonetheless, different studies exhibit some discrepancies which will be hereinafter described.

Moreover, some of the constitutive models used to describe the mechanical behaviour of ligaments will be slightly explained in Section 6.2.

6.1.1 **Sample collection**

Post-mortem, sample collection is the first step to take into account. After death, the *rigor mortis* (stiffness of death) starts chemical changes that will lead to stiffening of the soft tissues. In humans, they begin three to four hours after death, approximately. Stiffness will have reached its maximum after twelve hours and gradually dissipates after twenty-four hours [10]. Depending on the aim and set up, the whole knee can be collected, including 12 to 20 cm [28], [29], [44], [127] of the distal part of femur and tibia or the ligaments can be isolated from the joint, keeping only the bone blocks from the insertions.

Kennedy et al. (1976) [83] excised the ligaments from the knee joint twelve hours after death and analysed within four hours after extrusion. In Butler, Kay et Stouffer (1986) [18] ligaments were removed within eighteen hours *post-mortem*. On the other hand, for instance, Pioletti, Rakotomanana et Leyvraz (1999) [75] removed the ligaments of a bovine's knee after twenty-four hours *post-mortem*.

6.1.2 **Storage**

After the sample is collected, the storage procedure needs to be considered. The sample should be transported in a fresh storage no more than fifty hours after being removed from the cadaver [128]. If the samples need to be stored prior to the assay, the temperature of storage (the most used in literature) should be of -20 ° C in plastic bags [35], [48], [74], [75], [82], [84], [118], [127]–[131]. At this temperature it is possible to maintain the physical and mechanical properties of the specimens [82], [128].

For instance, in Su, Chen et Luo (2008) [129] the specimens of MCL and patellar tendon of a rat were wrapped in moistened gauze (0.9% normal saline), sealed in plastic Petri dishes with Parafilm M film (Alcan Packaging, WI, USA) and stored at -20 °C until testing within 24 h.

On the other hand, Butler, Kay et Stouffer (1986) [18] stored the joints in plastic bags and placed them in a freezer at -30º C for three weeks. Similarly, Duenwald, Vanderby et Lakes (2009) [123] wrapped tendons in saline-soaked gauze, covered with aluminium foil and sealed in plastic bags to be stored at -30 ºC in a freezer until the time of testing. It was referred that such careful freezing procedures have little effect on the biomechanical properties of collagenous tissues, such as tendon and ligament [118].

6.1.3 **Thawing**

The thawing procedure does not need special attention. Usually the specimens are left thawing, in a vertical position [35], at room temperature in plastic bags for six to ten hours [48], [74], [129]. It also could be done like in Butler, Kay et Stouffer (1986) [18] who left it thawing for twenty-four hours in a refrigerator at 4ºC. There is no evidence of differences between both methods, but the method of Butler, Kay et Stouffer (1986) could be more advantageous, since the specimen gradually defrosted at low temperatures, avoiding possible modifications in mechanical properties. On the other hand, Krokon et al. (1993) [131] and Dota et al. (2007) [130] thawed the knee parts in a recipient with physiologic solution (also known as saline solution or sodium chloride solution 0.9%) for four hours.

Haut et Haut (1997) [108] left the tendon of study thawing at room temperature in 0.1 molar (M) phosphate- buffered saline (PBS) for forty-five minutes before the mechanical test.

6.1.4 **Clamping**

The complex histological composition of ligaments confers hardly measurable mechanical properties. The ligaments are moisty, viscous and, consequently, slippery when gripped. In earlier studies, Kennedy et al. (1976) [83] modified the standard vacuum-controlled grips from Instron® Universal Testing Instrument TT-C for manually controlled clamps with coarse serrations on their jaws.

Butler, Kay et Stouffer (1986) [18] griped the entire distal bones in aluminium tubes mold with poly (methyl methacrylate) (PMMA), a bone cement. Other studies, proposed the use of cream hardener (similar to bone cement) in molds [123], custom made clamps [122] or total devices [75] according to the purpose.

Mommersteeg et al. (1995) [74] created a custom made setup, using a two-tier mold, in which the bone block was embedded in PMMA. Moreover, the bones were drilled and trimmed to ensure good mechanical interlock with PMMA. This mold was specially designed for positioning the insertion sites of the ligaments to study the effect of the variable insertion orientation on the tensile stiffness. Similarly, Pioletti et al. in 1999 developed a custom made device to perform uniaxial dynamical tests on isolated ligaments. To guarantee the right clamping, special clamps were

designed, in which the bone is involved in synthetic resin (monomer beracryl) and closed with a metallic ring and screws.

Su, Chen et Luo (2008) [129] potted the femur and tibia into a plastic tube with fixation of bone cement. The evolution from plastic tubes to aluminium tubes in this study was explained by the lower ductility of the plastic ones, which may break easily due to the loads imposed on it during testing.

Later, Bonner et al. (2014) [48] sawed the LCL femoral attachment in blocks of 15 x 15 x 25 mm^3 and removed its rounded proximal margin, diving it transversely at 40 mm in length. Afterwards, the blocks were placed in cylindrical aluminium pots, secured by alignment screws and embedded in PMMA. Petroleum jelly and saline soaked gauze were used to keep the ligament hydrated particularly due to the exothermic reaction of the bone cement polymerization.

6.1.5 **Testing conditions**

The temperature and moisture of the sample are very important, as the stiffness of the sample increases when the temperature decreases and so does the hydration [121]. This is due to the fact that the mechanical properties of these soft tissues are determined in large part by solid-liquid interaction structure [108]. To recreate the physiological conditions of tissue in experimental tests, the ligaments should be immersed in fluids, such as water, physiological fluid or isotonic saline solution.

Kennedy et al. (1976) [83] and Momersteeg et al. (1995) [74] kept the ligaments wrapped in gauze soaked in isotonic saline while awaiting testing. Moreover, in Momersteeg et al., Su, Chen et Luo (2008) [129] and Bonner et al. (2014) [48] tests, the ligaments were kept hydrated by frequently spraying it with 0.9% saline solution while testing process. While in Pioletti, Rakotomanana et Leyvraz (1999) [75] the specimens were continuously kept hydrated using a drip with a physiological fluid (1/3 NaCl 0.9%, 2/3 glucose 5%).

Pioletti, Rakotomanana et Leyvraz, Su, Chen et Luo, and Bonner et al. performed experiments at room temperature (±21°). However, Dota et al. (2007) [130] fixed the ligaments to an instrument, with a compartment similar to an aquarium, full with saline solution, simulating a physiological environment in order to minimize the effect of ligaments dehydration, thus, avoiding changes in the results.

6.1.6 **Load speed and strain rate**

The effect of strain rate on the mechanical properties of the ligaments has been reported, about which there are some studies available on the scientific community. The value of strain rate influences on the stress-strain curve obtained. Moreover, when tensile tests are performed at different strain rates, the resulting stress-strain curves are usually presented without a specific

method. A few examples of studies with different velocities are presented subsequently, trying to quantify the dependency of the stress on the strain rate. The strain rate is defined by the division of velocity by the original length.

Kennedy et al. (1976) tested the major knee ligaments (ACL and PCL) at two different velocities (125 and 500 $mm.min^{-1}$) in order to demonstrate the viscoelastic properties of ligaments [83]. Eight years later, Noyes et al. used a displacement rate of $100\%.s^{-1}$ of the original length of the sample to examine the mechanical properties of a substitute ACL graft [109].

In 1993, the cruciate ligaments were subjected to a uniaxial tensile test at velocity of 20 $mm.min^{-1}$ by Kokron et al. The average ligament length was considered 38 mm and a 60% rate of displacement was applied to 70 % of the total length of the samples. The aim of this study was to evaluate the mechanical properties of the ACL and compare it with the PCL [131].

Jones et al.(1995) [127] studied the ACL and conducted the tests with 50 and 500 $mm.min^{-1}$ at different degrees of joint flexion.

Haut et Haut (1997) [108] tested patellar tendon stretching at a rate of 125 $mm.s^{-1}$ up until to 3 % strain. After pre-tensioned the ligaments were stretched to failure at either 50 or 0.5 $\%.s^{-1}$. The study concluded that the tendons were significantly stiffer for $50\%.s^{-1}$ against $0.5\%.s^{-1}$.

In Dota et al. (2007) [130], a load application speed equal to 20 $mm.min^{-1}$ was applied to eleven PCL and fourteen patellar ligament. The aim of the study was to investigate the effects of radio frequency taking into account characteristics of rigidity and maximum deformation.

Bonner et al. (2014) [48] tested sixty porcine ligaments, so that the material properties of LCL of the porcine stifle joint could be measured. The test was performed in a uniaxial tension model through strain rates in the range from 0.01 to $100.s^{-1}$.

6.2 CONSTITUTIVE MODELS

The stress and strain are the quantification of action and its deformation, respectively, related by physical laws, the so-called constitutive laws. How these quantities relate to each other can depend on the material or material class. A constitutive model is a set of constitutive laws, which rely on the mechanical properties as parameters. Their solutions are used to describe the mechanical behaviour (not materials) [2]. Many constitutive models have been proposed, but they still remain a huge challenge for computer modelling, since they are validated only under certain conditions [2], [51]. In general, material's behaviour is grouped under constitutive models that include one or more behaviours such as elasticity, plasticity, viscoelasticity, viscoplasticity, among others. The following is an overall review of the last theories on constitutive models.

6.2.1 **Elasticity**

The materials are classified as having elasticity, when, after an intern loading and consequent deformation, they can be observed recovering their original shape. The material presents a reversible deformation followed by a conservation of its internal energy. In this kind of materials, the deformation state is reached immediately after load application [132].

Linear elastic materials obey to the Hooke's law which can be stated as a relationship between stress and strain, where the Young's modulus (E) is an intrinsic material property. The linear elastic material's constitutive relation is then defined by Equation 6.1, known as Hooke's law.

$$\sigma = E\ \varepsilon(t)^{e} \tag{6.1}$$

6.2.2 **Hyperelasticity**

In contrast to linear elastic materials, the stress-strain curve of hyperelastic materials is nonlinear. The hyperelastic constitutive models derive from a strain energy density function (W) as function of deformation gradient tensor: W=W (F). Also, in these constitutive models, the material is usually assumed to be isotropic, i.e. having identical values of a property, thus, responding equally in all directions with respect to the loading.

The neo-Hookean model is one of the hyperelastic material models used for plastics and rubber-like substances. This model is convenient due to its simplicity and serves as a basis for more complex material models, such as viscoelastic and viscoplastic models. The strain energy density function for an incompressible material is given by Equation 6.2 (neo-Hookean's law) [133].

$$W = C1\ (\lambda_1^2 + \lambda_2^2 + \ \lambda_3^2 - 3) \tag{6.2}$$

Where λ are the principal stretches, and C1 the material constant. As far as the transversely isotropic hyperelastic model is concerned, the neo-Hookean model is used to the ground substance modulation and Cauchy energy equation that defines the fibres behaviour [89], [117], [134].

The Holzapfel, Gasser and Ogden (HGO) model is an anisotropic, nonlinear, hyperelastic constitutive model that was developed to model the arterial wall mechanics [135]. Additionally, this model was developed with distributed collagen fibre orientations [136] and later on was successfully implemented for modelling the hip capsule following total hip arthroplasty [137]. More importantly, in 2013 this model was applied to model the knee ligaments by Westermann et al. in a knee joint obtained from the Open Knee project. The strain-energy potential U is in the form of the Equation 6.3:

$$U = C_{10}(\bar{I1} - 3) + \frac{1}{D}\left(\frac{(J^{el})^2 - 1}{2} - lnJ^{el}\right) + \frac{k_1}{2k_2}\sum_{\propto=1}^{N}\left(e^{\left[k_2\left(k\,(\bar{I}_1 - 3) + (1-3k)\left(\bar{I}_{4(\propto\propto)} - 1\right)\right)^2\right]} - 1\right) \quad (6.3)$$

Where,

- $\bar{I}_1$ is the first strain invariant;
- $\bar{I}_{4\propto\propto}$ are pseudo-invariants of the deviatoric part of the right Cauchy-Green deformation tensor;
- J^{el} is the elastic volume ration;
- N is the number of fibre families;
- C_{10}, D, k_1, k_2 are material coefficients;
- K is a parameter quantifying the degree of heterogeneity in the distribution of fibre directions locally within the material.

The material parameters are obtained from tissue's histology analysis and from mechanical experiments. This way, the parameters used in this part of the work were obtained by Kelleher et al. (2013) when studied the vocal ligament specimens [138].

6.2.3 **Viscoelasticity**

According to some studies [123], [139], the most suitable model is the one which considers viscoelasticity. The ligaments fall under viscoelastic behaviour, since they exhibit both viscous and elastic characteristics under deformation. Within this type of features there are several constitutive models that can be used to predict ligament behaviour. The following is a review of the theories that are used within this context.

In 1993, Fung [140] developed the quasi-linear viscoelastic (QLV) theory, one of the most successful models ever since to describe time and history dependency (creep and relaxation) of viscoelastic properties of ligaments, and the most commonly used in the biomechanics literature, e.g, in [118], [141]. The QLV assumes that a non-linear elastic response and a separate time-dependent relaxation function can be combined and subsequently predict equal time dependence across various strains [51], [118], [123], [141]. The basic equation for stress in QLV is given by the Equation 6.4.

$$\sigma(t) = \int_0^t E_t(t - \tau)g(\varepsilon)\frac{d\sigma}{d\varepsilon}\frac{d\varepsilon(\tau)}{d\tau}d\tau \quad (6.4)$$

Where E_t (t) is the reduced relaxation function (time dependent) and g (ε) represents the nonlinear strain dependence (independent of time) [142]. Viscoelastic properties as stress (τ) and strain (ε) are determined by experimental testing, and used in the equation above to obtain values of stress at any time (t).

Despite its great success, the theory is not valid for high stress and strain levels under creep and relaxation loading, respectively [139]. That is to say that when it incorporates low strain rates (0.06-0.75% s^{-1}) the results are satisfactory [143], whereas at higher strain rates (up to 10% s^{-1}) they are more imprecise [144]. These experimental observations ([143], [144]) proved the inadequacy of the QVL theory, proposed by Fung [140] in representing the ligament nonlinear viscoelastic behaviour.

As a consequence, alternative viscoelastic models have arisen, such as the single integral finite strain (SIFS) theory, described by Johnson (1996) with the formulation of the general continuum model [145]. This new theory introduced the ligament representation for finite deformations of a nonlinear viscoelastic material and can be used to model viscoelastic behaviour resulting from large deformations in 3D [145].

Up until now, new theories have been published, as is the example of Pioletti (1998) where a realistic 3D viscoelastic constitutive law was developed [70]. This new model describes the non-linearity of the stress-strain curves and takes into account the strain rate effect in soft tissue. In 2011, Sopakayang presented a model which intended to describe the relaxation, creep and strain stiffening phenomena characteristic of the ligament's parallel-fibred. This model added physical meaning and relation to the micro-structural changes that are associated with creep and relaxation [69].

Through the numerous studies done during the last decades, e.g. [69], [70], [118], [123], [139], [141], [146]–[148] the use of these theories proved quite helpful in investigating the relation between stress and strain in nonlinear viscoelastic domain of soft tissues like ligaments and tendons.

7 EXPERIMENTAL WORK

7.1 PREVIOUS APPROACH

Previous papers that studied mechanical properties through mechanical testing have already reported difficulties during the ligaments' clamping. A pioneer on this field was Kennedy et al. who published results of tensile tests made with an Instron ® machine in 1976. The standard clamps were substituted by manually controlled clamps with coarse serrations (Figure 7-1) in order to minimize tissue slipping [83].

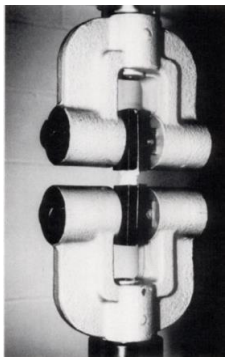

Figure 7-1*- Manually controlled clamps for Instron® machine used by Kennedy et al.*[83].

Therefore, a previous approach of this thesis was based on tensile tests performed for each major porcine knee ligament with three types of clamping: hook (Figure 7-2- a), clamp with serrations (similar to the ones used by Kennedy et al) (Figure 7-2 - b) and clamp with sandpaper (Figure 7-2-c) [149]. The machine used was an Instron ElectroPlus® E1000 with 2 kN load cell. The results of the ultimate load until slippage or partial rupture of each major porcine knee's ligament with each type of clamping are presented in Table 7-1.

(a) **(b)** **(c)**

Figure 7-2 *–Tensile tests performed with porcine knee ligaments using three types of clamping.* ***(a)*** *Hook,* ***(b)*** *clamp with serrations and* ***(c)*** *clamp with sandpaper.*

Table 7-1 *– Recorded ultimate load (N) of the major porcine knee ligaments, according to each type of clamping. From* [149].

	Ultimate Load (N)			
	ACL	**PCL**	**MCL**	**LCL**
Hook	19.3	17.3	40.1	14.0
Clamp with coarse serrations	34.5	77.8	28.1	45.5
Clamp with sandpaper	206.4	468.0	357.6	475.8

The hook method revealed to be the most inappropriate, since the ligaments started to tear on the hook's insertion region, invalidating the test. Moreover, using the clamp with serrations, the bone was crushed and its properties, for instance, tissue hydration, were changed. This is mainly due to the clamp's strength upon the bone and, consequently, the ligament started to tear on the clamped area. Finally, the last method included sandpaper to increase friction between the clamp and the ligament. Despite being the best results achieved, during the tests, it was possible to detect the ligament slippage between the clamps by looking for imprints of serrations on the ligament.

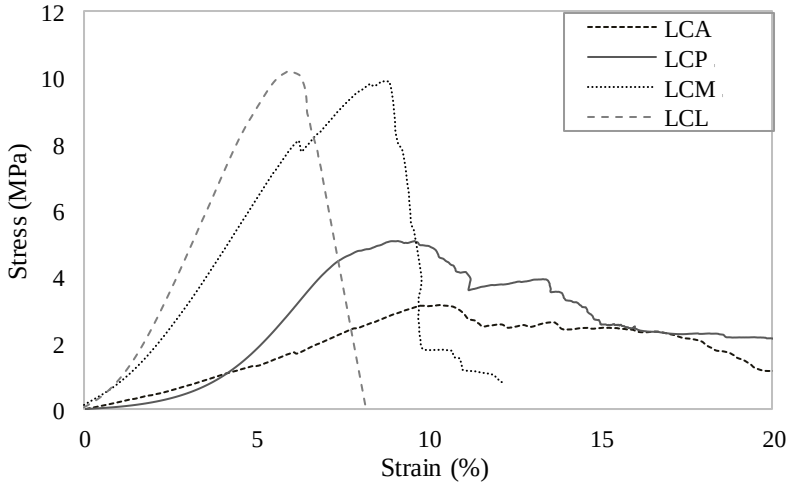

Figure 7-3- *Stress-strain curve obtained from the tensile tests for each major ligament.*

The Young's modulus (in Table 7-2) of each knee ligament was determined from the slope of the elastic region (linear region of the graphic) of each curve from Figure 7-3. In some cases, the acquired stress-strain curve was clearly distorted and the maximum stress achieved was not correct, once the slippage was not avoided. Therefore, the clamps with the same principle as the ones used by Kennedy et al. proved to be inadequate, as the variables were difficult to control. Consequently, a new solution was needed.

***Table 7-2**- Maximum stress (MPa) and Young's modulus of the major porcine knee ligaments, using the clamp with sandpaper, under a slow strain rate* [149].

Ligament	Maximum stress (MPa)	Young's Modulus (MPa)
ACL	3.15	33.3
PCL	5.09	112
MCL	9.92	163
LCL	10.21	224

7.2 CUSTOMIZED CLAMPS

In 1995, a study by Mommersteeg et al. was published, which investigated the effect of the variable relative insertion orientation of the ligaments during knee motion. In order to do that, the bone-ligament-bone complexes were set up in a material testing machine, where bone blocks were embedded in PMMA (Figure 7-4-a) [74]. Later, in 1999, Pioletti et al., analysed the strain rate effect on the mechanical behaviour. To achieve that, bovine knee ACL were used in a custom made device that performs uniaxial dynamical tests. The clamps were specially designed to prevent slippage where, similar to Mommersteeg, the ligament bone insertions were involved with synthetic resin (monomer beracryl) in a mold (Figure 7-4-b) [75].

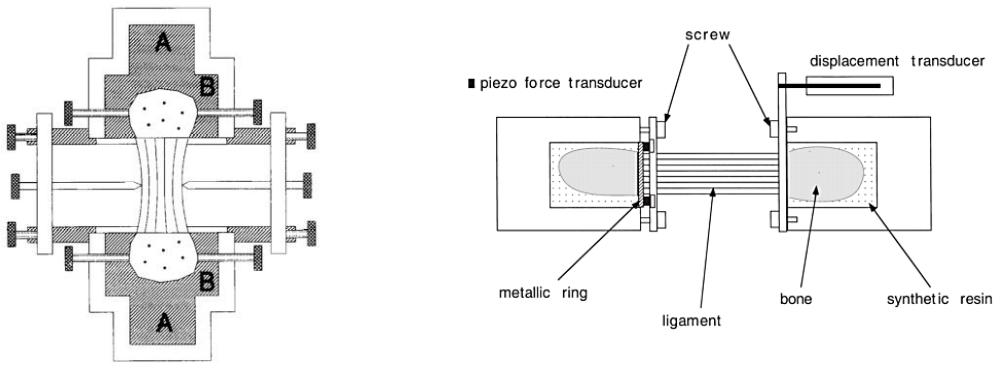

(a) **(b)**

***Figure 7-4**- Scheme of the clamps used by **(a)** Mommersteeg and **(b)** Pioletti. Both schemes use a synthetic resin which embedded the bone insertions of the ligament. In the left scheme* [74]*, screws were used to hold the bone and in the right one* [75]*, a metallic ring was placed between the synthetic resin and the piezo force transducers.*

These type of custom setups show to be very complex with a quantity of requirements that need to be fulfilled, and, consequently, with variables that could adulterate the results. For instance, during the solidification of the synthetic resin, in the Pioletti approach, an exothermic reaction occurs. As a result, there is a need to place it into a freezer in order to minimize the heat effects on the ligaments. In this step, a considerable problem can arise due to the mix of the heat (coming from the reaction) with the cold of the freezer, and, subsequently, the ligaments' properties may also be affected. Therefore, the most probable thing to happen is the bone or the ligament necrosis that will resultantly rupture at a lower tensile strength. In order to overcome these difficulties, a less aggressive mold should be used.

The available Instron® clamps (Figure 7-2– b) were not able to avoid the slippage. Then, the bone-ligament-bone complex was tested on a set of standard clamps in another uniaxial tensile machine (TIRAtest 2705 with a 5 kN load cell) available in INEGI Porto. For the sake of the evaluation of the standard clamp efficacy, porcine knee ligaments were tested and the data acquisition was performed with the suitable program. During the graft positioning, fibre direction was oriented vertically and each bone block was compressed with the standard clamps (Figure 7-5- a). These TIRAtest standard clamps were different at the level of the serrations from the Instron® standard clamps (Figure 7-5-b). It was possible to identify the major facts that have influenced the slippage. Owing to the compression by the clamps, the bone properties were changed and, then, these regions became more propitious to fractures. Moreover, during the specimen collection, there is an inherent difficulty to remove the bone block flawlessly and this can bring about some consequences in the clamping, rising the odds of slippage or rupture in this area.

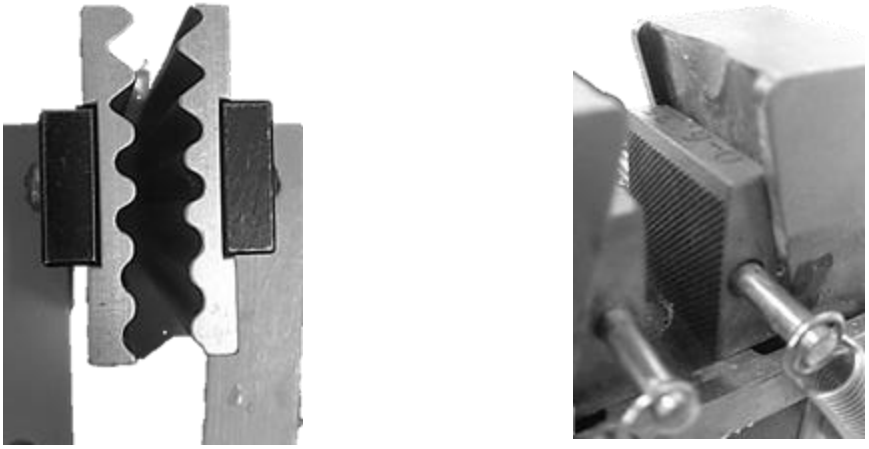

(a) **(b)**

Figure 7-5 – (a) *TIRAtest and* ***(b)*** *Instron® standard clamps' serrations.*

7.2.1 **Clamp Design**

Special clamps inspired in previous studies were designed to improve effectiveness and to prevent any slippage of the specimen. Hence, a 3D clamp was designed using a leader CAD software: SOLIDWORKS®. The clamps design is based on a parallelepiped made of two parts with two round openings on the top and bottom (Figure 7-6).

The upper opening is the docking area in the TIRAtest machine fixed by a pin through the clamp horizontally. The rectangular compartment, similarly to Pioletti's clamp (Figure 7-4-b), is where the bone insertion of the ligament will be wrapped by a polymer. Thus, to do the polymer insertion by injection, a canal through one of the parts was designed. Moreover, two pins were added to drive the clamp's closure in order to ensure the perfect fit. Finally, the whole clamp is closed by five screws, four in the corners and one in the middle[3].

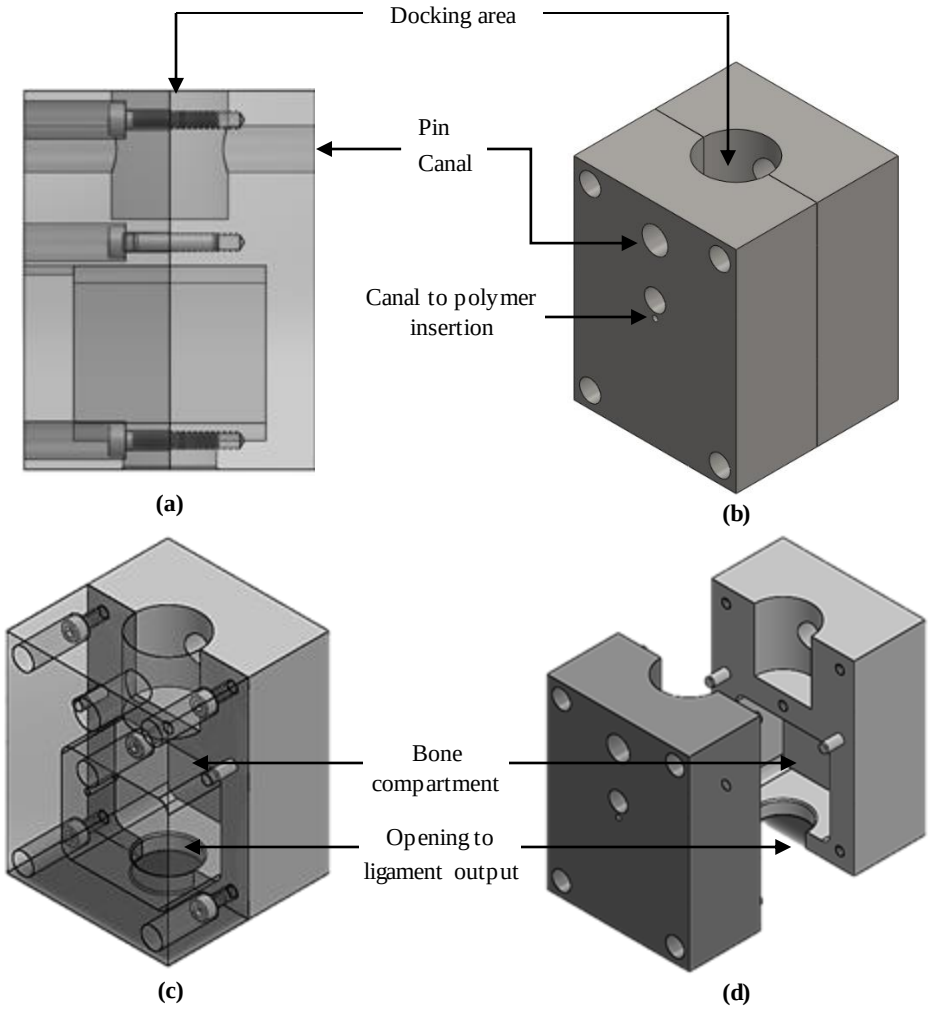

***Figure 7-6- (a)** Lateral and **(b), (c), (d)** isometric views of the customized clamps.*

[3] For more details about the clamp design, consult Annex I.

7.2.2 **Clamp Simulation**

When the technical drawings were completed, using the SOLIDWORKS® simulator, it was possible to foresee the clamp stress and strain under different materials. The tensile stress on the clamp, caused by the tension of the ligament and the mold, was calculated by fixing the pin tunnel and by applying a 5 kN force distributed through the sectional area perpendicular to the tensile test (Figure 7-7).

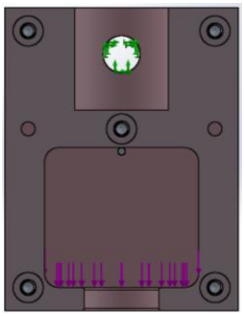

***Figure 7-7**- Boundary conditions of the clamp, simulating the uniaxial tensile test.*

Then, the clamp was meshed by a standard mesh with four Jacobian points consisting of 65295 nodes and 43147 elements.

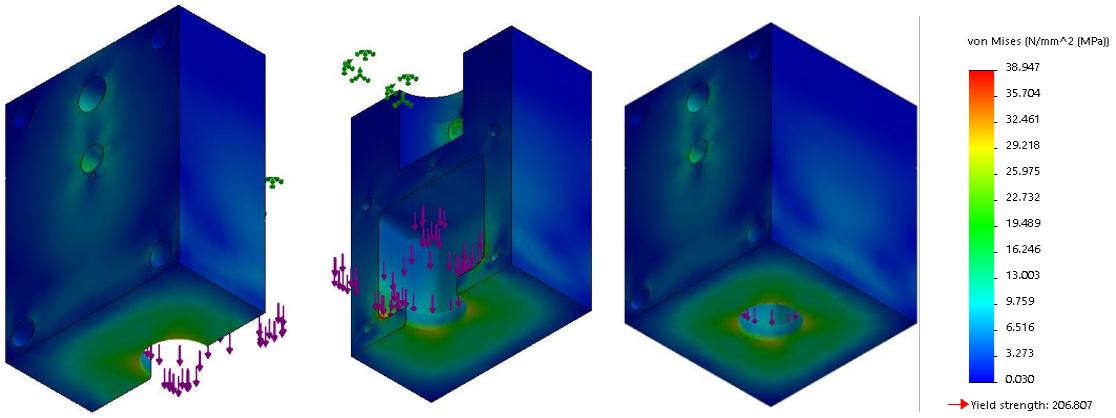

***Figure 7-8** – Clamp simulation yield strength results with steel AISI 304.*

Analysing the simulations results (Figure 7-8), it was possible to understand that the geometry conceived was suitable for the intended outcome. The maximum yield strength observed during a simulated tensile test was 39 MPa, therefore, all the materials with a higher yield strength are suitable for clamp construction.

Since the ligaments are highly hydrated tissues, the choice fell on stainless steel. Thus, an AISI 304 bar with 220x65x25 mm of dimensions was bought and sent to the mechanics manufactory at FEUP. As a result (Figure 7-9), two clamps composed of two parts each were accomplished, made of a stainless steel 304 type.

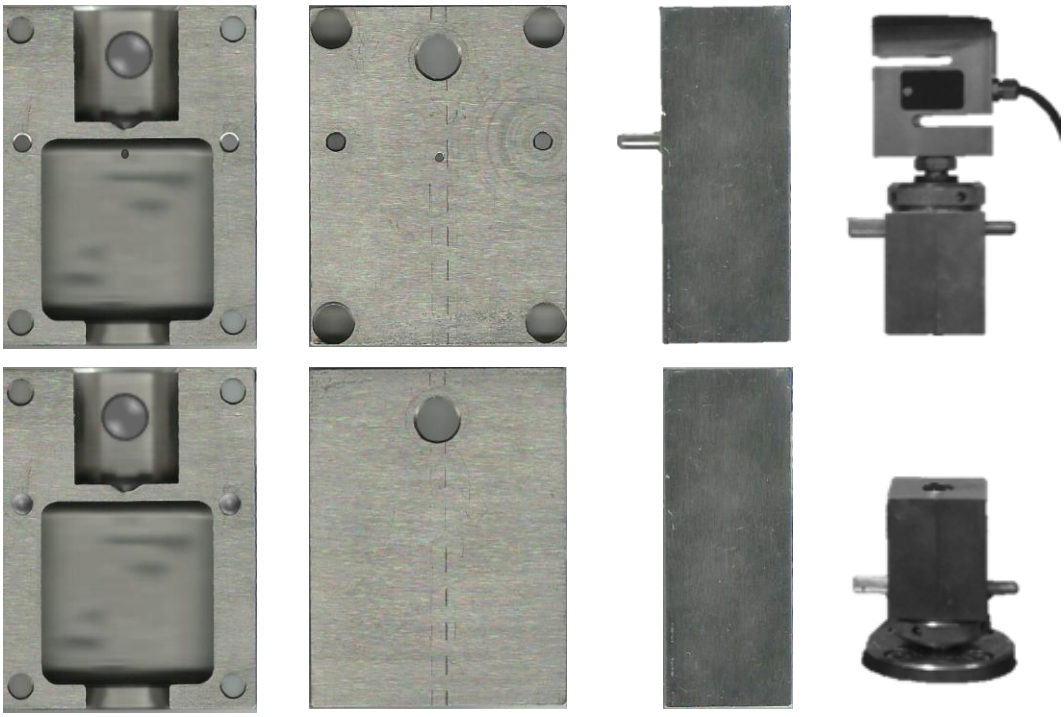

(a) **(b)** **(c)** **(d)**

Figure 7-9- *Final product: Two clamps, four parts:* ***(a)*** *insides,* ***(b)*** *outsides,* ***(c)*** *laterals and* ***(d)*** *set on the TIRAtest.*

7.3 METHODS

7.3.1 **Specimen Preparation**

The mechanical properties characterisation of the major ligaments from the knee were assessed through porcine knees. The similarities of porcine knee ligaments and the human knee ligaments are described in the previous work [149]. During the collection, all the knees were inspected. The ones showing signs of putrefaction were rejected. There was also a preference for knees from young porcine (4-5 months). Thus, 7 fresh porcine knees were collected from the local slaughterhouse. In the end, 7 ACL, 7 PCL, 7 MCL were extracted. There were only 2 LCL available for the mechanical tests, due to damages on the lateral side in the slaughterhouse.

The entire knees were extracted from the porcine limb and transported to São João Hospital in a fresh storage unit. The dissection was performed by a Doctor with suitable tools and at room temperature. After skin removal, muscles, joint capsule and menisci, the different ligaments were isolated as bone-ligament-bone units (Figure 7-10) using cutting tools and a hammer. When the assay occurs within the following 24 hours after the extraction, the samples were stored in an isotonic saline solution (0.9%) at 2°C, whereas, exceeding the period of 24 hours, the samples were stored at -7°C in plastic containers properly identified with isotonic saline solution (0.9%). Note that this procedure does not significantly affect the ligament mechanical properties [82],

[118], [128]. Twelve hours before testing, the specimens were thawed at room temperature within isotonic saline solution (0.9%). The conducted protocol was performed according to the ones proposed in literature [35], [48], [74], [75], [82], [84], [118], [127]–[131].

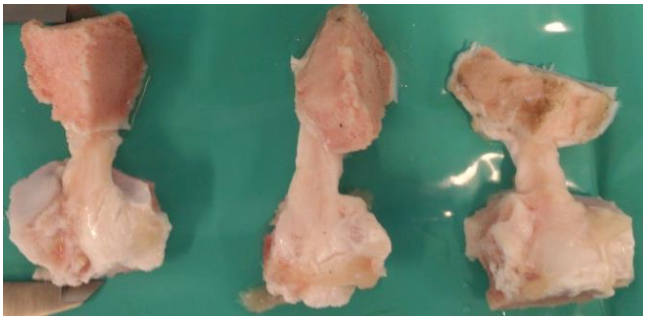

Figure 7-10 *– Bone-ligament-bone specimens prepared for the mechanical tests.*

The samples were prepared and measured with digital callipers before all the mechanical tests. The width was measured at three points of the ligament: proximal, medial and distal. Then the average width was used to calculate the cross-sectional area, which was calculated with the equation that assumes an elliptical geometry [129].

$$Cross\ sectional\ area = \frac{\pi w\, t}{4} \tag{7.1}$$

Where *w* is the width and *t* the thickness. Resorting to the measurements of the ligaments used on this work and on the previous work [149], the means and standard deviations were calculated from the Annex III and registered in Table 7-3. The ligaments were kept moist within an isotonic saline solution (0.9%) through the mechanical testing to avoid drying. All tests were performed at room temperature.

Table 7-3- *Porcine knee ligaments' measurements before the mechanical testing (mean ± standard deviation). Detailed measurements are available in the Annex III.*

Porcine Knee Ligaments	Length (mm)	Width (mm)	Thickness (mm)	Cross-Sectional Area (mm^2)
ACL (n=12)	50.04 ± 3.70	10.10 ± 2.23	4.59 ± 1.09	37.52 ± 15.38
PCL (n=12)	54.49 ± 14.5	11.42 ± 3.66	4.12 ± 0.43	37.74 ± 13.95
MCL (n= 12)	73.80 ± 8.68	12.55 ± 3.93	2.86 ± 0.70	26.12 ± 5.84
LCL (n= 5)	93.74 ± 10.9	12.26 ± 4.27	2.69 ± 0.40	25.83 ± 6.88

The mechanical tests performed were mainly tensile tests with 7 ACL, 7 MCL and 2 LCL. The PCL was submitted to a tensile test with three ligaments and additionally submitted to stress-

relaxation (2 PCL) and creep (2 PCL) tests. In this case, the tensile testing group aims to determine the stress-strain curve of each ligament, allowing to measure the material properties. Moreover, this group will also be used to normalise the stress levels for the stress-relaxation and creep groups. It is known that the ligaments exhibit time-dependence relaxations when subjected to stress or strain. Thus, the stress-relaxation is the measure of the reduction of the stress with time under a constant strain and creep is the measure of increase in strain with time under a constant stress [69], [141], [147], [150].

7.3.2 **Tensile Tests**

Young's modulus and failure stress are useful measurements to compare the material properties of different ligaments. The ultimate load, in the PCL case, was determined to normalise the stress levels for the stress-relaxation and creep groups. Additionally, these material properties measurements are useful input parameters to FE models of human knee joint.

Therefore, one of the aims of this work was to investigate the material properties of the ligaments with the uniaxial tensile test machine (TIRAtest) with the customized clamps. Hence, according to the experimental procedure from an amount of published studies (see at the Annex II), the mechanical tensile tests were performed at a medium and fast velocity: 125 and 500 $mm.min^{-1}$, respectively. Moreover, in the MCL and LCL cases, the results achieved in the previous work at 5 $mm.min^{-1}$ were added [149]. The main goal of comparing the tests at three velocities is to evaluate its effect on the mechanical properties of the ligaments.

***Table 7-4** – Total number of each specimens submitted to tensile test, grouped per type of velocity.*

	5 $mm.min^{-1}$	**125 $mm.min^{-1}$**	**500 $mm.min^{-1}$**
PCL	-	3	-
ACL	-	4	3
MCL	3	4	3
LCL	1	2	-

7.3.2.1 **Protocol**

Following the preparation of the bone-ligament-bone units, they were carefully placed into the customized clamps. Preceding each test, the bone compartment of the clamps were treated with three layers of FREKOTE®, a mold release agent (see data sheet in Annex VI). Between each treatment with the FREKOTE®, it was left to dry for 5 minutes. During the ligament placement into the clamps, a bone block of the ligament was carefully adjusted inside the upper clamp and

was left to hang freely, seeking its own orientation. Then, the lower clamp was applied, with special attention not to twist the ligament and both clamps were closed properly.

In order to fulfil the compartment of the clamp where the bone is placed, the PALAMED®, (see data sheet in Annex V), a quick-setting bone cement, was used. This bone cement, besides having a quick-setting property, also exhibits low viscosity feature, which is ideal for the current situation, since the filling of the clamp's compartment is made through needle injection. The product is obtained by mixing a polymer powder component with a liquid monomer component (Figure 7-11-a). First, the liquid is poured into a metallic bowl, as recommended, and the powder is added next. With a metallic spoon, the mixture was carefully stirred for approximately 30 seconds (s), according to the user instructions accompanying the material (Figure 7-11-b). The bone cement was then inserted into the clamp, with a disposable needle through the proper canal (Figure 7-11-c). While performing this action, saline soaked gauze was used to keep the ligaments hydrated.

(a) **(b)** **(c)**

Figure 7-11 - (a) *Sterile powder and liquid for the bone cement,* ***(b)*** *Colour and texture of the bone cement after mixing and* ***(c)*** *injection with a disposable needle of the bone cement.*

Before testing, the ligaments were preconditioned with 10 cyclic loading between 1 and 10 N at 10 mm.min^{-1} (Figure 7-12). Based on previous studies, the preconditioning was chosen to avoid plastic deformation or damage to the specimen [48], [84], [129], [151]. After preconditioning, ligaments were elongated to failure at two velocities: medium (125 mm.min^{-1}) and fast (500 mm.min^{-1}).

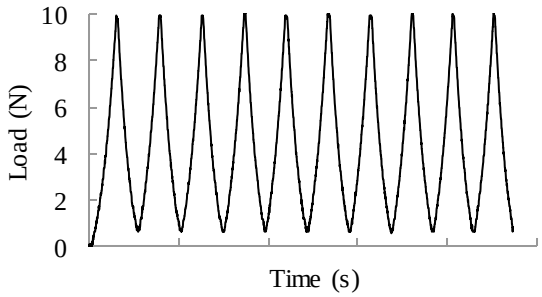

Figure 7-12 *– Schematic plot showing the standard preconditioning for the beginning of all tests.*

7.3.2.2 Results and Discussion

During the uniaxial tensile tests, the ligaments were uniformly stretched as the clamps moved apart at the designated velocity. Overall, the collateral ligaments rupture occurred abruptly, whereas, for the cruciate ligaments, it occurred more gradually, according to the tearing of the bundles. Furthermore, the ligament failure occurred within the range available of the machine's load cell for all specimens. The collateral ligaments used in this study failed within the middle portion of the structure, while the cruciate mainly failed close to the bone insertion. Moreover, no slipping of the ligaments between the clamps was observed in the experimental data. Thus, for each individual, the load-displacement and the stress-strain curves were analysed and displayed after that.

The TIRAtest machine recorded the load and displacement values through time until the point of failure (visible gross disruption of the fibres). The stress was defined by dividing the load by the cross-sectional area, as the strain was defined by dividing the variation of length by the initial length. Each respective measurement of the ligaments is available in the Annex III, where each ligament was labelled by an ID, used in the graphs. For each curve obtained, the Young's modulus was calculated by the slope of the linear region of the stress-strain curve, whereas the stiffness was given by the slope of the linear region of the load-displacement curve.

Figure 7-13- *Bone-ligament-bone complex type used in the customized clamps. In this case, an ACL is displayed.*

The ACL (Figure 7-13) were submitted to mechanical tensile tests at two different velocities, also used by Kennedy et al. [83]. Four ACL were tested to a medium velocity and three at a faster pace. The load-displacement curves obtained for two specimens presented similar trend, whereas the other two showed macro failures after a while, until total rupture. This may be explained by the shorter size of the bundles, which leads to a more gradual rupture with abrupt peaks. Notwithstanding, the stress-strain curves were defined and the Young's modulus and the stiffness were determined.

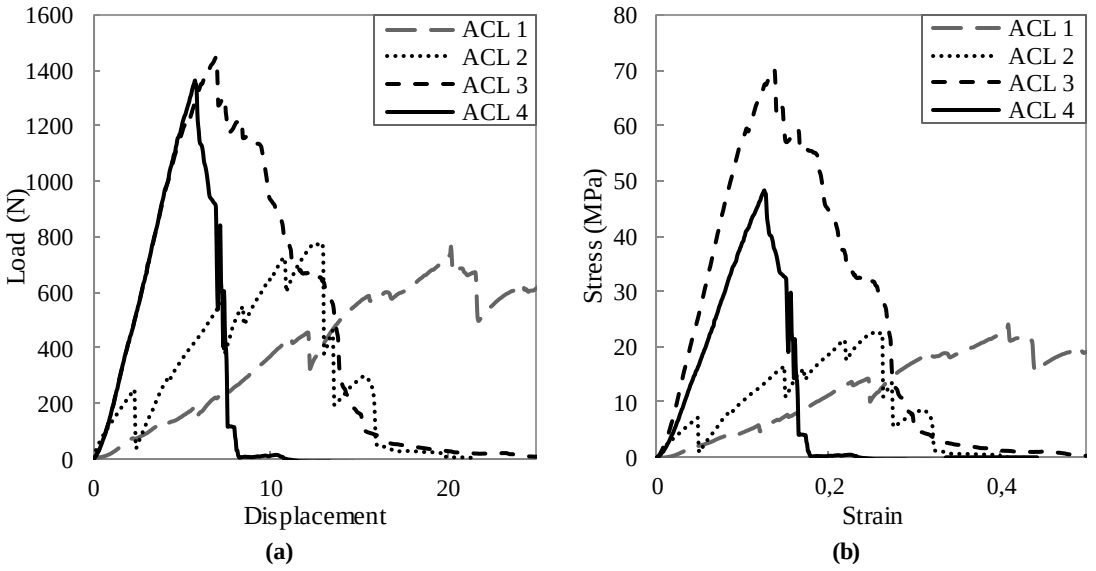

Figure 7-14 - *ACL results at 125 mm.min^{-1}: **(a)** load-displacement curve and **(b)** stress-strain curve.*

At a higher velocity (500 mm.min^{-1}) the stress-strain curves presented similar pattern. Overall ultimate load increased from 1087 to 1347 N. Consequently, as it was expected, the Young's modulus decreased from 340.3 to 270.8 MPa and the stiffness slightly increased from 163.1 to 178.2 N.mm^{-1}, respectively.

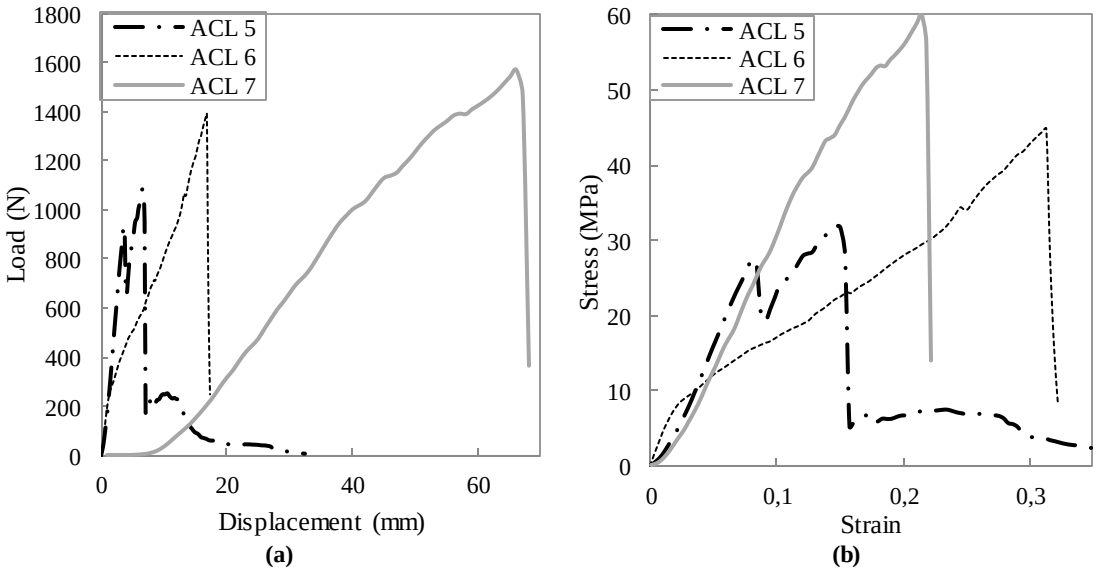

Figure 7-15- *ACL results at 500 mm.min^{-1}: **(a)** load-displacement curve and **(b)** stress-strain curve.*

Comparing Figure 7-14-(b) and Figure 7-15-(b), the failure stress decreased, whereas the ultimate load increased at the highest velocity. Consequently, the Young's modulus decreased with the ACL response of the ligament according to the velocity. Table 7-5 resumes the mechanical properties of the ACL at both velocities, statically analysed and treated.

Table 7-5- *ACL results at 125 mm.min^{-1} and 500 mm.min^{-1} for the young's modulus, failure stress and strain, ultimate load and stiffness (mean ± standard deviation).*

Nº of ACL	Velocity (mm.min^{-1})	Young's Modulus (MPa)	Failure Stress (MPa)	Failure Strain (%)	Ultimate Load (N)	Stiffness (N.mm^{-1})
3	125	340.3 ± 238.7	41.35 ± 22.63	23.10 ± 13.15	1087 ± 371.6	163.1 ± 104.6
4	500	270.8 ± 142.1	45.29 ± 11.71	23.23 ± 11.92	1347 ± 245.6	178.2 ± 114.3

Figure 7-16- (a) depicts a tensile test performed with the PCL, leading to a total rupture near to the bone insertion. Figure 7-16- (b) depicts the opened clamp after the tensile test performed. It is possible to distinguish the effectiveness of the bone cement, wrapping all the bone insertion. Moreover, it also proves the efficacy of the mold release agent, FREKOTE®, in the bone cement removal.

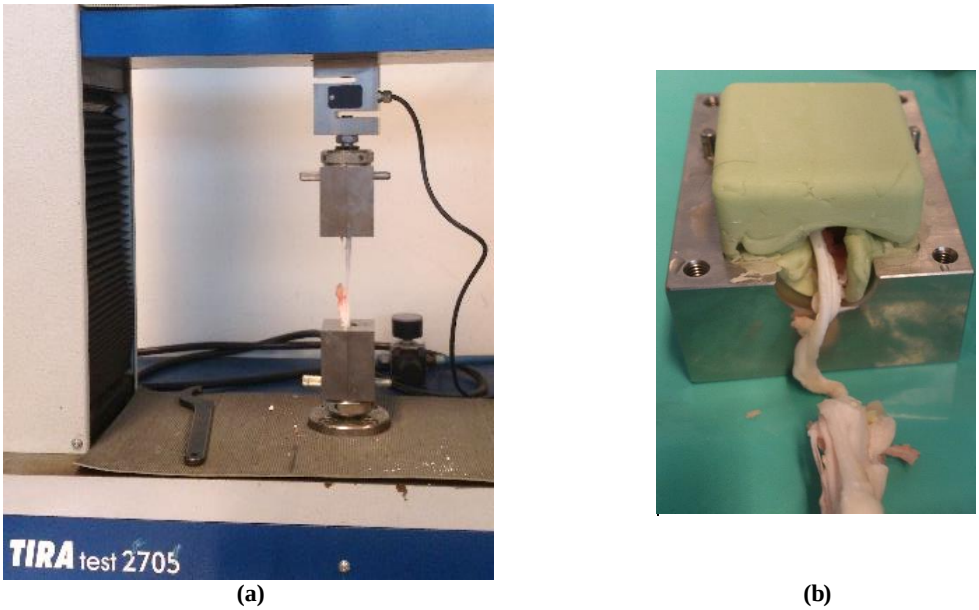

(a) **(b)**

Figure 7-16- (a) *TIRAtest performing the tensile test on the PCL.* ***(b)*** *PCL after the mechanical test, with the clamp opened.*

Regarding the PCL, only three ligaments were tested under the medium velocity. This test, as mentioned before, was performed to determine the mechanical properties under tension in order to normalise the stress levels for the relaxation and creep groups. The results, depicted in Figure 7-17), demonstrated a general trend, except the PCL 1, which demonstrated a deviation from the other two. Therefore, the mean was 1460 ± 642.5 N and the ultimate strain was 17.75 ± 2.147 %. These two values are of interest to use in the creep and stress-relaxation tests performed and described further on Section 7.3.3.

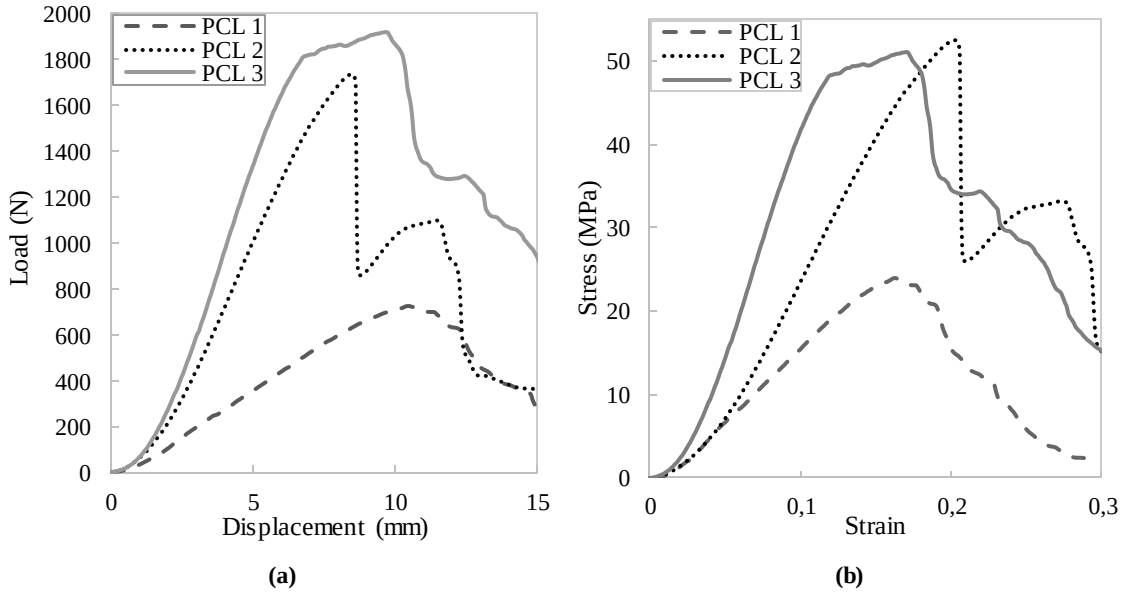

***Figure 7-17** – PCL results at 125 mm.min^{-1}: **(a)** load-displacement curve and **(b)** Stress-strain curve.*

Regarding the load-displacement and stress-strain curves of the PCL, a deviation occurs between them. As the ligaments have different lengths and cross-sectional areas, they present some dispersion and, consequently, have a broader range of values. Table 7-6 resumes the mechanical properties of the PCL statically analysed. Comparing to the ACL, the PCL has similar Young's modulus at the same velocity (340.3 MPa and 347.3 MPa, respectively).

***Table 7-6** - PCL results at 125 mm.min^{-1} for the Young' modulus, failure stress and strain, ultimate load and stiffness (mean and standard deviation).*

Nº of PCL	Velocity (mm.min^{-1})	Young's Modulus (MPa)	Failure Stress (MPa)	Failure Strain (%)	Ultimate Load (N)	Stiffness (N.mm^{-1})
3	125	347.3 ± 174.0	42.49 ± 16.15	17.75 ± 2.147	1460 ± 642.5	228.4±134.2

Following, ten MCL were tested at three different velocities. Besides the medium and fast velocity, a slower velocity (5 mm.min^{-1}) was also added to the group of tensile tests in order to compare with the other velocities [149]. Thus, at a slow velocity, three ligaments were tested (Figure 7-18), four for the medium velocity (Figure 7-19) and, finally, three to the fast velocity (Figure 7-20). The velocities selection aims to investigate the sensitivity of the MCL in a wider range of velocities, and, therefore, measure the mechanical properties of the material. Similarly to the previous studies, the failure stress and strain, stiffness and Young's modulus were calculated by taking the ligament until failure. The MCL responses according to each type of velocity are depicted and defined below.

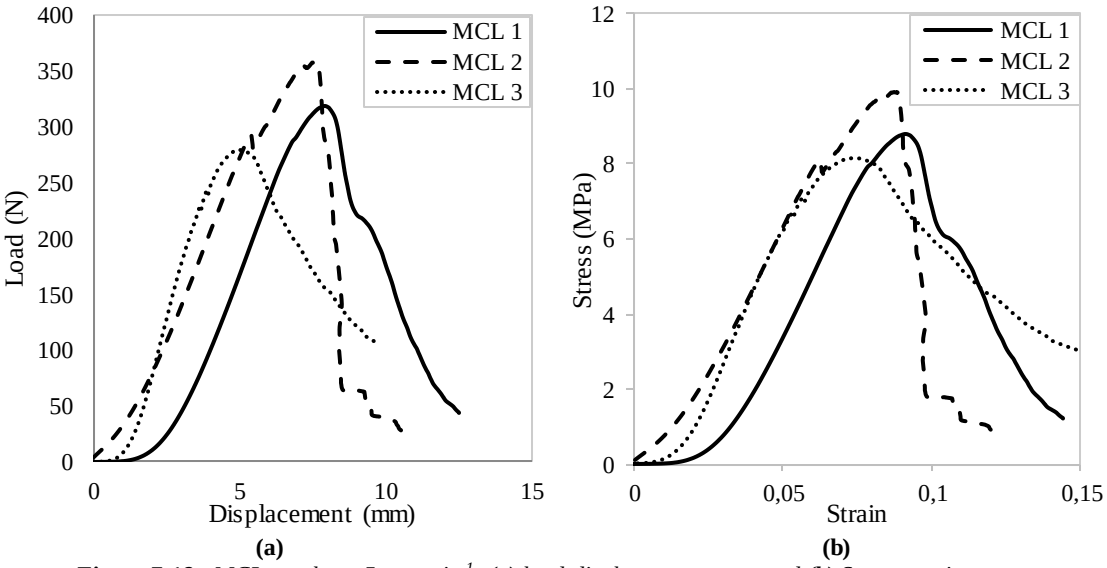

***Figure 7-18** - MCL results at 5 mm.min^{-1}: **(a)** load-displacement curve and **(b)** Stress-strain curve.*

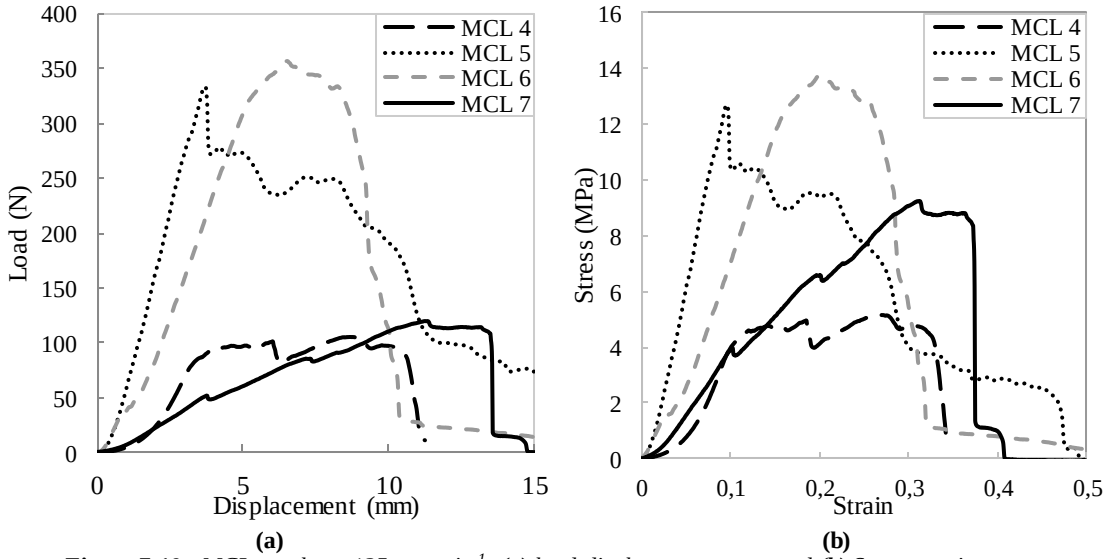

***Figure 7-19** - MCL results at 125 mm.min^{-1}: **(a)** load-displacement curve and **(b)** Stress-strain curve.*

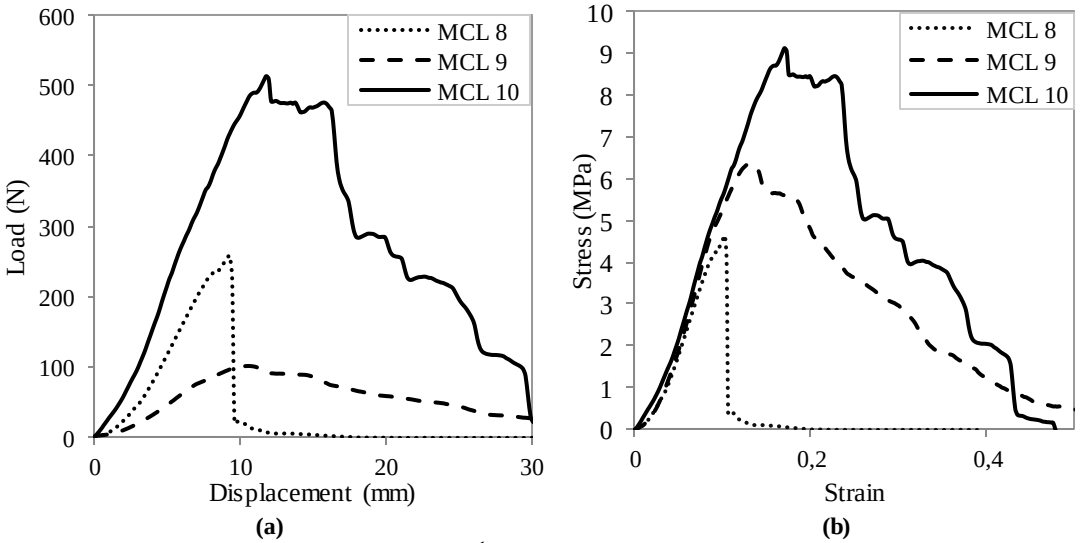

***Figure 7-20** - MCL results at 500 mm.min^{-1}: **(a)** load-displacement curve and **(b)** Stress-strain curve.*

The MCL were the ones which showed the lowest difference in lengths and cross-sectional area between groups of specimens. The MCL results at 5 mm.min^{-1} and 500 mm.min^{-1} presented similar trends, according to the test, for all the specimens, whereas at 125 mm.min^{-1} two ligaments (MCL 4 and 7) displayed irregularities and lower ultimate load comparatively to the other two ligaments. Nonetheless, normalizing with length and cross-sectional area, the stress-strain curve moved closer to the other two.

(a) **(b)** **(c)**

Figure 7-21- *Three examples of the MCL disruption on the middle portion of the ligament in a uniaxial tensile test:* ***(a)*** *and* ***(b)*** *at 125 mm.min^{-1} and* ***(c)*** *at 500 mm.min^{-1}.*

According to the different velocities imposed during the uniaxial tensile test, the ultimate load, failure stress and strain were defined. Consequently, it was possible to calculate the stiffness and the Young's modulus from the obtained curves. Analysing the detailed data at Table 7-7, there is a trend; when the velocity increases, the Young's modulus and stiffness decrease. Contrasting to the cruciate ligaments, the ultimate load is lower, which is in accordance to the data found in literature [63], [83], [86], [152], [153].

Table 7-7- *MCL results at 5 mm.min^{-1}, 125 mm.min^{-1}and 500 mm.min^{-1} for the Young's modulus, failure stress and strain, ultimate load and stiffness, respectively (mean and standard deviation).*

N° of MCL	Velocity (mm.min^{-1})	Young 's Modulus (MPa)	Failure Stress (MPa)	Failure Strain (%)	Ultimate Load (N)	Stiffness (N.mm^{-1})
3	5	168.9 ±14.45	8.920 ±0.9491	8.408 ± 0.8975	318.0± 39.59	75.08 ± 18.83
4	125	85.42 ± 51.75	10.22 ± 3.899	21.96 ± 9.492	228.7± 135.0	28.13 ± 19.95
3	500	66.27 ± 4.777	6.708 ± 2.271	13.44 ± 3.384	291.7± 208.0	35.00 ± 18.73

As mentioned before, due to damages in the lateral part of the knee in the slaughterhouse, only three LCL were in conditions to submit to tensile test. Therefore, only one was analysed at 5 mm.min^{-1} velocity [149], whereas the other two were submitted to 125 mm.min^{-1} of velocity. The load-displacement and stress-strain curves for the LCL 1 and 2 were acceptable, whereas the LCL 3 curves were not suitable after the toe region (Figure 7-22 and Figure 7-23). In both cases (LCL 1 and 2), the ultimate load was up to 250 N.

The Young's modulus and the stiffness were calculated in the toe region for the results at 125 mm.min^{-1}. Thus, comparing the Young's modulus and stiffness, it is observed that, as it is expected, when the velocity increases, the Young's modulus and stiffness decrease, which is in accordance to literature [18], [74]. On the other hand, the failure strain increased, when the velocity increased. The data achieved from the uniaxial tensile tests were statistically treated and displayed in Table 7-8.

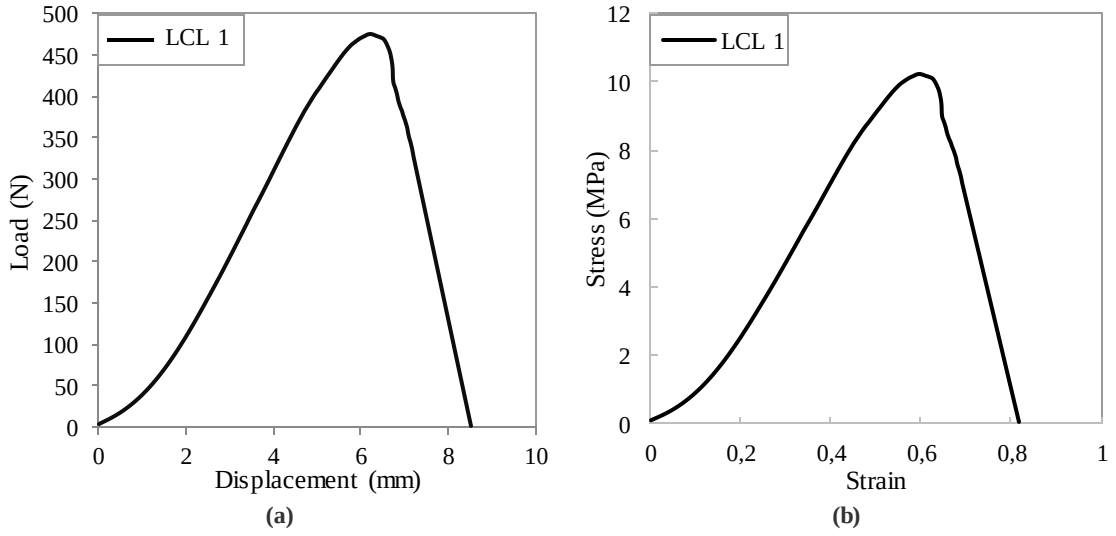

Figure 7-22- *LCL results at 5 mm.min^{-1}: **(a)** load-displacement curve and **(b)** Stress-strain curve.*

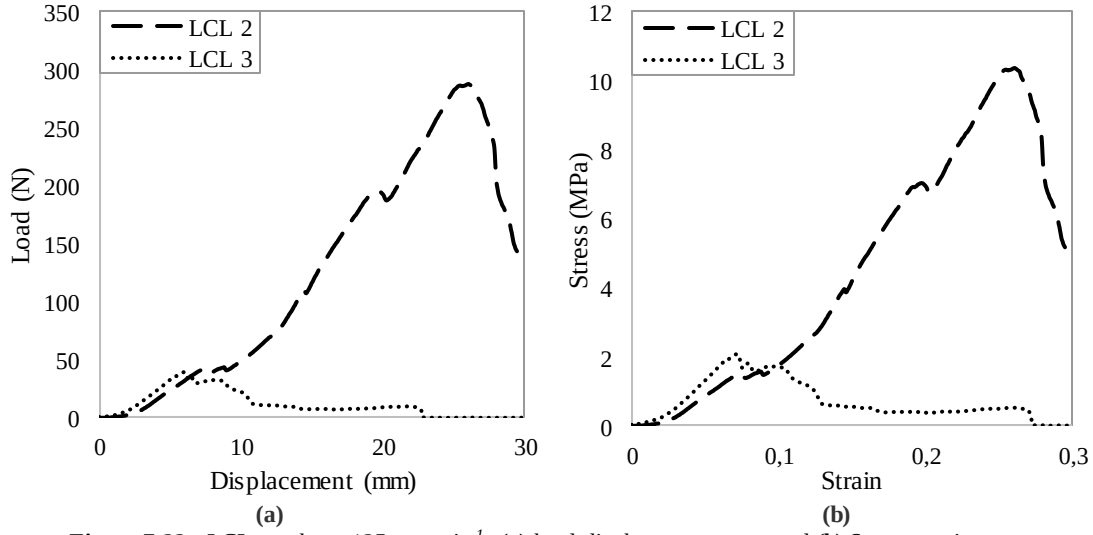

Figure 7-23 *- LCL results at 125 mm.min^{-1}: **(a)** load-displacement curve and **(b)** Stress-strain curve.*

Table 7-8- *LCL results at 5 mm.min^{-1} and 125 mm.min^{-1} for the Young's modulus, failure stress and strain, ultimate load and stiffness, respectively (mean and standard deviation).*

N° of LCL	Velocity (mm.min^{-1})	Young's Modulus (MPa)	Failure Stress (MPa)	Failure Strain (%)	Ultimate Load (N)	Stiffness (N.mm^{-1})
1	5	224.7	10.21	5.980	475.8	96.92
2	125	30.41 ± 4.448	6.225 ± 5.882	16.62 ± 13.33	162.6 ± 175.5	7.534 ± 0.0255

7.3.3 **Creep and Stress-Relaxation Tests**

Ligaments are constantly in vivo exposed to lower stresses than tendons, about 3 to 8 times lower relatively to the ultimate load [154], which may lead to different ligaments' response from tendons and damage at higher stresses [11]. The creep and stress-relaxation tests are two standard experimental tests used to illustrate the viscoelastic, time-dependent and nonlinear behaviour of the ligaments.

The creep test involves subjecting the ligament to a constant load over a period, in which the ligaments' length exhibits a slow continuous increase in strain [11], [69]. The common graph pattern for the creep results is represented by a quick increasing of the deformation up until the load imposed and, then, a progressive, but slower, continue at a low rate.

On the other hand, the stress-relaxation tests involve subjecting the ligament to a constant stretching over an extended period (i.e., the amount of elongation is constant). Therefore, the strain is kept constant over time allowing the stress to vary with time, in order to fulfil the elongation requested [11], [155]. The common graph pattern achieved in a stress-relaxation test is a first quick decrease of the load and then more slowly until stabilization.

When this type of tests are cyclically performed, the increase in strain gradually becomes less pronounced for the creep and for the stress-relaxation tests it is expected that the decrease in the stress gradually becomes less pronounced during an extended period [11]. This is what will be tested and investigated.

Two PCL were tested for cyclic creep deformation at maximum (peak cycle) stresses equal to 5% of the ultimate load and at a minimum stress of 50% of the maximum peak (see Table 7-9). This settings of the test intends to avoid structural damage to the tissue. Each step was applied with a constant rate of 0.5.s^{-1} for approximately forty minutes and then were taken until the zero load. The ligaments were remained hydrated during the test. This protocol was repeated for all the following tests.

Table 7-9- *Parameters of the creep test. The ultimate load is the one achieved in the tensile tests; Maximum peak is 5% of the ultimate load and the minimum peak is 50% of the maximum peak.*

Ultimate Load (N)	Maximum peak (N)	Minimum peak (N)
1460 ± 642.47	72.98	36.49

Regarding the cyclic stress-relaxation tests, similarly to the creep tests, two PCL were submitted to test at the deformation equivalent to the peak deformation recorded at the tensile test (Table 7-10). The strain rate was $0.5.s^{-1}$, maintaining the ligaments hydrated during the test. This protocol was repeated for approximately forty minutes and then taken until the zero load.

Table 7-10 *– Parameters of the creep test. The ultimate strain is the one achieved in the tensile tests; Maximum peak is 5% of the ultimate strain and the minimum peak is 50% of the maximum peak.*

Ultimate Strain (%)	Maximum peak (%)	Minimum peak (%)
17,75 ± 2,15	0.89	0.44

Following the previous series of tests, the ligaments never showed signals of failure. Therefore, the ligaments submitted to the creep test were then subjected to step strain test (maximum and minimum from Table 7-10). Moreover, the ligaments submitted to the stress-relaxation test were then submitted to a step load test (maximum and minimum from Table 7-9). Thus, the ligaments were taken until the maximum peak in one second, and maintained for 300 s, remaining hydrated. After that the clamps were returned to the minimum peak in one second and the ligament recovered for 300 s. Finally, the ligaments were taken back to the maximum peak in one second and maintained for 300 s. In the end of the test, the load and strain were taken until zero, respectively.

7.3.3.1 Protocol

In contrast to the tensile tests, the creep and stress-relaxation tests were performed with a universal testing machine, an Instron® ElectroPlus E1000 with 2 kN load cell. The clamps used were the ones which presented coarse serrations. In this case, it was not necessary to use the customized clamps, since the range of loads was not critical to occur ligament slippage, and the load cell was sufficient. Moreover, this machine is more precise to perform this kind of tests.

The bone-ligament-bone units were carefully prepared and placed into the Instron® standard clamps. It was necessary to cut the bone to have the thickness of 6 mm (Figure 7-24) to fit into the opening of the clamp. During the placing, the bone block was carefully adjusted inside the upper clamp and was left to hang freely, seeking its own orientation. Then, the other end of the ligament was placed into the lower clamp, with special attention not to twist the ligament and,

finally, the clamps were closed properly. Similarly to the tensile tests, the ligaments were preloaded with 10 cycles between 1 to 10 N at 10 mm.min^{-1}.

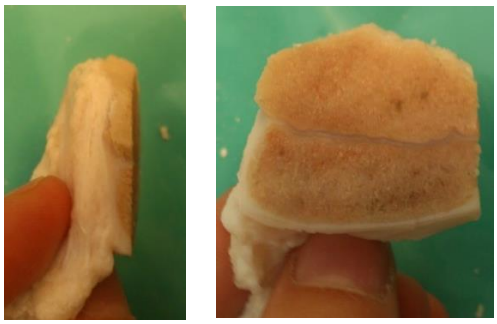

(a) **(b)**

Figure 7-24- (a) *Lateral and* ***(b)*** *interior views of the bone to fit into the standard Instron® clamps.*

7.3.3.2 Results and Discussion

The bone-PCL-bone complex was placed into the standard Instron® clamps (Figure 7-25). Then, the creep tests were conducted with regular loading/unloading cycles between 72.98 N and 36.49 N. The test was interrupted after 2348 seconds, including the time for preconditioning. The Figure 7-26 displays the imposed settings on the creep test.

Figure 7-25 *– Instron® clamps with the bone-PCL-bone complex.*

The results of the ligament response under the imposed creep test are displayed in Figure 7-27 and in Figure 7-28. In both graphics, a quick increase of the deformation up until the maximum peak cycle is found. Then, gradually, there is a stabilization of the deformation for the imposed range of loading. The PCL 4 stabilized at approximately 6% of the strain with a 0.03 % of variance in the last cycle. On the other hand, the PCL 5 has stabilized at approximately 8% of the strain, with 0.04 % of variance in the last cycle. Note that, during the preconditioning, there was an accumulation of deformation of about 0.46% for PCL 4 and 0.74% for PCL 5. After the creep tests, the ligaments showed no damages and, therefore, one more test was conducted for both PCL.

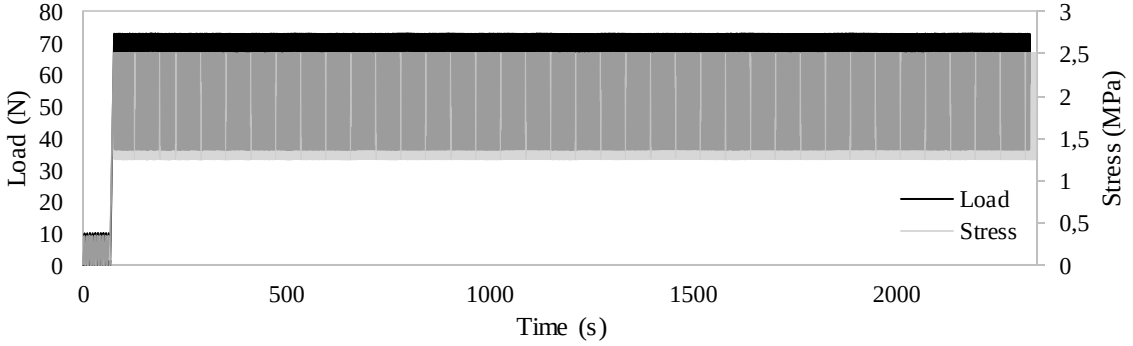

(a)

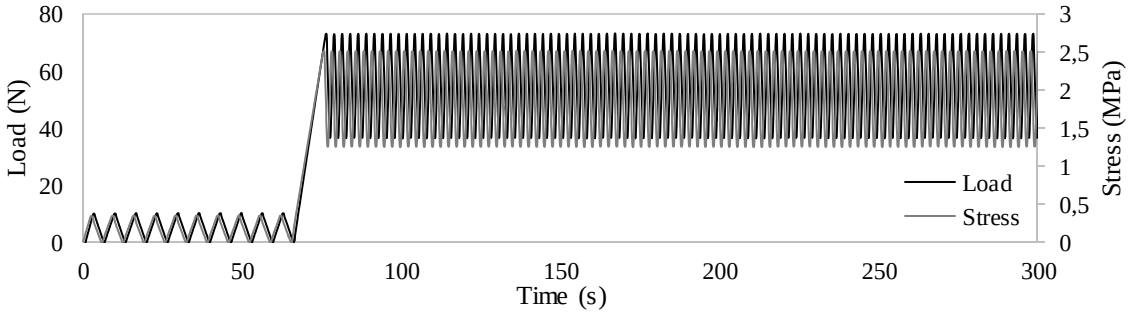

(b)

Figure 7-26*-Creep test imposed in both posterior cruciate ligaments (PCL 4 and 5).* ***(a)*** *Complete and* ***(b)*** *enlarged graph.*

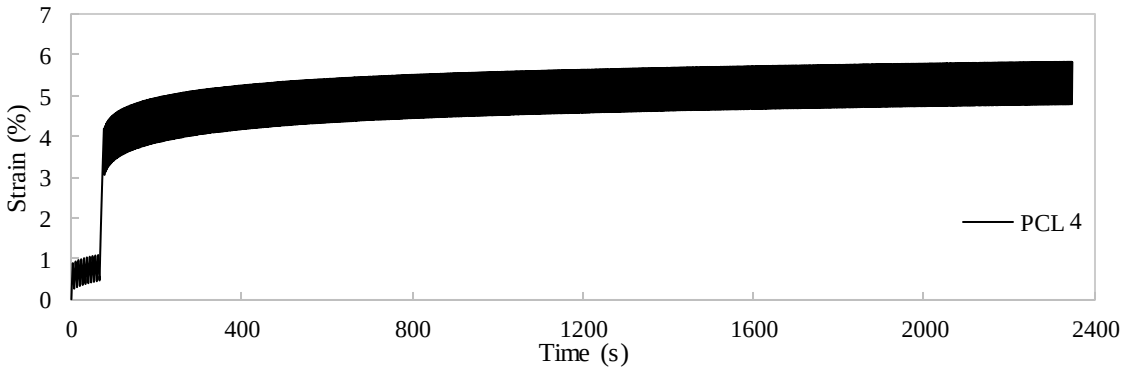

Figure 7-27 – *Response to loading/unloading cycles at 0.5 s^{-1} for a posterior cruciate ligament (PCL 4).*

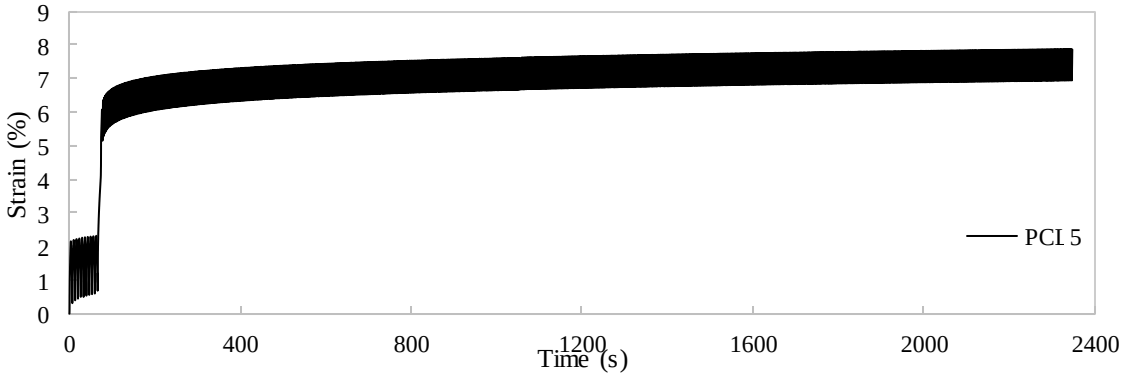

Figure 7-28*- Response to loading/unloading cycles at 0.5 s^{-1} for a posterior cruciate ligament (PCL 5).*

The preconditioning was controlled by load and the step-strain was controlled by strain. Figure 7-29- (a) and Figure 7-30-(a) depict an increase in strain to maintain the imposed load cycles. This behaviour is similar to the creep tests, where, due to the cycles applied, a residual deformation was obtained. Moreover, these variations do not have influence in the subsequent test. The tests were conducted with regular steps at 0.89% and 0.44% with 300 s duration each. Analysing Figure 7-29, the results showed that for PCL 4, the requested stress for the first step was 0.45 MPa (13.0 N of load) with a decay to 0.38 MPa (11.2 N of load). The second step presented an increase of the requested load to maintain the input strain. Starting with 0.12 MPa (3.50 N of load) up until stabilization at 0.15 MPa (4.30 N of load). Finally, the last step indicated a decrease relatively to the first step at 0.89%. The step started at 0.42MPa (12.3 N of load) and dropped to 0.38N (11.0 N of load) at a constant strain of 0.89%

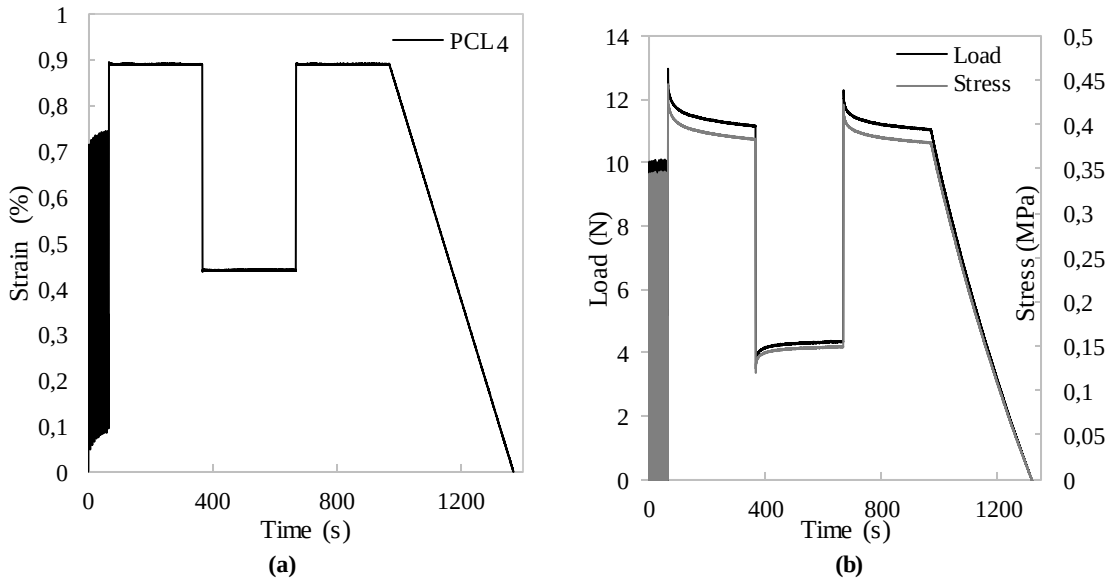

Figure 7-29 – (a) *Imposed step-strain and* ***(b)*** *response of the step-strain test for the PCL 4.*

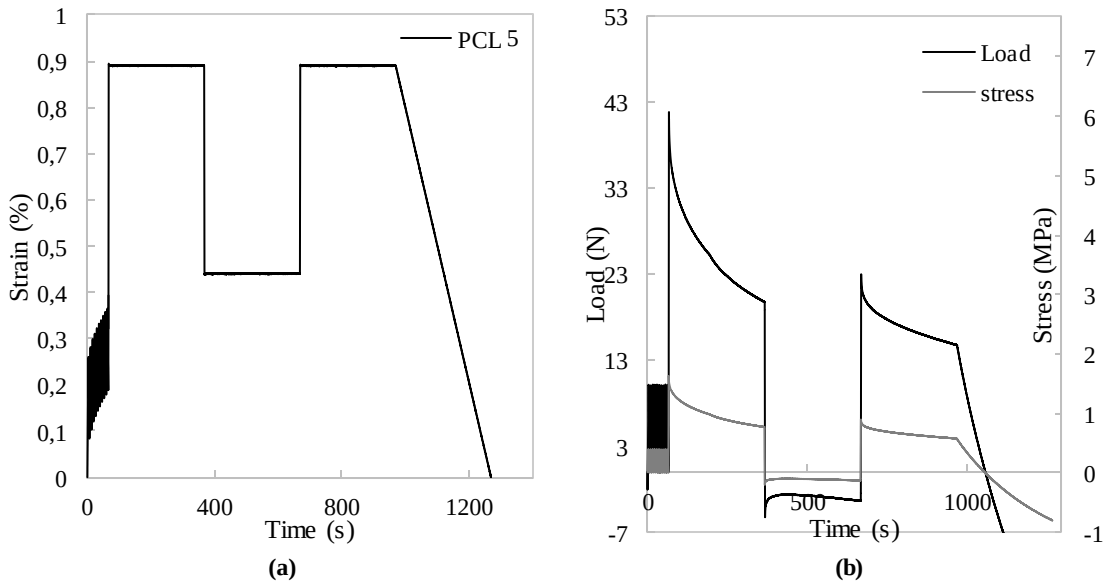

Figure 7-30- (a) *Imposed step-strain and* ***(b)*** *response of the step-strain test for the PCL 5.*

Relatively to the PCL 5, whose results are depicted in Figure 7-30, the slope of the steps is more pronounced. In relation to the first step, it initialises at 1.63 MPa (41.8 N of load) and decreases up until 0.77 MPa (19.7 N of load). The second step extends from -0.17 MPa (-4.32 N of load) to -0.12 MPa (-3.33 N of load). Finally, the last step decreases from 0.89 MPa (22.9 N of load) until 0.57 MPa (14.7 N of load).

The differences between steps of each ligament are presented in Table 7-11. Comparing both results, there are larger declines in PCL 5. This meets the previous results, where the PCL 5 showed a higher strain in the creep cycles imposed. Thus, a trend is revealed according to a ratio. The organic tissues present divergence among the ultimate load and geometries, which have influence on the mechanical characteristics. The ratio mentioned before must thus be investigated in the future in order to normalize the mechanical behaviour under creep and relaxation.

***Table 7-11** – Summary table of the difference between initial and final stress (MPa) according to each step-strain.*

	PCL 4			PCL 5		
Step	**Initial Stress**	**Final Stress**	**Variation**	**Initial Stress**	**Final Stress**	**Variation**
0.89%	0.45	0.38	-0.07	1.63	0.77	-0.89
0.44%	0.12	0.15	0.03	-0.17	-0.12	0.05
0.89%	0.42	0.38	-0.04	0.89	0.57	-0.32

Finally, the last two PCL were subjected to cyclic relaxation tests, where a constant strain was applied over a defined period, and, subsequently, a step-load test was performed. Hence, the ligaments were preconditioned and tested cyclically between 0.89% and 0.44% for approximately forty minutes (Figure 7-31 for PCL 6 and Figure 7-33 for PCL 7). Both ligaments showed a gradual decrease in stress during the relaxation cycles. Thus, in the PCL 6 to fulfil the strain requested, there was a gradual decrease from 0.22 MPa to 0.017 MPa (Figure 7-32). Regarding the PCL 7, the stress decreased from 0.57 MPa maximum peak until 0.27 MPa (Figure 7-34).

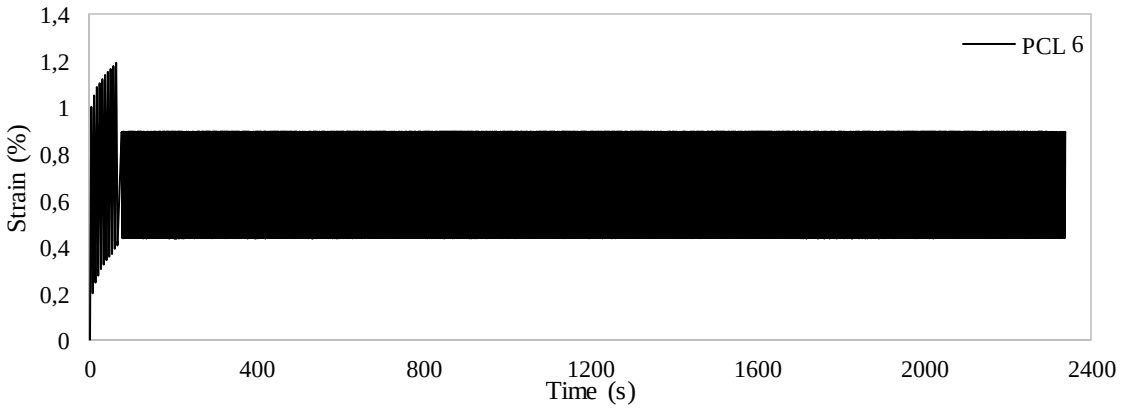

***Figure 7-31**- Imposed cyclic relaxation test in PCL 6.*

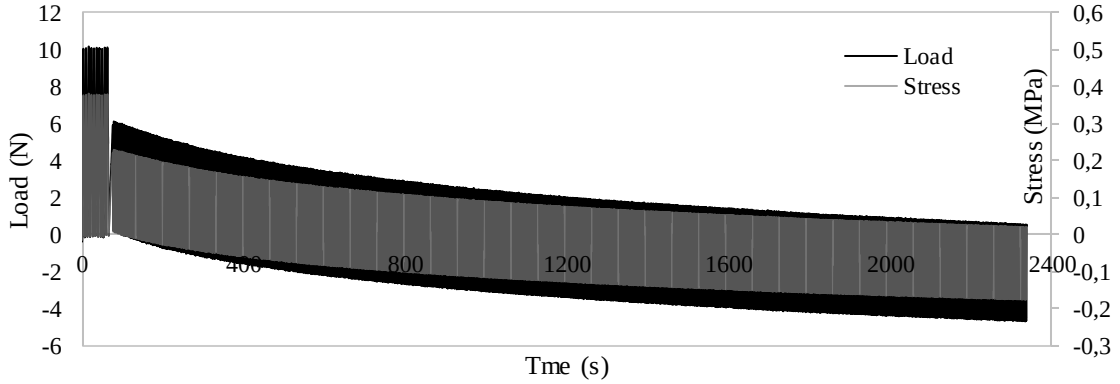

***Figure 7-32** - Response to relaxation cycles at 0.5 s^{-1} for the PCL 6.*

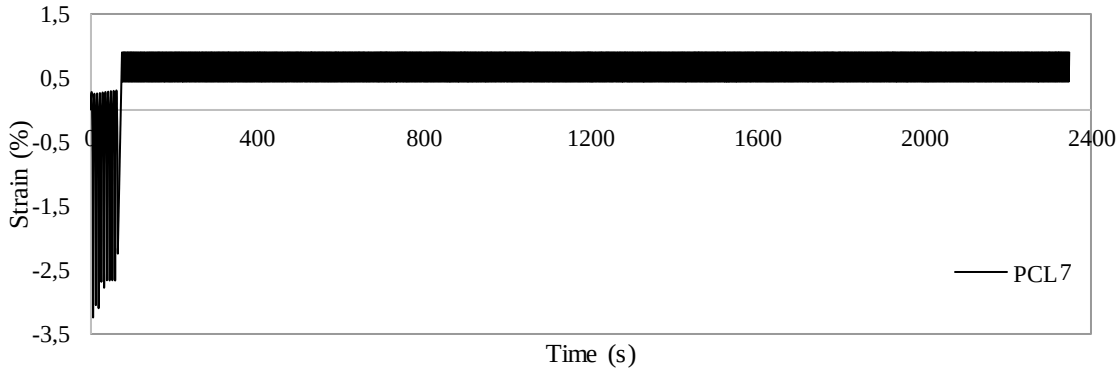

***Figure 7-33**- Imposed cyclic relaxation test in PCL 7.*

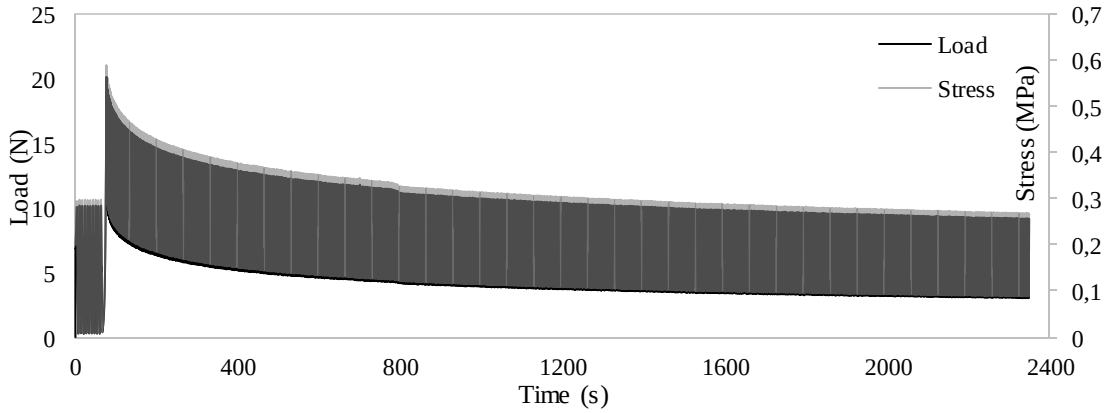

***Figure 7-34**- Response to relaxation cycles at 0.5 s^{-1} for the PCL 7.*

After the relaxation cyclic test, both ligaments did not show any sign of damages. Therefore, they were submitted to a step-load test with three steps: two at 72.98 N and one lower step at 36.49 N. Each step, similarly to the previous tests, were maintained by 300 s. In both results, depicted in Figure 7-35-(b) and in Figure 7-36-(b), there is a gradual increase in load to maintain the steps-load.

First, in Figure 7-35-(b) reveals that the PCL 6 started at 8.14% of strain for the requested load and increased up until 8.82%, whereas, in PCL 7 (Figure 7-36-(b)), it reached lower values,

increasing from 5.50% to 6.08%. Subsequently, in the minimum step-load (36.49 N), the variance was minimal. The PCL 6 had a variation of 0.04% between 7.74 % and 7.78%, while the PCL 7 had a lower variation (0.01%), from 5.07% to 5.08%. Finally, in the last step, going back to 72.98 N, there is evidently an increasing of the initial strain in both ligaments, comparing to the first step. Thus, the PCL 6 reached 8.97% of initial strain, 0.83% higher than the first step, finishing off with a maximum strain of 9.19%, 0.37% more than the maximum strain obtained in the first step. Regarding the PCL 7, there is a similar trend in the patterns relatively to the PCL 6. The initial strain for the third step presented a 0.59% value higher than the initial strain required in the first step. Thus, the third step ranged from 6.09% to 6.29%, finishing off with 0.11% higher than the final strain in the first step.

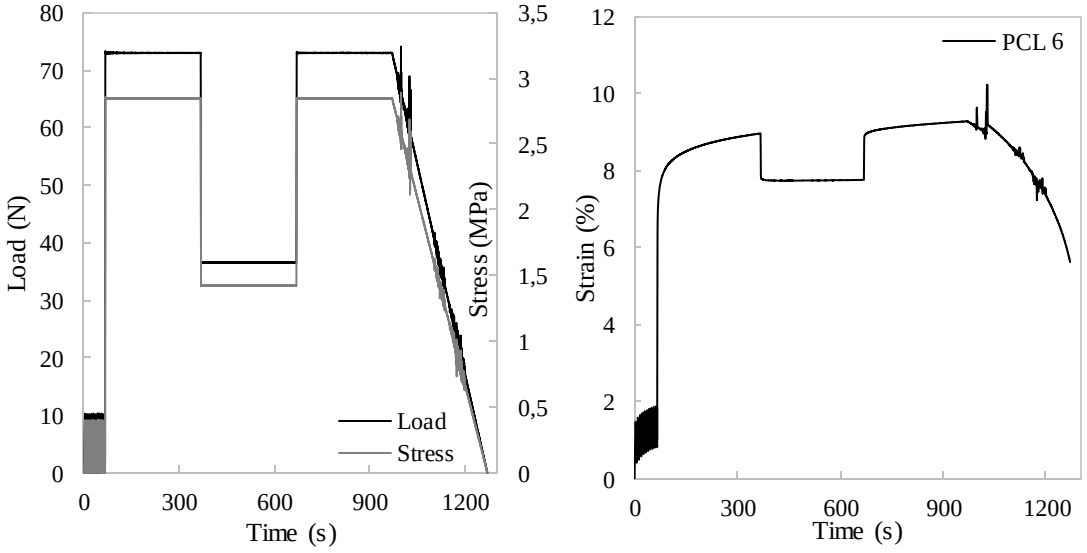

Figure 7-35-(a) *Imposed step-load and* ***(b)*** *response of the step-load test for the PCL 6.*

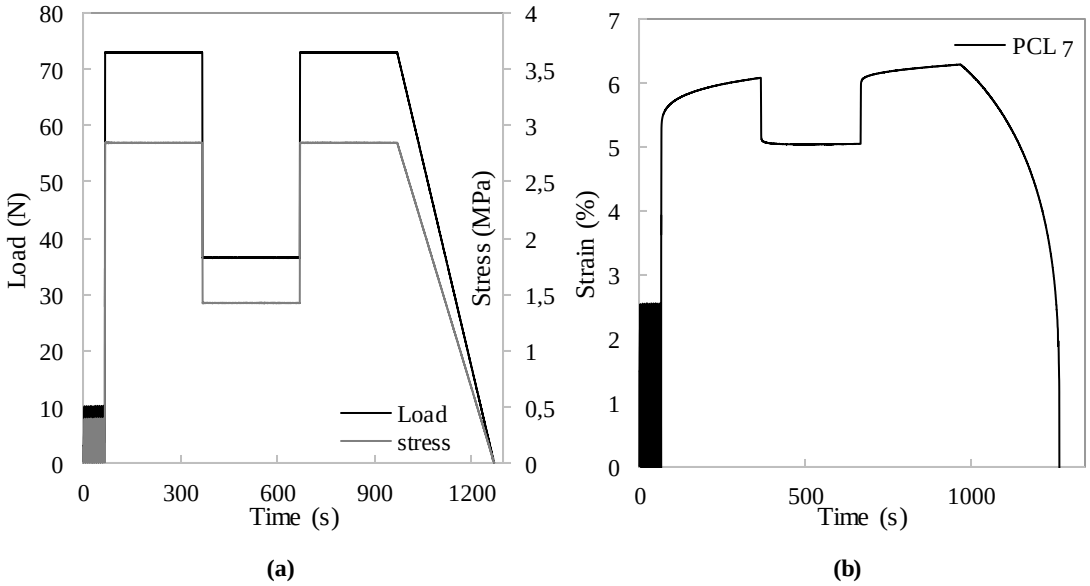

Figure 7-36-(a) *Imposed step-load and* ***(b)*** *response of the step-load test for the PCL 7.*

The differences between steps are presented in Table 7-12. Analysing the data, it is proved that both ligaments display a similar trend. There is an evident increasing in strain during each step in order to maintain the required load. Nonetheless, for the maximum step (at 72.98N), there is a clear decrease in variation with the time evolution. This is explained by the adaptation of the fibres and by the loss of elasticity. Contrasting with the cyclic relaxation tests, the step-load test exhibited consistency with data, since the PCL 7 showed a higher stress than the PCL 6 for the same required strain. Thus, for the same load applied, the PCL 7 deforms less than the PCL 6, which is what the data reveals.

Table 7-12- *Summary table of the difference between initial and final strain (%) according to each step-load.*

	PCL 6			PCL 7		
Step (N)	**Initial Strain**	**Final Strain**	**Variation**	**Initial Strain**	**Final Strain**	**Variation**
72.98	8.14	8.82	0.68	5.50	6.08	0.58
36.49	7.74	7.78	0.04	5.07	5.08	0.01
72.98	8.97	9.19	0.22	6.09	6.29	0.20

7.4 OVERALL RESULTS AND DISCUSSION

This section is reserved to analyse the overall response of the knee porcine ligaments. The results were compiled according to each velocity. In the overall, the collateral ligaments were the only analysed at 5 $mm.min^{-1}$ (Table 7-13). Every category of the ligaments were studied at 125 $mm.min^{-1}$ (Table 7-14) and to complete the tensile tests, the ACL and the MCL were also investigated under a faster velocity: 500 $mm.min^{-1}$ (Table 7-15). Moreover, the type of rupture was added to the tables in order to investigate a pattern of ligament tearing under uniaxial tensile tests. It was observed that the collateral ligaments' rupture mainly occurred in the mid-substance, whereas the cruciate ligaments have failed close to the bone-ligament junction.

The collateral ligaments have less fibres density than the cruciate ligaments, thus, this may be the reason why they are more easily ruptured in the middle. On the other hand, the cruciate ligaments are being recognized by their multi-bundle composition, which may explain this type of rupture. Additionally, they have an elliptical shape of the bone attachment, of which, under a uniaxial tensile test, the shorter bundle is the first to tear and it is the closest to the bone-ligament junction.

At the slowest velocity (see Table 7-13), the LCL revealed to have a higher value for the Young's modulus, suggesting to be more rigid than the medial collateral ligament. Also, the ultimate load and the failure stress are higher for the LCL, whereas the failure strain is lower. These values are similar to the results in literature [48], [63], nonetheless, more tests regarding this velocity are required in order to get more conclusive data.

***Table 7-13**- Material properties of the knee porcine collateral ligaments at 5 mm.min^{-1}; (mean ±SD). Type of rupture: BLJ -close to the bone-ligament junction and MS- Mid-substance.*

Ligament	N° of specimen	Young's Modulus (MPa)	Failure Stress (MPa)	Failure Strain (%)	Ultimate Load (N)	Stiffness (N.mm^{-1})	Type of rupture
MCL	3	168.9 ±14.45	8.920±0.9491	8.408±0.8975	318.0±39.59	75.08±18.83	MS
LCL	1	224.7	10.21	5.980	475.8	96.92	MS

Relatively to the major porcine knee ligaments tested at 125 mm.min^{-1} are depicted in the Table 7-14. Similar velocity values have been previously investigated in human, rabbit and porcine by other authors [48], [83], [156]–[158]. The results suggest that the PCL revealed to be the strongest knee ligament, followed by the ACL, whereas, the LCL revealed to be the weakest, which is consistent with previous studies [74], [83], [156].Contrasting the values achieved for the collateral ligaments at 5 mm.min^{-1}, in this case, the most rigid ligament appeared to be the MCL, nonetheless, these relation must be explored. Overall, these results suggest that the viscoelastic properties depend on time and the loading rate. Thus, future tensile tests, combined with microscopic analysis, should be taken into account to a deeper investigation of this behaviour.

***Table 7-14** - Material properties of the knee porcine ligaments at 125 mm.min^{-1}; (mean ±SD). Type of rupture: BLJ-close to the bone-ligament junction and MS- Mid-substance.*

Ligament	N° of specimens	Young's Modulus (MPa)	Failure Stress (MPa)	Failure Strain (%)	Ultimate Load (N)	Stiffness (N.mm^{-1})	Type of ruptur
ACL	3	340.4 ± 238.7	41.35± 22.63	23.10±13.15	1087±371.6	163.1±104.6	BLJ
PCL	3	347.3 ± 174.0	42.49 ± 16.15	17.75±2.147	1460 ± 642.5	228.4±134.2	BLJ
MCL	4	85.42 ± 51.75	10.22 ±3.899	21.96±9.492	228.7±135.0	28.13±19.95	MS
LCL	2	30.41 ±4.448	6.225 ± 5.882	16.62±13.33	162.6±175.5	7.534±0.0255	MS

In order to finalize the tensile studies, the ACL and MCL, the most susceptible to damages, were studied at a faster velocity, which may approach the rates in the mechanisms of injury situation [7], [83], [159]. Both ligaments have decreased the Young's modulus and increased the stiffness and the ultimate load. There is an evident trend according to the increasing of the velocity of the test.

***Table 7-15**- Material properties of the knee porcine ligaments at 500 mm.min^{-1}; (mean ±SD). Type of rupture: BLJ-close to the bone-ligament junction and MS- Mid-substance.*

Ligament	N° of specimens	Young's Modulus (MPa)	Failure Stress (MPa)	Failure Strain (%)	Ultimate Load (N)	Stiffness (N.mm^{-1})	Type of rupture
ACL	4	270.8 ± 142.1	45.29 ± 11.71	23.23 ± 11.92	1347 ± 245.6	178.2 ± 114.3	BLJ
MCL	3	66.27 ± 4.777	6.708 ± 2.271	13.44 ±3.384	291.7 ±208.0	35.00 ±18.73	MS

In conclusion, the results of the creep and relaxation cyclic tests for the posterior cruciate are showed in Table 7-16. The steps were defined by 5% of the ultimate load and strain obtained in the tensile test. To compare both results, the strain and load outcomes expected were calculated. For the creep cyclic test, if we take into account the relaxation cyclic test for the requested peaks, it is expected to achieve 7.1% of max strain. On the other hand, regarding the results of the creep cyclic test, the ultimate load requested for the strain peaks imposed is between 8 and 11 N. It is demonstrated that the results are the awaited, except for the 0.50 N obtained in the relaxation cyclic test for the PCL 6.

Table 7-16- *Creep and relaxation cyclic test summary. Max strain and load for each step of each PCL (4-7).*

	Creep cyclic test		**Relaxation cyclic test**	
	Load (N) peaks	**Max strain (%)**	**Strain (%) peaks**	**Max Load (N)**
PCL	72.98 – 36.44	6 – 8	0.89 – 0.44	0.50 – 9.11

PART III

COMPUTER MODELLING

FINITE ELEMENTS METHOD

STATE OF THE ART

3D FINITE ELEMENT KNEE MODEL

CONSTITUTIVE MODELS ANALYSIS

MECHANISM OF INJURY ANALYSIS

[This page was intentionally left in blank]

8 COMPUTER MODELLING

Nowadays, computational techniques are extremely useful to simulate the biomechanical behaviour of human body parts, individually or as a whole. Therefore, the study of joint mechanics can elucidate their anatomic and kinematic function and further yield information that is really difficult or even impossible to obtain under experimental investigation [2]. Nevertheless, it is important to validate the model with data obtained from the experimental investigation in order to predict extreme physiological conditions, as in the example of high competition sports, in which the knee ligaments are under dangerous conditions.

8.1 FINITE ELEMENT METHOD

A novel approach to display the mechanical behaviour of knee ligaments is computational modelling which may use the finite element method. FEM is a numerical technique by mathematical analysis which allows to predict spatial and temporal variations in stress, strain and contact area/forces [2], [160]. FEM discretises (in a proper manner) a continuum into a set of finite elements. Each of these finite elements is defined by element equations, assuming simple forms of displacement (variation, pattern and profile). Thus, a global problem domain can be solved by a global finite element equation achieved by assembling equations obtained for each element together with concern about the adjoining elements [117], [160]. Many FEM models described by constitutive equations have been suggested to describe the knee's mechanical behaviour [90], [91], [93], [96], [161] and the ligament material's behaviour [2], [89], [117], [124], [148], [162]–[164]. The use of the FEM is exponentially becoming more frequent, allowing the advance of the understanding of a broad range of topics regarding the knee, such as pathologies, injuries, surgical techniques and reconstruction design.

8.2 STATE OF THE ART

In the last few decades, the FEM has been able to provide deep insights on the ligament's mechanical properties, broadening visualisation of strain and stress distributions and enlightening how they affect the structure. On the other hand, it predicts behaviours effectively and provides information that otherwise (for instance, through experimental measurements) would be extremely difficult to obtain. Withal numerical modelling is an important tool in qualitative and quantitative assessment of the biomechanical behaviour of the knee components. This section is subdivided according to the focal point of each study. It concerns computer modelling studies on the knee as structure (including bones, menisci, cartilage and ligaments), and on the ligaments alone (either as individual units or including bone structures), multi-bundle ligament, and reconstruction models. Each study has different assessments and purposes, and the most interesting ones will be described further along in the following sub-sections.

8.2.1 **Knee Modelling**

In this sub-section, some three-dimensional finite element studies of the human knee are presented. These studies include bone structures, ligaments, cartilages and menisci. Overall, the bones are considered to be isotropic rigid bodies [2], [45], [90], [165], [166], whereas soft tissues are considered elastic, hyperelastic or viscoelastic materials.

Li, Gil, Kanamori et Woo (1999) presented a 3D FEM tibiofemoral joint model of a human knee validated using experimental data achieved by a robotic/universal force-moment sensor. The aim was to demonstrate the accuracy of the prediction of kinematics and forces in knee models. In this model, the ligaments were represented by their functional bundles and modelled by a force-displacement relationship in a nonlinear spring element. The methodology used in this study can be useful to calculate the forces of individual ligaments and contact pressure of the cartilage under normal activities. Nonetheless, the menisci might not be suitable to simulate the function with the same degree of precision. This model was used as a step toward the development of more advanced computational knee models and is believed to be a useful tool for further analysis of knee joint function [90].

In Peña, Calvo, Martínez et Doblaré (2006) a complete 3D FE model of the healthy human knee was suggested, including all the relevant structures, bones and soft tissues. The ligaments were modelled as transversely isotropic hyperelastic, acknowledging the effect of one family of fibres. They were pre-tensioned in an initial position. Using experimental and numerical data available in literature, this model was validated despite some limitations that are implicit in the paper. The main goal of this study was to analyse load transmission and stability in the combined behaviour of ligaments and menisci. The results were compared to published data from other

authors and demonstrated the model's good performance and accuracy. The kinematic results revealed to be strongly dependent on the distribution of initial strains. Further research will be needed on how different joint angles modify the contact areas in the menisci and the stresses in ligaments. This study clearly states the importance of the combined role of menisci and ligaments in the stability of the joint as primary or secondary restrainers [167].

In the Junior, Fancello, Roesler et More (2008) study, the main goal was the construction of a 3D computational knee model in order to obtain information from the major ligaments by simulating joint kinematics, mainly during knee flexion. As result, a 3D model of a knee was achieved with kinematic aspects reproduced, compared to data available in literature. It was pointed out that the initial pre-tension and the positioning of the ligaments were relevant variables in the results [161].

Au, Liggins, Raso, Carey et Amirjazli (2010) aimed to properly represent the heterogeneous distribution of bone tissue material properties in a finite element (FE) knee model. In this regard, it was used a new application of an image processing technique to characterise the heterogeneity of bone density using CT image data. This technique was applied to estimate an optimal level of heterogeneity required to minimize computational effort, while maintaining solution convergence. Resultantly, they accomplished a substantial computational time saving of 60% from the application of the new technique to assign bone mechanical properties [96].

The main objectives of Haindong et al. (2012) were to achieve two tibiofemoral joints with special concern for the cortical and cancellous bone. The threshold segmentation method on MRI images was used to distinguish these models. After establishing the two kinds of finite element models, those were subsequently tested by imposing three types of combined load. Finally, based on the FEM results, they were compared by analysis, disclosing the differences between bearing stress of all single material soft tissues and bone tissue as distinguished materials. In conclusion, the study provided techniques and data for definition of tibiofemoral joint material properties during the mechanical analysis of knee motion [92].

Vairis et al. (2013) evaluated the efficiency of a numerical model of a human knee joint with static load cases (knee joint mechanical behaviour in all life conditions and in sports activities) to use for comparison with experimental data presented in literature in order to validate it. Two different studies were implemented for this evaluation. The first study employed linear material properties, while in the second, non-linear material properties were chosen. This twofold methodologies have the purpose to investigate the differences in analysis affected by linear material properties as opposed to nonlinear ones. As conclusions of the the model's behaviour, its responses and differences were analysed, employing the results calculated for the studied load cases as a basis [93].

8.2.2 **Ligament Modelling**

Limbert, Taylor et Middleton (2004) presented an FE model of the human ACL as a transversely isotropic hyperelastic material. According to the authors, this law embodies a reliable representation. The aim of this work was to compare stress and strain patterns with a stressed ACL to the ones attained with a stress-free. Moreover, the simulation results were compared to existing experimental data in order to verify the model. This paper's conclusion was that the ACL has no stress-free state at any flexion angles [168].

Ozkan, Akalan et Temelli (2007) investigated the effects of ligament bundles and articular contacts on knee motion through a simplified 3D tibio-femoral dynamic model. The approach taken for the suggested model has shown to be capable of properties and geometrical modifications that enable the study of bone shape and ligament-related abnormalities of knee kinematics. The results were compared to the ones achieved with a 3D anatomical model based on normal cadavers or found in literature data. In conclusion, this paper illustrates the relation between bundles and the articular structure. It shows that any change in bundle's length or location (for instance, after surgical reconstruction from injury or maltreatment of the related ligaments) may change natural constraints and force the articular structure and, therefore, the knee's behaviour [169].

Zhang, Jiang, Wu et Woo (2008) developed a subject-specific FEM of the human ACL. The model is composed of bony structures and the ACL, which is represented by a transversely isotropic hyperelastic material, concerning the orientation of its fibre bundles. The results showed that the average stress in the ACL was between the ranges of 4.7 to 5.9 MPa, with a peak stress between the ranges of 9.8 to10.9 MPa, which shifted from the PL bundle to the AM bundle as the knee flexed. Future studies are left with the suggestion to use their model to predict ACL stress under other loading solicitations of common activities [89].

For Wang, Hao et Wan (2009) the purpose of their study was to understand the effect of ACL injury on the biomechanical behaviour of the human knee joint. Three cases (intact ACL, partially injured ACL and totally ruptured ACL) were compared under the same load conditions. In this case, the ligaments were assumed to be hyperelastic with the New-Hooker model. In spite of the acquired results, which showed there are several limitations on this model, a quantitative analysis of the effect of ACL injury on the biomechanics of other knee tissues was reported [170].

Zhong, Wang, Rong et Xie (2011) studied the stress changes of LCL at different knee flexions with or without displaced movements. The results showed that the LCL is vulnerable to adduction motion in almost all knee bending positions and susceptible to anteroposterior tibial translation or internal-external rotation at early 30^{o} of knee flexion [171].

Gaolong et al. (2012) studied the effects of posterior cruciate ligament rupture on the biomechanics of other major ligaments. The 3D FE knee model includes all the bony structures

assumed to be isotropic elastic material; Cartilage and menisci were considered to be linear elastic material; whereas, the major ligaments were assumed as transversely isotropic hyperelastic material. This study was conducted at different flexion angles (0^o, 25^o, 60^o and 80^o). The results indicated that the ligaments' tensions significantly changed at 0°and 60° flexion angles and were more sensitive to flexion angles than load conditions. Another important result was that at four flexion angles, but especially at 60°, a larger maximum von-Mises equivalent stress is generated [172].

Wan, Hao et Wen (2013) focused on the effect of the variation in an ACL constitutive model on knee joint kinematics and biomechanics under different loads. The three constitutive models corresponded to an isotropic hyperelasticity model, a transversely isotropic hyperelasticity model with neo-Hookean ground substance description, and a transversely isotropic hyperelastic model with nonlinear ground substance description. It was revealed that the last model mentioned was the best representation of the realistic ACL property by a linear regression between the simulated and the experiment's deformation results [117].

8.2.3 **Preventive Modelling**

Zhang, Liu et Xie (2011) quantified in vivo ACL strain by computer simulation, which includes a marker-based biomechanical model and a skeletal geometry model of the leg. Case studies (jump landing, running and sidestep cutting activities) were conducted to understand ACL injury mechanisms related to sports activities. The simulation results showed that FEM can be extended to increase understanding on the differences in global AM and PL bundle strain related to different sports activities [124].

Mo et al. (2014) is addressed to pedestrian safety, in which the injury threshold of major knee ligaments is investigated by the parametric study of car-pedestrian impact conditions. A complete FEM, including detailed anatomical structures of the lower limb from the hip joint to the toe region, was created for the study case. Moreover, the entire front-end shape of a car model was employed and tested under impact conditions. The simulations were developed regarding the influences of three impact factors (impact heights, locations and velocities). The results provide a deep understanding of the knee ligament injuries of pedestrians in collisions with cars, allowing a faster intervention and treatment [1].

Orsi et al. (2014) investigated which effects of knee joint motion led to ACL injury and other concomitant knee injuries. The ligaments were characterised as transversely isotropic hyperelastic using a 3D FE knee model. As knee joint orientation and tissue failures can present some susceptibility for knee injuries, this was analysed and verified in the results. In conclusion, this study provides a deep understanding of how ligament ruptures occur, as well as the associated concomitant soft tissue injuries. Furthermore, a simplified version of the full 3D model showed

close correlation to the complete model. This is an important achievement, once it drastically decreases the computational time and, therefore, it permits a *quasi*-instant action during a specific injury analysis [173].

8.2.4 **Reconstructive Modelling**

Veselko et Godles (2000) observed the various surgical techniques for reconstruction of the ACL to study graft biomechanics with computer simulation. An important aspect mentioned is that during the reconstruction, the complex structure of the normal ACL must be built into the graft. As a conclusion, the computer simulation of various surgical techniques of reconstruction can be implemented in the field of biomechanics. Their study also showed that the multi-fibre bundle can be used in reconstruction by adjusting the position and orientation of the femoral ACL attachment [174].

Peña et al. (2006) was used as a basis for many subsequent studies. The purpose of this paper was to study the influence of the tunnel angle in ACL graft on the biomechanics of the knee joint. Therefore, a 3D FE model of the human knee was used with different tunnel angles, and the outcomes were compared to experimental data obtained in available literature. The results demonstrated that the angles in the femur as well as in the tibia have different effects, such as laxity or meniscal stresses and strains [175].

Two studies of Zelle et al. (2009 and 2010) examined the posterior cruciate ligament biomechanics and properties on total knee arthroplasty by a prosthetic FE knee model, including a PCL with adjustable properties. They revealed that the PCL balancing is an important surgical aim in knee arthroplasty [163], [164].

Vairis et al. (2010) designed a new device for handling on ligament repair surgery. The intention is to reduce damage of the ligament grafts so that post-surgery complications are minimised. In this paper, the efficiency of the device was evaluated by computer modelling. The results showed that the device suits most of the load requests, but needs further research [116].

Zheng et al. (2011) developed models of the intact knee (not injured) and two reconstructions of the ACL with double-femoral double-tibial tunnel (DF-DT) and single-femoral double-tibial tunnel (SF-DT). The ligament material properties derived from stress-strain curves available in literature. Ultimately, these three models were compared and the study determined that the technique of SF-DT is more suitable, once the results showed the stresses in bone around the tunnel are closer to those registered with the intact ACL [113].

Wan, Hao et Wen (2011) developed a 3D FE knee model, including cartilages, menisci and four main ligaments. The purpose of this study was to investigate the effect of ACL reconstructions (bone-patellar tendon-bone, double and quadruple semitendinosus) on the

biomechanics of knee joint. The study drew attention to the fact that the quadruple semitendinosus graft reconstruction was better than the others, but can only restore ACL function partially [176].

Westermann et al. (2013) simulated the Lachman testing in order to evaluate the effect of ACL reconstruction graft size. Therefore, similar to what is proposed in the present thesis, the OpenKnee project was used to evaluate reconstructions analysing joint biomechanics according to the ACL graft size. The ACL graft was constructed as a single bundle and it was represented as anisotropic (fibre direction-dependent) using the hyperelastic constitutive model introduced by Holzapfel, Gasser and Ogden (HGO). As conclusions of this work, ACL reconstructions showed a dramatic effect of the knee biomechanics as smaller as the graft is [177].

Recent studies of reconstruction are based on materials to replace the ligament. Thus, the studies use the FEM to compare results from the ACL's own biomechanics and properties to the outcome derived from artificial ACL built of different materials. For instance, Bogdan et al. (2013) used a material with super-elasticity, shape memory and corrosion resistance (Nitinol) for further usage in artificial ligament. The results confirmed that stress values are low and the material recovers from such strain [178].

[This page was intentionally left in blank]

9 THREE DIMENSIONAL FINITE ELEMENT KNEE MODEL

9.1 OPENKNEE PROJECT

In this work, a right human knee joint, whose details are in Table 9-1, was used for the construction of a FE knee model made available online by OpenKnee Project [165].

The FE model is achieved by following these steps:

- **Image acquisition** by scanning techniques (for instance MRI or CT);
- Construction of the **geometric model** in a coordinate system;
- **Mesh generation**, with the most suitable shape of elements;
- Elements' **properties** and **materials'** definition;
- Definition of **kinematics, kinetics** and **boundary** conditions;
- Finally, **case simulations** regarding case-specific loading and boundary conditions.

The knee joint was scanned according to three major anatomical planes (axial, sagittal and coronal) by magnetic resonance imaging (MRI) (Orthone, ONI Medical Systems Inc, Wilmington MA) at the Biomechanics Laboratory of the Cleveland Clinic, under the following settings of image technique: a 3D spoiled gradient echo sequence was utilised with fat suppression, 1.0 Tesla (T), repetition time= 30 milliseconds (ms), echo time= 6.7 ms, flip angle=200 deg. The resolution operated was 150 mm x 150 mm field of view, with 1.5 mm slide thickness. Then, a three-dimensional tibiofemoral joint intact model, including femur, tibia, cartilage (femoral and tibial), menisci and the four major ligaments (Figure 9-1) were reconstructed and meshed with an appropriate software [165].

Table 9-1- *Specimen details. Adapted from* [165].

Side	Right
Donor age	70 years
Donor estimated body weight	77.1 kg (170 lbs)
Donor height	1.68 m (5'6'')
Donor gender	Female
Donor cause of death	Pneumonia/cancer

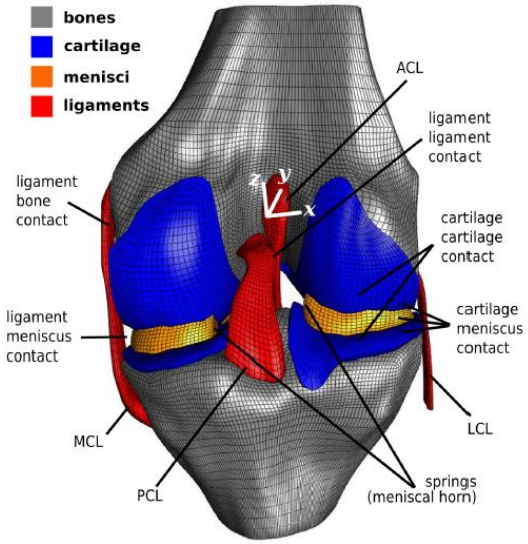

Figure 9-1- *An overview of the open knee project, with highlights on knee components: four major ligaments, menisci, cartilage femoral and tibial, and femur and tibia [174].*

Femur and tibia were assumed to be rigid in this model, so, they were meshed using S4 elements type (only their surface representation was needed). The ligaments were modelled as deformable bodies, and meshed using C3D8 elements (see Figure 9-2). The number of elements and nodes of each body is listed in Table 9-2.

Table 9-2 – *Listing of the number of nodes and elements of each structure.*

Structure	Type	Nodes	Elements
Femur	4 node- Shell section (S4)	13862	13860
Tibia	4 node - Shell section(S4)	11362	11360
ACL	8 node-linear brick (C3D8)	4653	4096
PCL	8 node-linear brick (C3D8)	5922	5248
LCL	8 node-linear brick (C3D8)	7425	6656
MCL	8 node-linear brick (C3D8)	5781	5120

Figure 9-2- (a) *S4 and* ***(b)*** *C3D8 element type used in bone and ligaments representation, respectively.*

This model was not supported by verification and validation studies, hence, it is not trustable for simulation predictions [2], [91], [179]. As far as this investigation is concerned, only the ligaments were harnessed, grasping the opportunity to explore and adjust the model and to compare it to the other ones available.

9.2 KNEE MODEL

Although the OpenKnee model files were from an open-source, it was only possible to edit it with specific software programs. Therefore, the model was generated using the file containing the mesh elements (tf_jont.inp). The mesh file is based on ABAQUS input file format, which is text based and could also be imported into FEMAP. The latter was used as a pre-processor for the finite element analysis and also to allow a better control of the mesh elements. Hence, the model was processed on FEMAP and exported as .inp file. Using ABAQUS standard analysis, the .inp file exported from FEMAP was separated and developed according to the requirements. Overall, it is as if the FEMAP makes the pieces and ABAQUS solves the puzzle.

The available mesh file included all nodes, elements and surfaces set definitions. Nonetheless, this raw file was recognized as one solid model when imported to ABAQUS or FEMAP (Figure 9-3- a). Consequently, the first step was to separate each knee component. In order to do that, a set of layers were created according to each part, in which the corresponding set of elements was saved in. In Figure 9-3- (b) and (c) the results of the FEMAP processing are depicted, with the separated knee's structures.

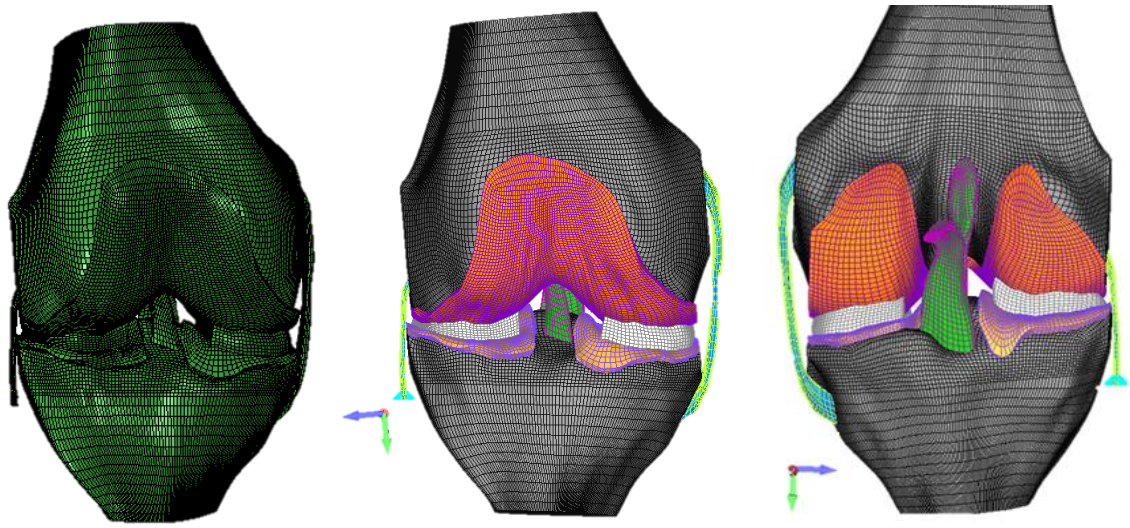

(a) **(b)** **(c)**

Figure 9-3- (a) *Openknee solid model without edition.* ***(b)*** *Anterior and* ***(c)*** *posterior views of the meshed model with all knee components separated in layers. Dark grey – femur e tibia; Green –anterior and posterior cruciate ligaments; Light grey – menisci; Blue and yellow- medial and lateral collateral ligaments.*

Eleven layers were defined for: femur, tibia, right and left tibial cartilage, femoral cartilage, anterior and posterior cruciate ligaments, lateral and medial collateral ligaments, and finally the menisci (medial and lateral). Hence, each component became able to be edited individually. Ultimately, once the model was partitioned, it was necessary to define the connecting regions between components. Twenty-eight connection regions were defined by selecting the corresponding elements. Subsequently, the adjacent faces method was chosen for the selection of faces with the "match normals only" option turned on.

The model exported to the .inp file was separated into different .inp files relatively to each component and connecting region. In the main file (joelho.inp), the parts were assembled concerning all matching files of each component and connection region. Since the ligaments are the main subject of this work, the cartilages[4] and the menisci[5] were removed in order to only focus on ligaments. This way, the model was less complex and the time of solving was lower.

Note that the fibula is not included in the model, and, therefore, the distal nodes of the LCL were constrained using the “encastre” method, holding any movement. Moreover, with regard to the tibia and femur, the rotations and translations were applied in conformity with the activity modelled.

---

[4] The cartilages are the bone covering in a joint, they do not have a direct influence on this type of simulations to evaluate the ligament’s biomechanics.

[5] The meniscus mechanics is a rolling friction thereof with the condyles of the femur, which substantially complicates the problem and provides little information to the simulation.

9.2.1 **Ligament Fibres**

The ligaments are mainly distinct by their histological structure. They are structurally held by a matrix (or ground substance) responsible for the elasticity and by the collagen fibres in charge of the ligament stiffness and strength [60], [180]. The collagen fibre orientation of the ligaments was assumed to run partially parallel to the long axis of the graft, once the typical response of the ligaments is uniaxial tension along the fibre direction [122]. Therefore, to reinforce the matrix geometry, element bar were created to simulate the collagen fibres. One by one, each mesh element was separated and distinguished by different colours and saved on different layers. The cruciate ligaments and the lateral collateral ligaments were divided into six layers, while the medial collateral ligament was divided into five layers. Figure 9-4 left column represents the fibres support/structure elements. Upon each layer, the edge members' method was used to apply the link property and hence upgrade it to the bar property (type T3D2) (Figure 9-4 right column).

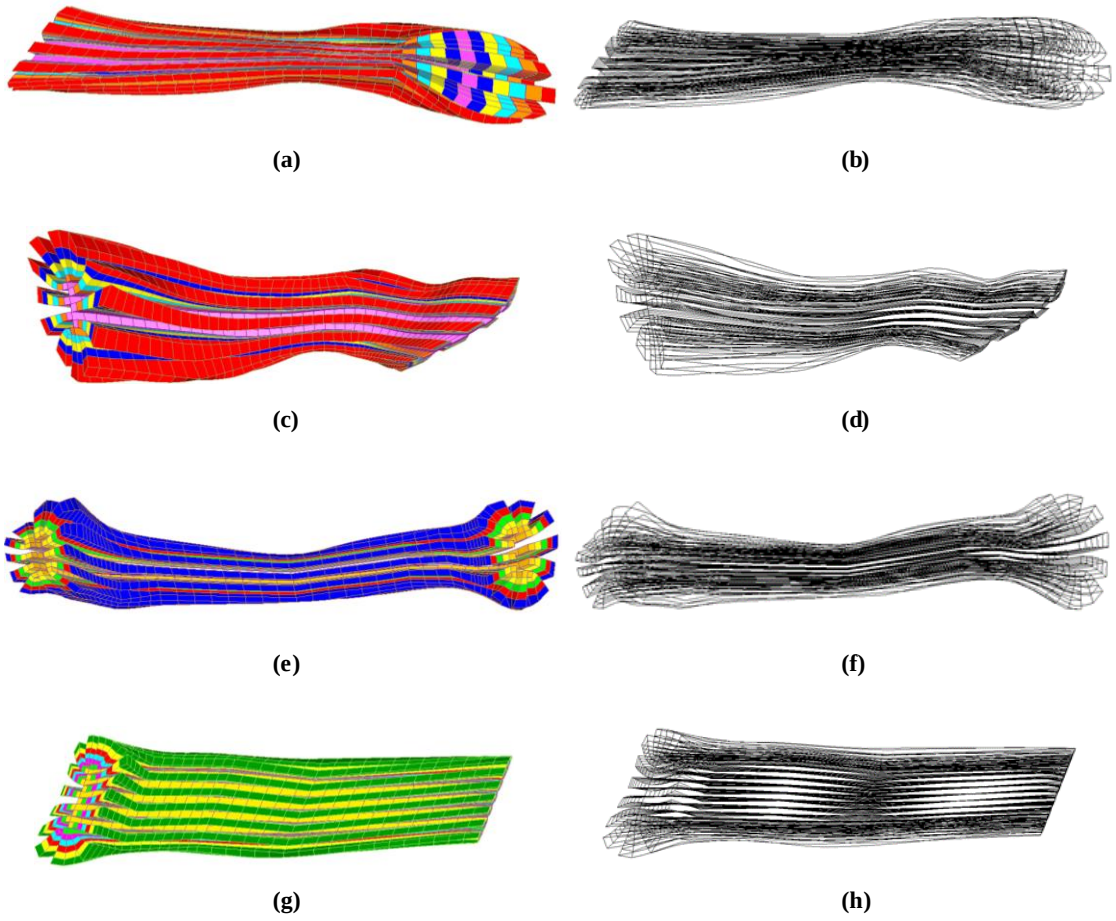

Figure 9-4 *- Illustration of the matrix and fibres selection for* ***(a)*** *ACL fibre structure elements and* ***(b)*** *ACL fibres,* ***(c)*** *PCL fibre structure elements and* ***(d)*** *PCL fibres,* ***(e)*** *MCL fibre structure elements and* ***(f)*** *MCL fibres,* ***(g)*** *LCL fibre structure elements and* ***(h)*** *LCL fibres.*

Each set of fibres was separated into .inp files and imported to the main file. To determine the average radius of the fibres, the following relation was used:

$$\frac{Ligament\ cross\ sectional\ area\ (mm^2)}{Number\ of\ fibres\ \times(\pi \times R^2)(mm^2)} \cong 1 \qquad (9.1)$$

Thus, for each ligament the radius of fibres to cover all the ligament cross sectional area of the matrix was calculated. In Table 9-3 all the concerning values of the ligament fibres are exhibited. Also, Figure 9-5 depicts the ligament fibres with the radius calculated previously for each major ligament.

Table 9-3- *Ligaments parameters of the knee model. Radius and error calculated with the Equation 9.1.*

Ligament	***Ligament cross-sectional area (mm²)[6]***	***Number of fibres***	***Radius (mm)***	***Error***
ACL	12.73	144	0.17	0.03
PCL	30.99	144	0.27	0.06
MCL	24.38	120	0.21	0.09
LCL	11.38	192	0.18	0.07

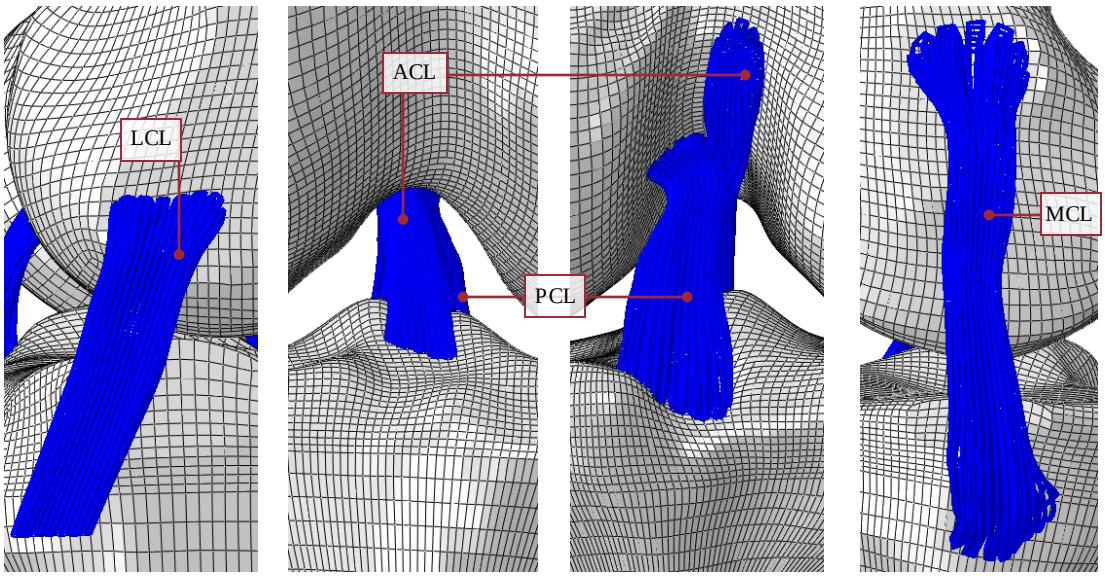

Figure 9-5 – (a) *Lateral,* ***(b)*** *anterior,* ***(c)*** *posterior and* ***(d)*** *medial view of the reinforcing fibres.*

[6] Ligaments measurements of the model available in Annex IV.

9.2.2 **Material Behaviour**

After the FE model reconstruction, the material properties were defined at the main .inp file. The physical and mechanical properties of each model structure are a very important step to obtain reliability of the results, since the characteristics of each component of the model have influence on the behaviour of what is intended to simulate. As described previously in the Section 6.2, the materials are described as linear, non-linear elastic material, viscoelastic material (deformation occurs and the return to the original shape, depends on time) and viscoplastic materials (deformation occurs without return to the original shape, depends on time). The viscoelastic material characterisation that considers the time factor would be the ideal, however, the knowledge about this behaviour is restricted and because of that, the application is limited.

As it has been reported in literature, due to its stiffness compared with the joint soft tissues the bone material was assumed to be a linear elastic and isotropic material with the parameters displayed in Table 9-4 [5], [92], [113], [181], [182].

***Table 9-4**- Bone parameters used to define the bone elasticity.*

Young's modulus (MPa)	Poisson ratio
1700	0.3

The constitutive models of soft tissues are a critical factor in the numerical simulation. Different constitutive models have been developed to describe the ligament material behaviour correctly. Thus, the effect of the variation of some constitutive model on ligament response under joint kinematics will be studied. The constitutive models were investigated in consideration of previous studies: the neo-Hookean [176], Holzapfel, Gasser and Ogden (HGO)[7] [177] and the polynomial hyperelastic constitutive models [5], [183]. Each one was studied concerning the material parameters available in literature. These four ligament representations were compared under a common situation to investigate the effect of the change in the four major ligaments and to compare it with the results available in literature. After revealing the best representative constitutive model, the simulation cases will be conducted.

The neo-Hookean and the polynomial hyperelastic constitutive models represent an isotropic (fibre direction-independent) behaviour, whereas the HGO represents an anisotropic (fibre direction-dependent) behaviour. The material parameters used in the first part of the computer modelling were found in literature and in further comparison of the experimental results. By

[7] Description of the constitutive models in Section 6.2.

analysing Table 9-5, the HGO and the polynomial hyperelastic model parameters were not differentiated for each ligament; However, ideally, they should have been, since, despite being histologically similar, their the location, geometry and mechanical function affect the material properties of each one.

***Table 9-5** – Material parameters for the knee ligaments available in literature.*

Ligaments	**Neo-Hookean (**[167], [176]**)**	**Polynomial hyperelastic n=2** ([5], [183])	**Holzapfel, Gasser and Ogden** [138]
ACL	C_{10}=5.83 MPa, D=0.00683 MPa^{-1}	C_{10}=10.5495 MPa, C_{01}=0, C_{20}=0.499 MPa, C_{11}=126.398 MPa, C_{02}=775.82 MPa, D_1=1.016 MPa^{-1}, D_2=0.00126 MPa^{-1}	Neo-Hookean material coefficients (C_{10}, D) k_1=0.00814 MPa, k_2=0.027.32 MPa, k=0.1444
PCL	C_{10}=6.06 MPa, D=0.0041 MPa^{-1}		
MCL	C_{10}=6.43 MPa, D=0.00126 MPa^{-1}		
LCL	C_{10}=6.06 MPa, D=0.00126 MPa^{-1}		

9.3 CONSTITUTIVE MODELS STUDY

The ligament behaviour will be studied, regarding to the constitutive models mentioned before: neo-Hookean with and without fibres, polynomial hyperelastic and the HGO. Nonetheless, to compare these four constitutive models, a common simulation case needed to be selected. According to Berry [184], a complete gait cycle is divided into two phases: stance and swing (Figure 9-6). In the swing phase, the flexion is between 60°-70°, whereas, for most of the stance phase, it is less than 20°, but increases up until to 45°-55° at toe off [13], [185].

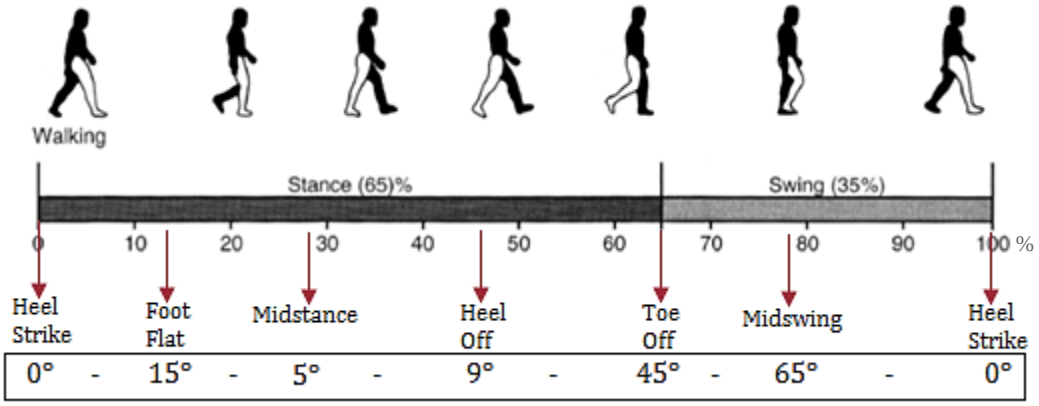

Figure 9-6- *Walking gait sequence. The stance phase is from the heel strike until the toe off, and the swing phase is from the toe off until the heel strike. Image adapted from* [185] *and flexion values adapted from* [13].

Thus, in order to examine the effect of each constitutive model, a region from the normal walking gait sequence was selected from literature [13], [40], [185]–[187]. The flexion was performed at 45° flexion (toe off region) with 2.5° of adduction and 12° of external rotation [13]. The 45° flexion was imposed strategically at the lateral side of the femur according to the rotation along the z axis. Moreover, in femur, 2.5° of adduction was imposed along the x axis. This way, the lack of menisci to control the displacement of the femur was overcome. It was also applied 12° of external rotation along the y axis in the tibia. Then, it is expected that, once the knee is flexed, the collateral ligaments become loose, the ACL relaxes and the PCL becomes tense [12], [155].

The dynamics is present in almost all types of structures, due to the existence of inertial forces being applied at each of its components. However, in certain cases, it is possible to consider that these dynamic actions are applied at substantially low velocity. Thus, in this work it was only implemented static analysis. Moreover, the stress analysis, for all the simulations, the Maximum Principal Stress (S. Max Principal) method was used for the visualization, wherein, the stress mentioned in the results, refer to these maximum stresses.

9.3.1 **Neo-Hookean Model**

In the Section 6.2.2 of this work, the neo-Hookean was mentioned as a simplistic model, that is used as basis for more complex material models. It is more frequently used in the study of ligaments in the matrix definition [89], [117], [188]. The ligament matrix is assumed to be incompressible and isotropic, as a result, the model becomes suitable to represent it. Therefore, the ligaments were modelled with the neo-Hookean model, firstly without fibres and lastly with inclusion of fibres.

9.3.1.1 Without fibres

Under a combination of 45° of flexion, and 2.5° of adduction applied on femur and 12° of external rotation applied on tibia, the stress distribution of the knee ligaments was calculated. The forward figures depicts the results of the neo-Hookean model without fibres representation.

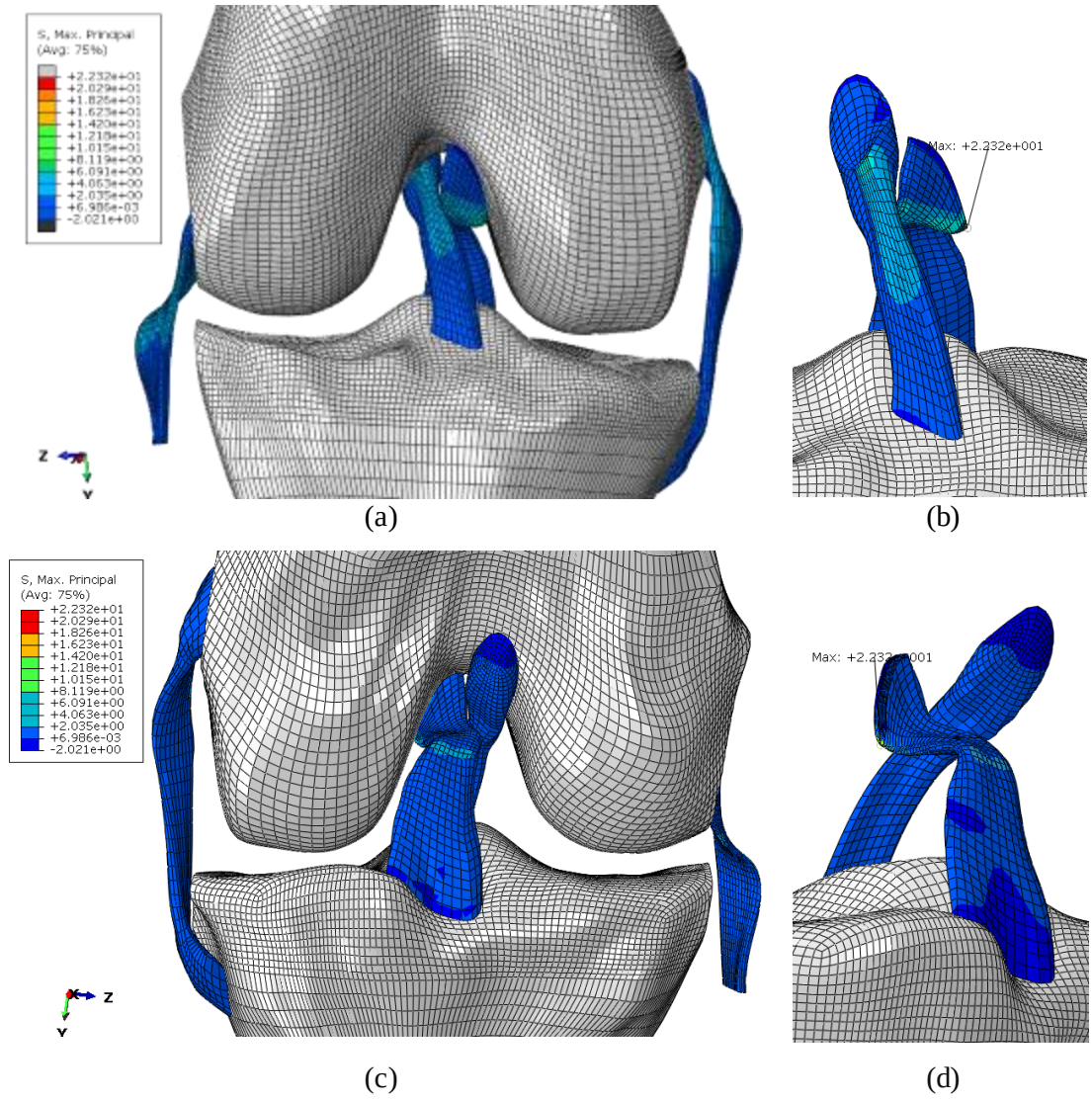

***Figure 9-7** –Neo-Hookean model. Knee under flexion at 45 °, 2.5° of adduction and 12° of external rotation.**(a)** and **(b)** anterior and **(c)** and **(d)** posterior views of the knee joint set and the cruciate ligaments, respectively.*

9.3.1.2 With fibres

Introducing the fibres mentioned in Section 9.2.1 and using the same boundary conditions previously stablished, the results are depicted in the following image. The ligament properties applied in the previous model were used to define the fibres material and the matrix was defined as a neo-Hookean material with baseline parameters C_{10} = 1.95 MPa and D_1 = 0.00683 MPa^{-1} [189].

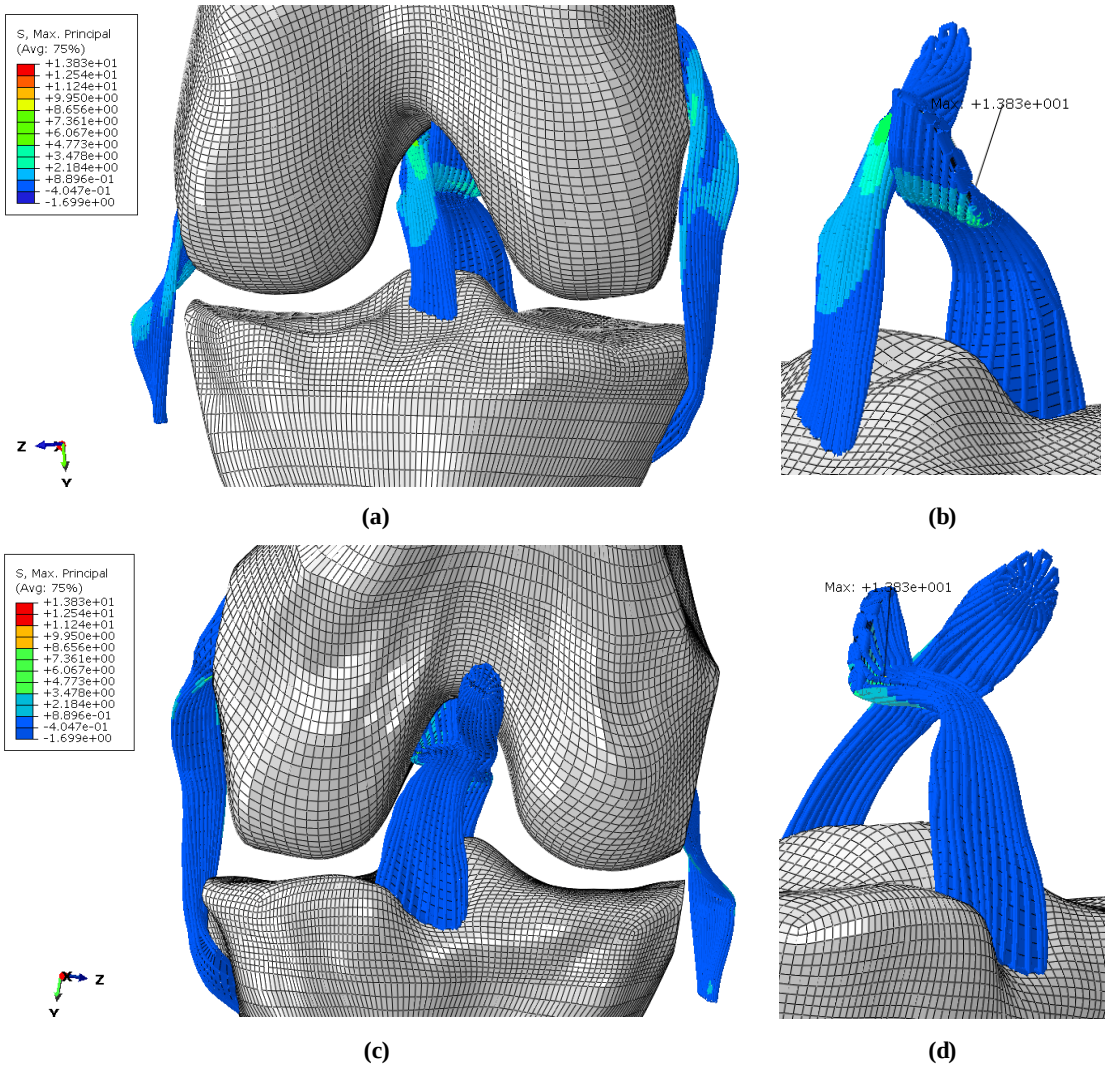

Figure 9-8- *Neo-Hookean model with ligament fibres. Knee under flexion at 45 °, 2.5° of adduction and 12° of external rotation.* ***(a)*** *and* ***(b)*** *anterior and* ***(c)*** *and* ***(d)*** *posterior views of the knee joint set and the cruciate ligaments, respectively.*

9.3.2 **Polynomial constitutive model**

The polynomial hyperelastic constitutive model is a nearly incompressible model. It is an approximation and an adaptation of the transversely isotropic hyperelastic used in Estefania Peña's thesis [5]. This adaptation was also used before in João Carneiro thesis [183]. The boundary conditions applied were the same as previously. The forward figures displays the results in the anterior and posterior views of the knee.

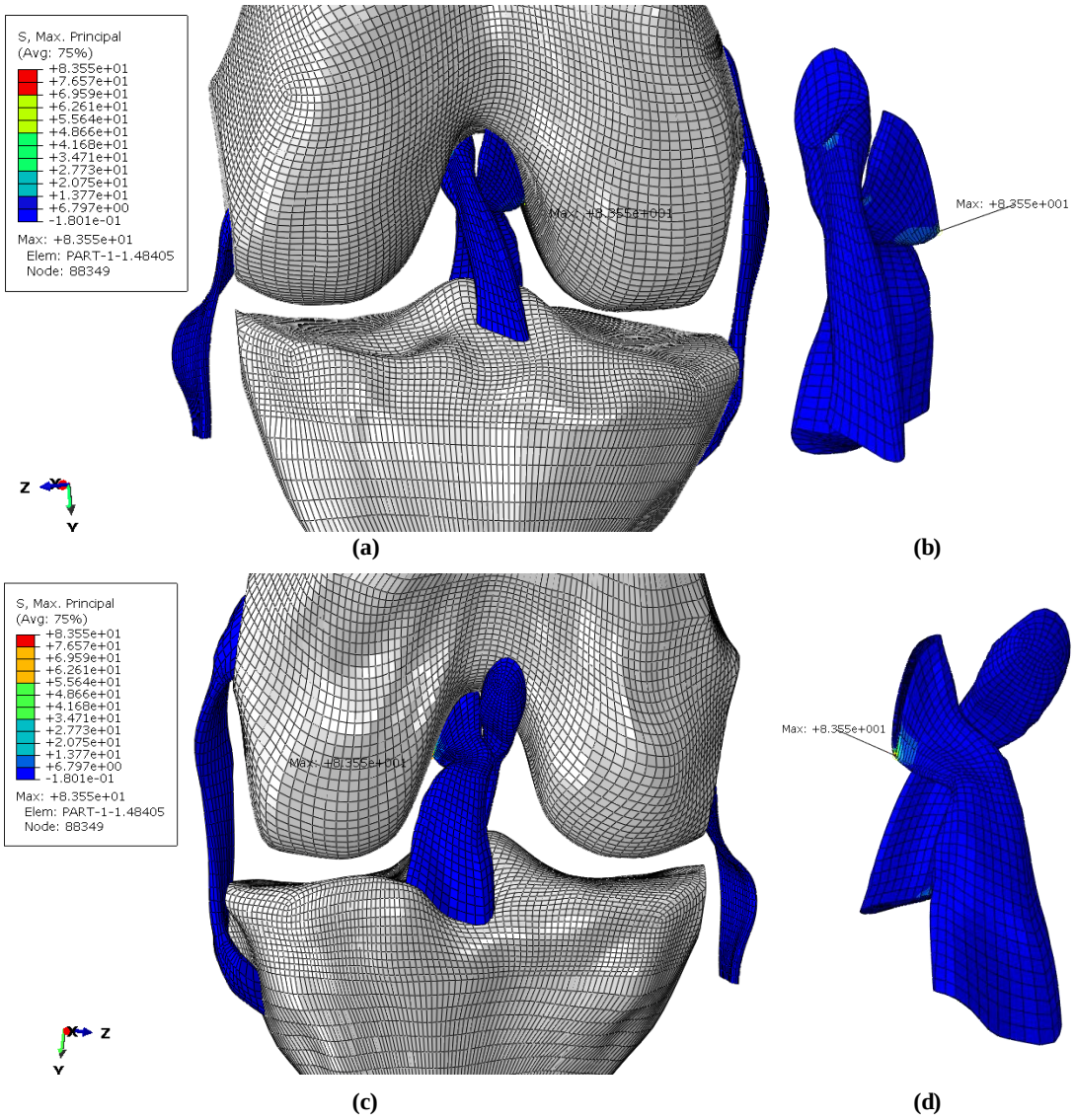

***Figure 9-9** – Polynomial hyperelastic n=2 model. Knee under flexion at 45 °, 2.5° of adduction and 12° of external rotation.**(a)** and **(b)** anterior and **(c)** and **(d)** posterior views of the knee joint set and the cruciate ligaments, respectively.*

9.3.3 **Holzapfel, Gasser and Ogden Model**

The HGO model is an anisotropic hyperelastic constitutive material model, described in Section 6.2.2. This model requires a determination of prevailing fibre orientation. Thus, the fibres were created automatically by an element-by-element function in a continuous orientation, parallel to the long-axis of the ligament. This way, an appropriate material response from tensile loads is defined.

The boundary conditions applied were the same as previously for comparison purposes with the other constitutive models. Therefore, the Figure 9-10 depicts the results of the applied motion with the HGO model.

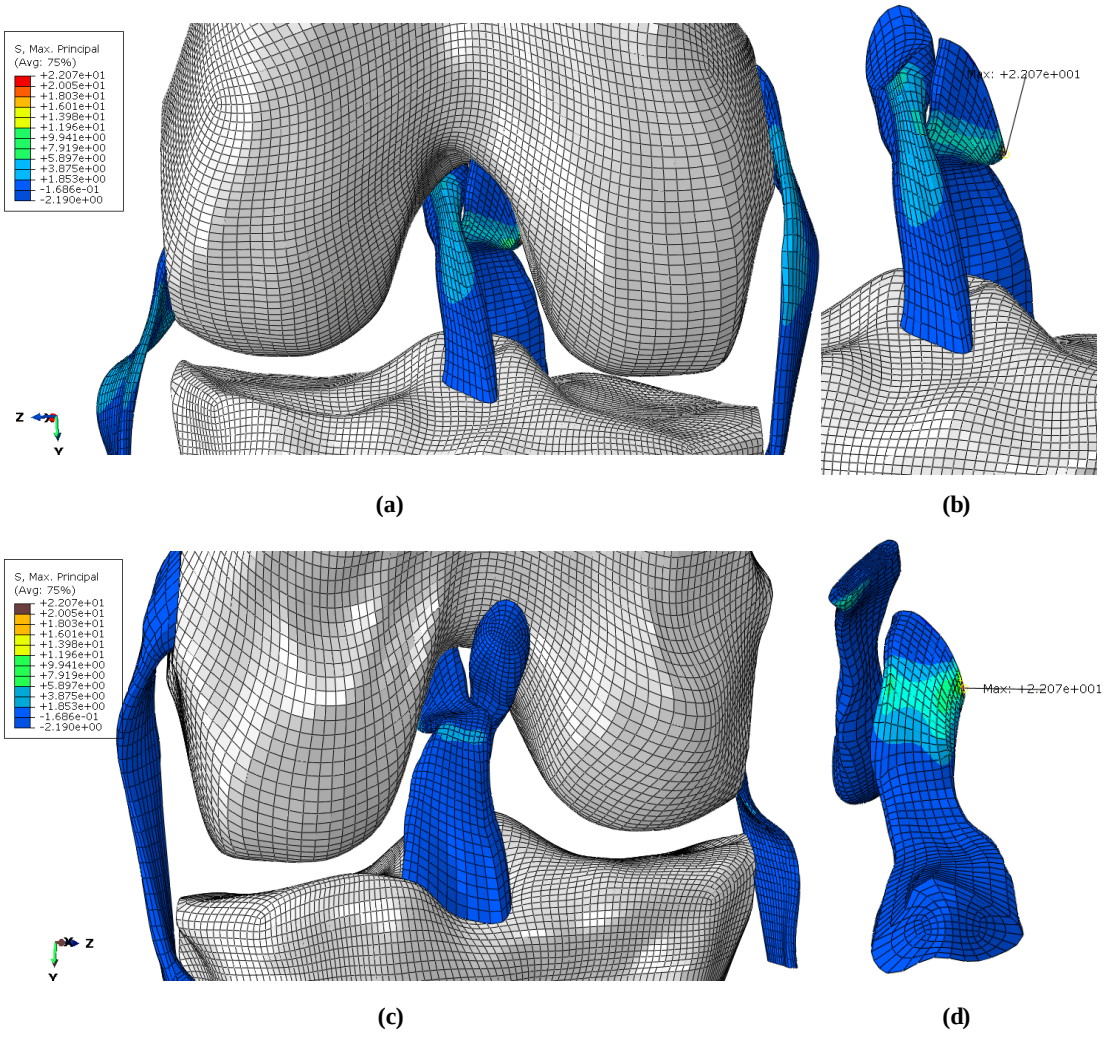

***Figure 9-10**- HGO model to define the ligaments. Knee under flexion at 45°, 2.5° of adduction and 12° of external rotation. **(a)** and **(b)** anterior view of the whole knee and the cruciate ligaments, respectively. **(c)** Posterior view of the knee and **(d)** inferior view of the cruciate ligaments.*

9.3.4 **Constitutive Models Comparison**

Evaluating the constitutive models results, the maximum stress values were analysed according to the toe region during normal walking. Recent studies show that the ligaments are initially pretensioned and this substantially changes the results [5], [64], [134], [161], [190]. In this work, the results were under pretension null, since the analysis was focused on qualitative analysis and on the influence of the ligaments on the knee kinematics.

In every simulations, the PCL was the one where the maximum stress was visualised, which is in agreement with the qualitative results, reported in literature, particularly by Peña (2004) [5]. Quantitatively, a relationship stress-angle of flexion, seen in the PCL, from the four models was displayed. Observing Figure 9-11, the polynomial hyperelastic model was the less accurate representation, since the maximum stress (83.55 MPa) was out of range (Annex II). This may be due to the fact that the model adaptation is not adequate. Although the coefficients are the same,

there are other parameters that are not respected. For the example, in the transversely isotropic hyperelastic model (used by Peña [5]), the ground substance is considered, whereas with the polynomial hyperelastic it is not. Thus, the transverse isotropic hyperelastic model must not be adapted to a polynomial hyperelastic model and, for that reason it was disregarded from the evaluation.

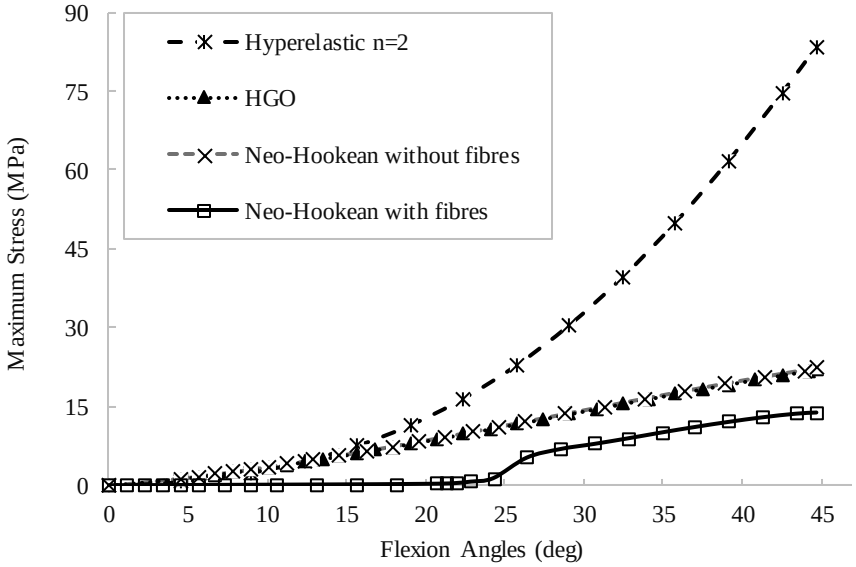

***Figure 9-11**- Evolution of the maximum stress (MPa) in the PCL during normal knee flexion (degrees) when walking according to the four constitutive models.*

In this study, despite of the limitation mentioned before, the results can be compared with the experimental and computational outcomes. Nevertheless, the study is more likely to be validated according to the stress distribution patterns. Therefore, with reference to the stress distribution data available in literature, the model's qualitative validation will be treated.

The lack of data in literature regarding the stress distribution during normal walking was constraining. Consequently, these results were compared with the data obtained in a plain flexion of 45°. In all three constitutive models' results, it was observed that, during flexion, the maximum stress was found in the anteromedial part of the PCL, which is in accordance with the Peña simulation results [5]. Hirokawa et al. quantified the non-uniform strains over the entire surface of ACL. Experimentally, resorting to a photoelastic coating technique, the ACL isochromatic fringe patterns were obtained according to different knee angles (from 0° to 120°) [191]. From 30° to 60°, their results demonstrate that, in an anterior view, the ACL is stressed close to the femoral insertion, which confirms the behaviour visualised in Figure 9-7, Figure 9-8 and Figure 9-10. Also, during the flexion, the ACL anteromedial portion becomes more tensioned, whereas the posterolateral becomes less tensioned, which is in compliant with other experimental data [5], [192], [193].

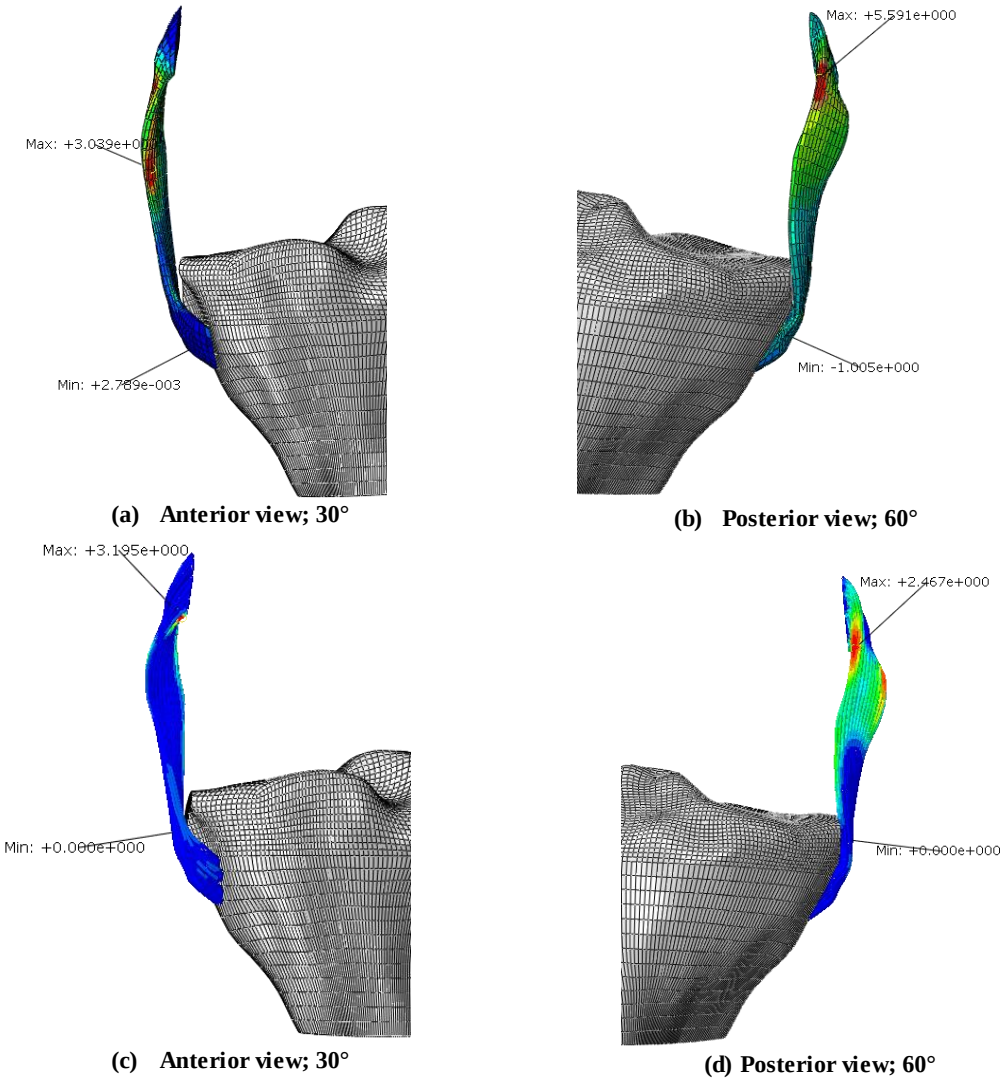

(a) Anterior view; 30° **(b) Posterior view; 60°**

(c) Anterior view; 30° **(d) Posterior view; 60°**

Figure 9-12*- Tibia and MCL representation with the knee flexing 30° and 60°. Being* ***(a)*** *and* ***(b)*** *characterized with HGO and* ***(c)*** *and* ***(d)*** *with neo-Hookean with fibres.*

Gardiner et al. investigated the MCL stress distribution in consonance with different flexion angles (0°, 30° and 60°) [166], [194]. Using markers attached to the MCL, it was possible to experimentally obtain the position of the markers and the ligament's geometry for the *in situ* strain analysis. According to their results, from the extension to flexion, the strain values in the posterior fibres decreased, increasing the anterior fibres and in tibial insertion. Visualizing the simulation results depicted in Figure 9-12, where the knee was flexed at 30° and 60°, the same trend can be perceived. I.e., the stress increase in the anterior region of the ligament and decreases in the posterior region, similarly to the results reported by Gardiner et al. It is important to bear in mind that, since the ligaments in this model were not pretensioned, when the knee is in extension, there is no stress in the ligament, i.e., at 0° of flexion, the model presents no stress distribution, but it should.

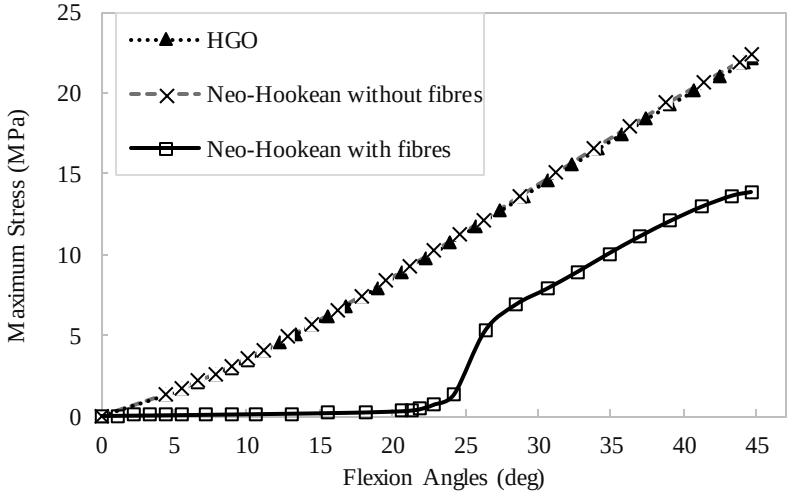

Figure 9-13- *Evolution of the maximum stress (MPa) in the PCL during normal knee flexion (degrees) when walking according to three different constitutive models.*

Quantitatively, the results may not be cross-referred with literature, nonetheless, they can be inserted in a range of values to verify their accuracy. Figure 9-13 displays the maximum stress versus flexion angle curves of three constitutive models considered to the analysis results. The maximum stress value (22.07 MPa in HGO, 22.32 MPa in neo-Hookean without fibres and 13.83 MPa in neo-Hookean with fibres) indicates the similar longitudinal behaviour among them. As stated in literature, Prietto (1988) and Race et Amis (1994) presented the lowest maximum stress values (26.8 MPa and 24.4 MPa) at rupture situations, relatively to other researchers [152], [153] (see Annex II – PCL table). Nonetheless, the other values found in literature, under uniaxial tensile tests, are higher, which means that, during walking, the ligament will not tear according to the results found with the three constitutive models.

In conclusion, making an exception to the hyperelastic polynomial model, the three models have qualitative results equivalent to literature, despite the limitations highlighted throughout this discussion. Moreover, the quantitative analysis suggests that the most suitable model is the one which presents the lowest maximum stress value, i.e., the neo-Hookean reinforced with fibres. Thus, with this model, some mechanisms of ligaments' injury will be studied in the following section.

9.4 KNEE MODEL STATIC ANALYSIS

9.4.1 **Introduction**

The ligaments' constitutive models analysis has concluded that the neo-Hookean model reinforced with fibres is the most suitable one. Thus, mechanisms of injury that frequently result

on ligament injury will be investigated in this section. The bone material model is maintained and the boundary conditions are variable according to the mechanism. Five simulation cases were considered: adduction and abduction, two mechanisms of injury mentioned by Dr. José Carlos Noronha and a PCL injury caused by a traffic accident.

MCL and LCL damages typically occur due to activities placing excessive strain because of a specific incident. The adduction and abduction knee rotations, when exceeded, can result in LCL and MCL injuries (Figure 9-14), respectively [166], [194], [195]. Each of these ligament injuries mechanisms will be investigated through computer modelling, where the collateral ligaments are more likely to tear.

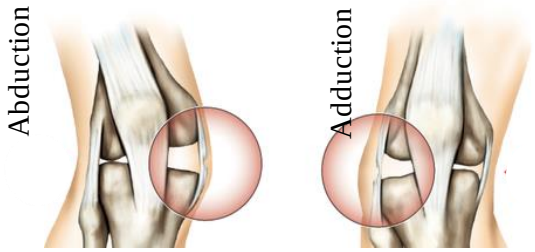

***Figure 9-14**- Abduction and adduction motion on the right knee, injuring MCL and LCL respectively. Adapted from* [196].

Dr. José Carlos Noronha, MD, PhD, a renowned doctor whose work in the knee is acknowledged and from extreme importance, mentioned two mechanisms of ACL injury in his book: flexion-abduction-external femoral rotation (Figure 9-15- a) and flexion-adduction-internal femoral rotation (Figure 9-15- b) [9].

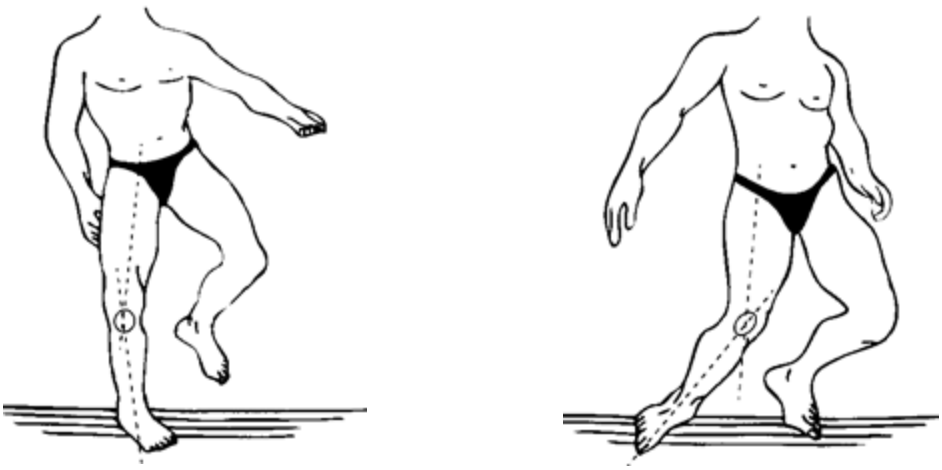

(a) **(b)**

***Figure 9-15**- ACL injury caused by **(a)** flexion-abduction-external femoral rotation and **(b)** flexion-adduction-internal femoral rotation. Adapted from* [9].

Dr. José Carlos Noronha suggested applying about 15° of flexion, 2.5° of adduction and abduction and about 12° of internal and external femoral rotation. The mechanism of injury lies on the combination of these rotations.

According to previous studies, the most common PCL injury cases are caused by traffic accidents (45%) [197]. Consequently, the most common mechanism of PCL injury is provoked by an posteriorly directed force on the proximal tibia (when the knee is in a flexed position) as it strikes on the dashboard or steering wheel during a car crash [101], [197], [198]. By analysing the stress - radiographs after PCL injury by traffic accident, it is reported that at 90° of flexion the posterior tibial displacement was 13.4 ± 4.7 mm, similarly to the mechanism represented on Figure 9-16 [198]. Therefore, this is the mechanism of injury that will be simulated for the PCL tearing.

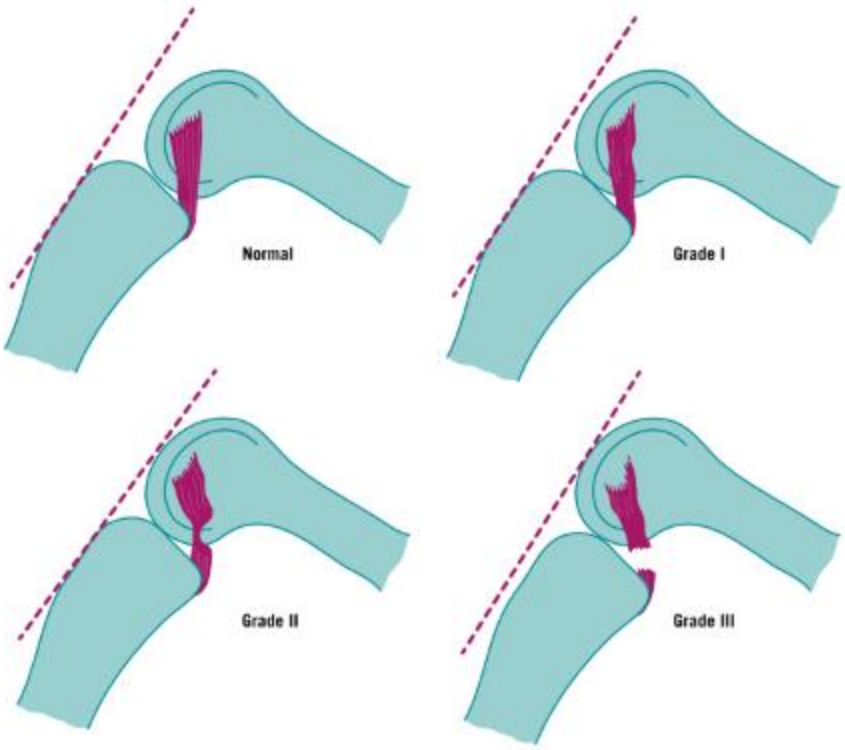

***Figure 9-16**- The three grades of posterior subluxation. The third grade represents a typical injury due to knee crash on the dashboard. Adapted from* [197].

9.4.2 **MCL and LCL Mechanisms of Injury**

The MCL and the LCL are the sideways knee stabilizers and they are easily damaged when under certain mechanisms of injury. Abduction and adduction are among the primary injury's mechanism of the MCL and LCL, respectively [166], [195]. Notwithstanding, the MCL is more frequently injured than the LCL, once it is more susceptible to external impacts, for instance, when practicing sports.

Therefore, for the abduction's mechanism injury, approximately 10° of flexion, 15° of abduction and 9° of internal tibial rotation was imposed on the knee model. Figure 9-17 and Figure 9-18 depict the results of the abduction simulation. It is visible that the MCL presented the

maximum value for the fibres during the movement applied. This enforces that the MCL is the ligament that suffers from injury under a knee abduction motion.

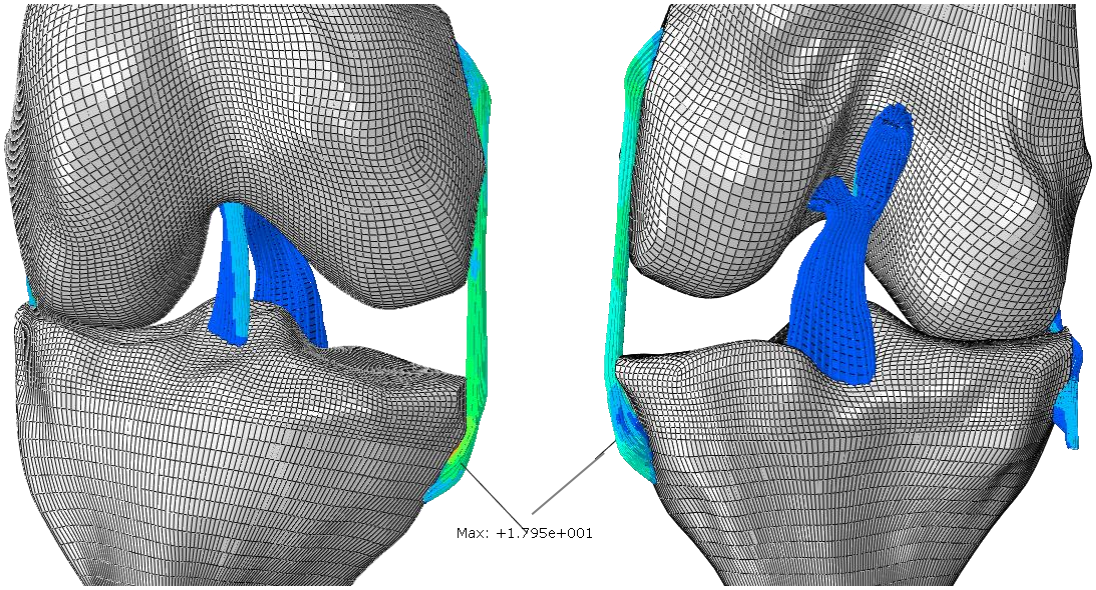

Figure 9-17- (a) *Anterior and* ***(b)*** *posterior view of the knee under abduction motion.*

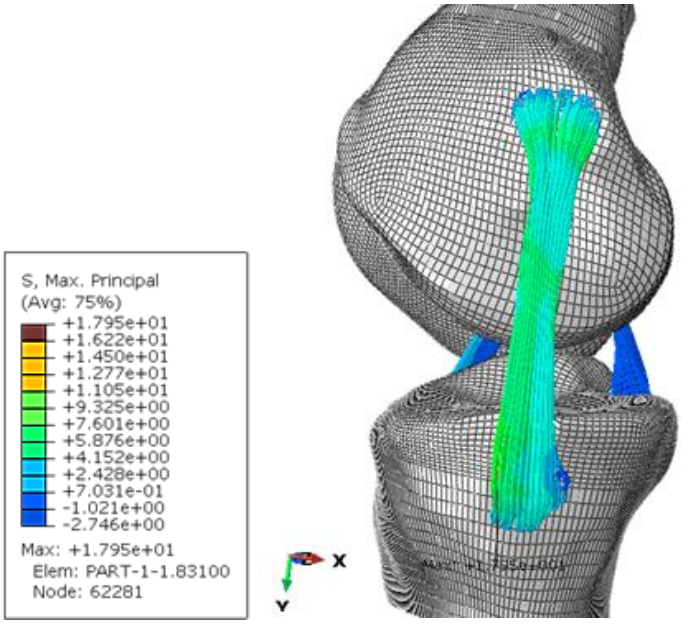

Figure 9-18- *Medial view of the knee under abduction motion.*

The adduction rotation have influence mainly on the LCL. This type of motion is rarer than the abduction rotation, once it is more difficult to be performed passively or under an external force. To simulate the adduction motion, approximately 10° of flexion, 18° of adduction and 6° of external tibial rotation was applied. Figure 9-19 and Figure 9-20 depict the results of the adduction simulation in the anterior, posterior and lateral view.

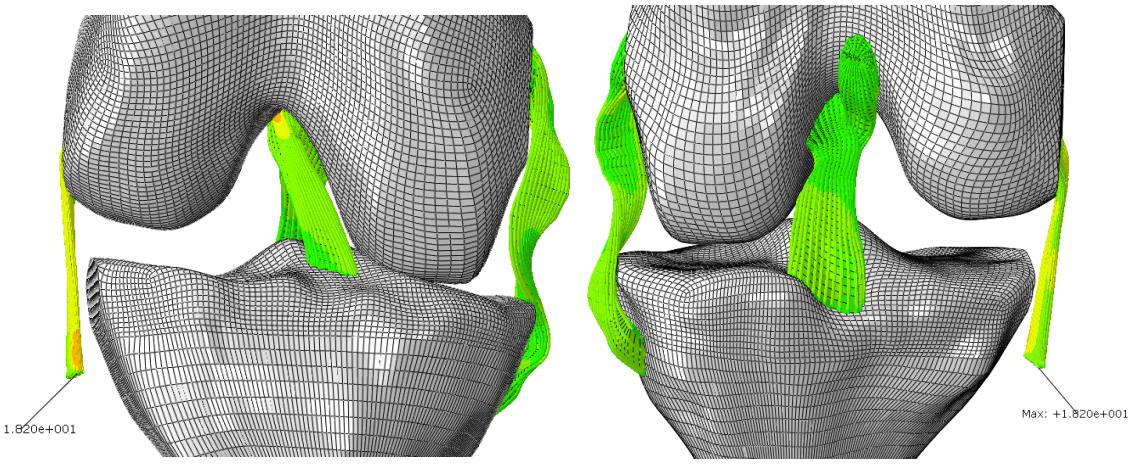

(a) **(b)**

Figure 9-19-(a) *Anterior view and* ***(b)*** *posterior view of the knee under adduction motion.*

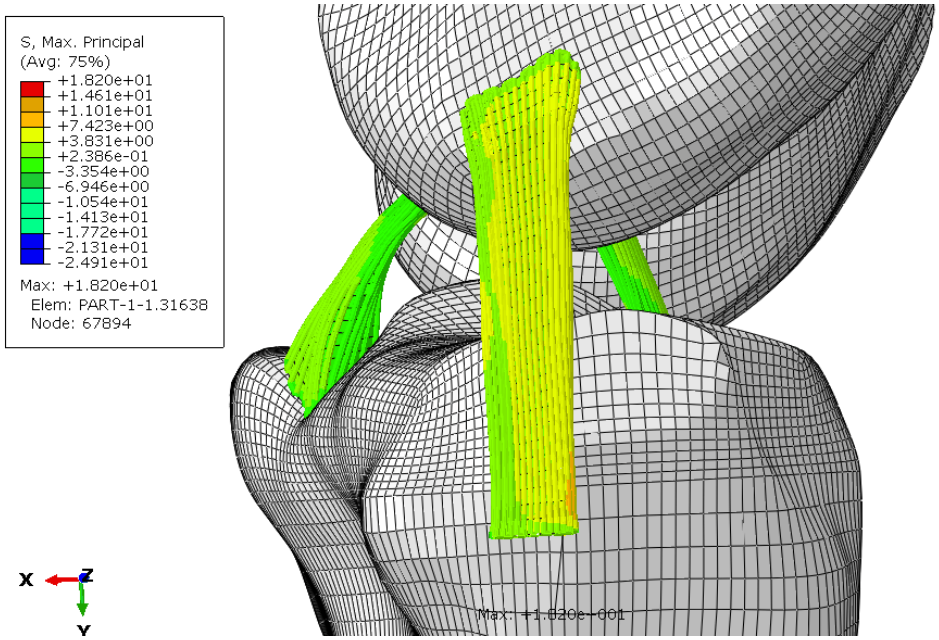

Figure 9-20 *- Lateral view of the knee under adduction motion.*

The results of the adduction rotation revealed that the LCL is the primarily affected. Moreover, both results indicate the maximum stress on the bone insertion site. This means that the ligament starts to fail on the attachment area under both types of motion.

9.4.3 **ACL Mechanisms of Injury**

According to Dr. José Carlos Noronha, the most frequent ACL's mechanisms of injury are caused by a specific set of movements including the flexion, abduction or adduction and external or internal femoral rotation, which may tear the ACL due to the tensile loading acting on. Thus, to

see what happens to the ACL during this type of mechanism of injury, two simulations were conducted.

The flexion-abduction-external femoral rotation is the most common mechanism to happen and to lead to an ACL tearing. To simulate this mechanism of injury, there was applied approximately 15° of flexion, 2.4° of abduction and finally 12° of external femoral rotation

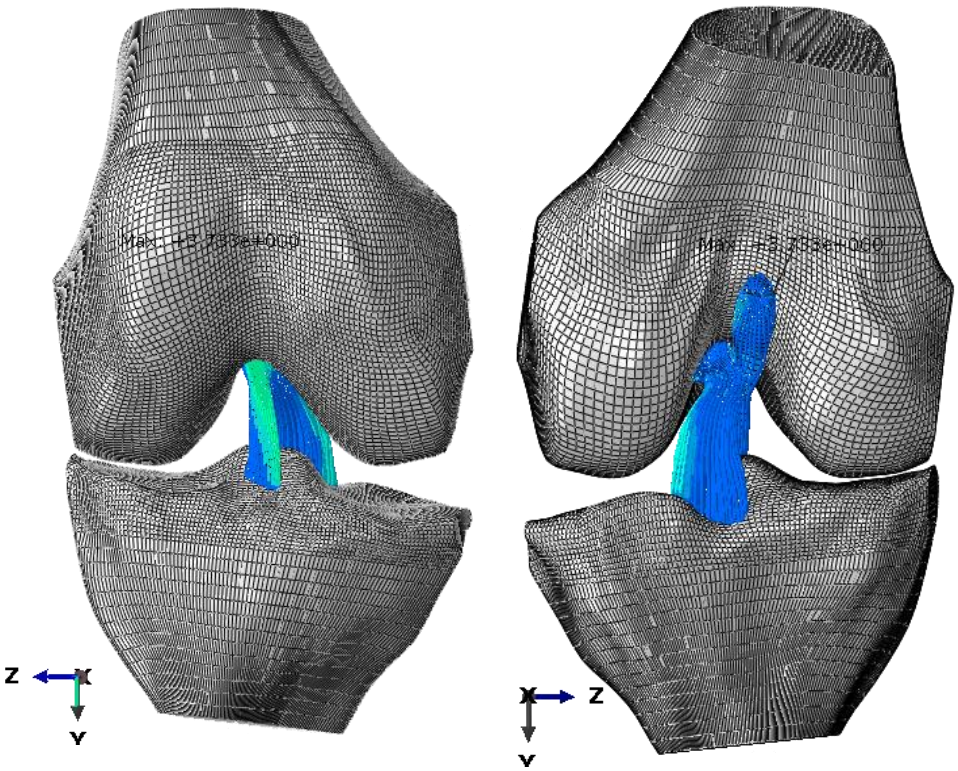

(a) **(b)**

Figure 9-21- (a) *Anterior and* ***(b)*** *posterior view of the flexion, abduction and external femoral rotation proposed by Dr. José Carlos Noronha.*

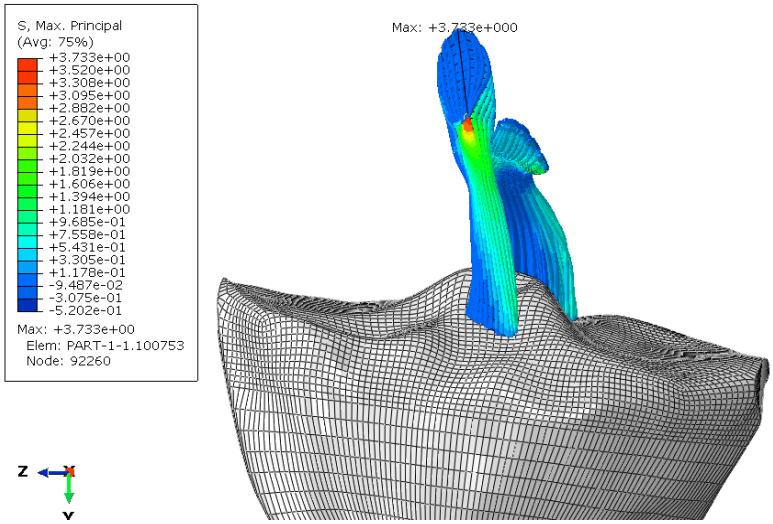

Figure 9-22- *Injury caused by flexion, abduction and external femoral rotation.*

In Figure 9-21, the global result of a flexion-abduction-external femoral rotation applied on the knee is depicted. It is possible to visualise that the ACL is the one under the maximum principal stress, whereas, on the PCL, it is only visible stress on the medial portion, mainly due to the abduction motion. Particularly in Figure 9-22, the highest stress is visible next to the ACL femoral insertion.

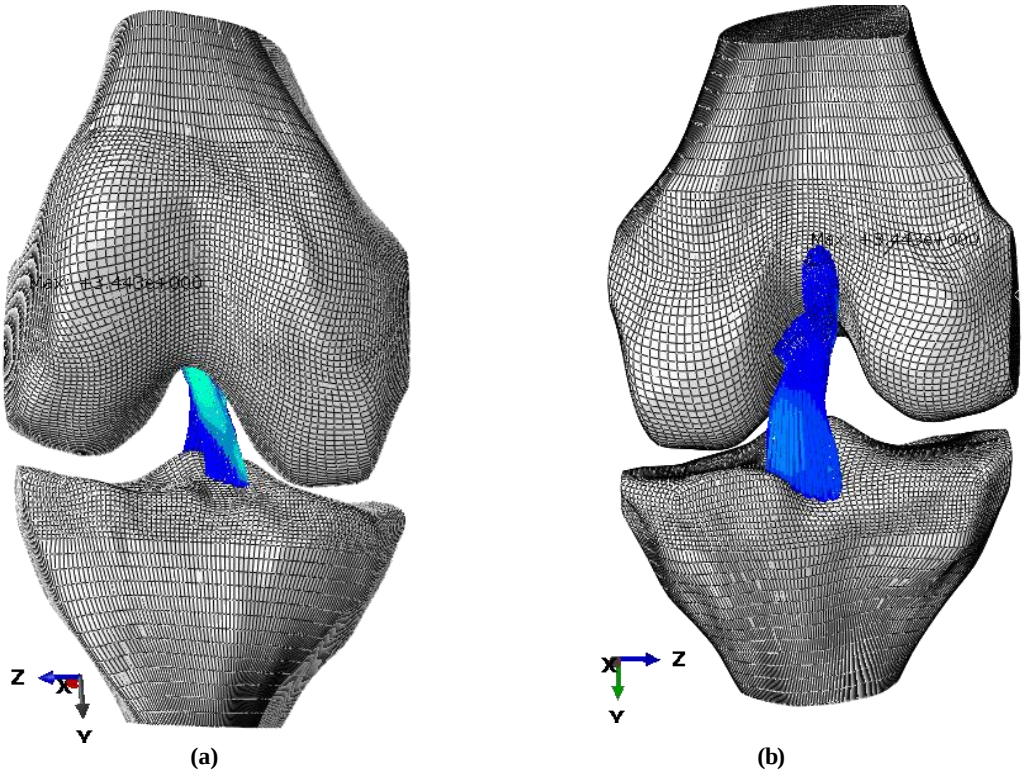

(a) **(b)**

Figure 9-23-(a) *Anterior and* ***(b)*** *posterior view of the flexion, adduction and internal femoral rotation proposed by Dr. José Carlos Noronha.*

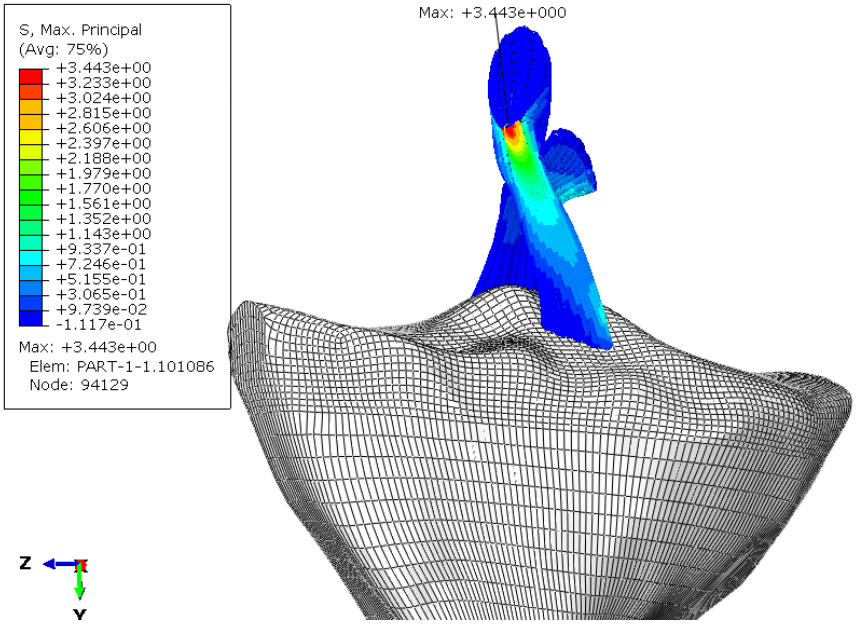

Figure 9-24- *ACL injury caused by flexion, adduction and -internal femoral rotation.*

In Figure 9-23, the orientation of the knee bones and the stress distribution of the cruciate ligaments are demonstrated. Similarly to the first mechanism of injury simulated, the maximum principal stresses are visualised on the anterior portion of the ACL (Figure 9-24).

As expected by Dr. José Carlos Noronha, the results prove that the ACL is the one that suffers the highest stress in both mechanisms of injury. The ACL presented a peak value of 3.733 MPa during the flexion-abduction-external femoral rotation and 3.443 MPa during flexion-adduction-internal femoral rotation. In both mechanisms of injury, the ACL starts to fail in the mid-anterior fibres close to the femoral insertion.

9.4.4 **PCL Mechanism of Injury**

In order to simulate the PCL mechanism of injury by car crash, the knee was taken at approximately to 90° of flexion and the tibia was dislocated posteriorly about 13 mm. Thus, for this simulation, there were two necessary steps: the first one to flex the knee with the tibia fixed and the subsequent one where the femur position is maintained and a posterior displacement on the tibia is applied.

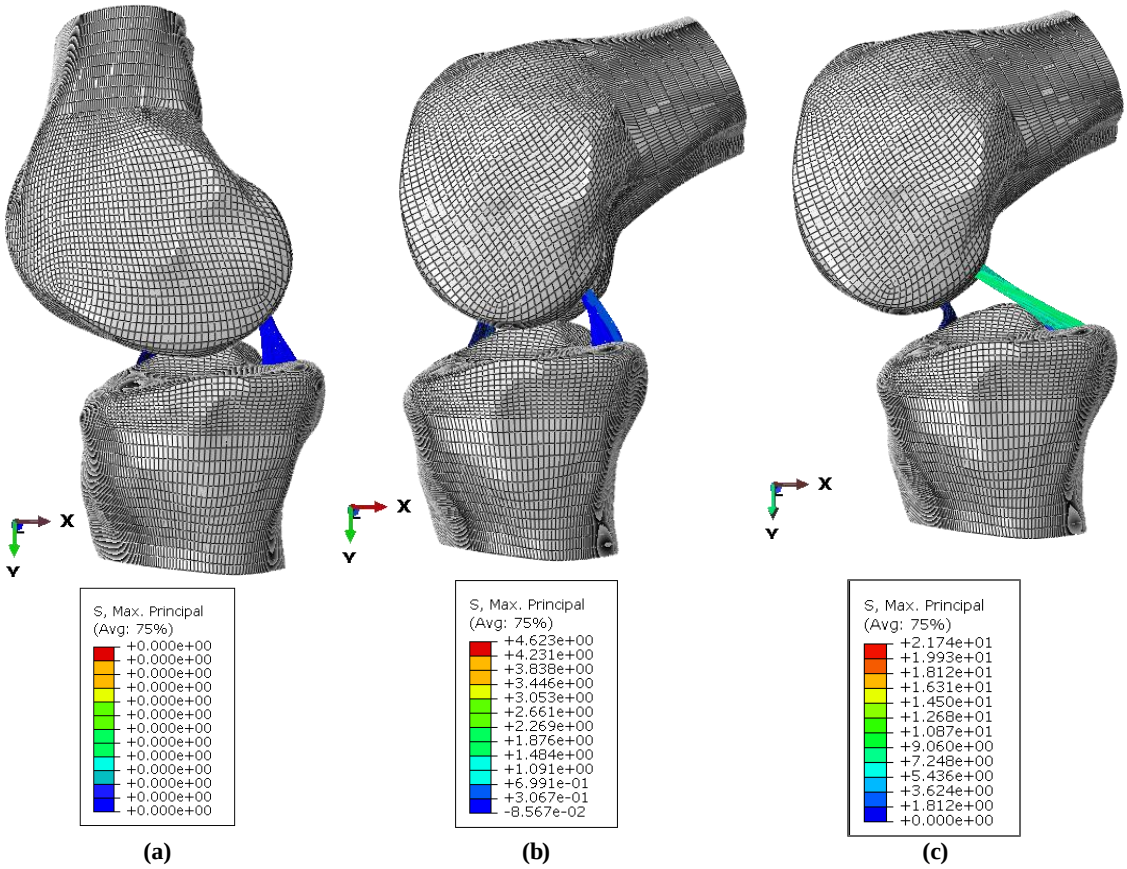

Figure 9-25- (a) *Initial position,* ***(b)*** *approximately 90° knee flexion and* ***(c)*** *tibial posterior displacement (approximately 13 mm).*

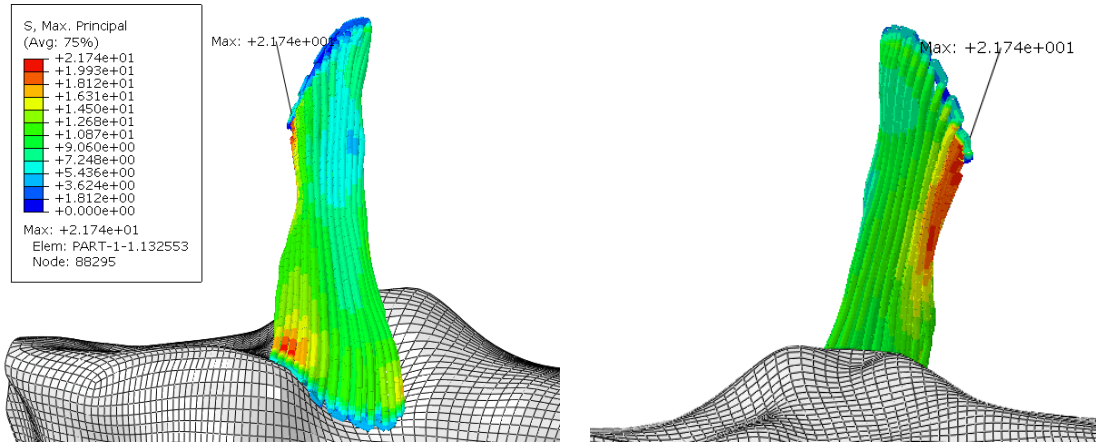

Figure 9-26- (a) *Posterior view and* ***(b)*** *anterior view of the PCL stress distribution.*

Figure 9-25 displays the three phases of this simulation case. In Figure 9-25 (a) the initial position is represented, whereas on (b) the knee flexion is illustrated and, finally, on (c) it is depicted the tibia dislocation. Also, on the last stress distribution results (Figure 9-26), it is visible the stretch of the PCL, which is evaluated by the stress distribution.

The results of the PCL's injury simulation by the shock of the knee on the dashboard revealed that the PCL may partially tear (grade I and II) or, more likely, completely tear (grade III). The maximum principal stresses are located in the proximal–medial portion of the PCL and next to the tibial insertion. Concluding, the stress values obtained are high sufficiently to admit that there was a complete rupture. However, depending on the load that the knee strikes the dashboard, the PCL injury could be studied in future works.

10 CONCLUSIONS AND FUTURE PERSPECTIVES

This chapter is reserved for the summary of the main conclusions of the investigation. First of all, an overview of the work accomplished is described. Furthermore, the main conclusions will be commented and summarized in a comprehensive manner. As a result of this thesis, there are original contributions that are emphasized in Section 10.3. Finally, in the last section, future perspectives of this work for the continuation of this investigation are suggested.

10.1 WORK SUMMARY

The main objectives of this thesis focus on two fields: mechanical testing and computer modelling. For the mechanical tests, a new approach of clamping was designed and, consequently, the mechanical characterization of the porcine knee ligaments was performed. On the other hand, the characterization and analysis of the constitutive models of the knee ligaments and further FE simulation of the knee biomechanical behaviour under injury were investigated. To achieve these aims, a summary of the tasks accomplished is listed below.

1. A comprehensive literature review, including all the theoretical fundamentals that contribute to the understanding of this work;
2. Detailed revision of the state of the art, serving as a base for the experimental work;
3. Several tests conducted with different types of knee ligaments' clamping to corroborate the need of a new clamping solution;
4. Design and evaluation of a new clamp in SOLIDWORKS taking previous studies into account;
5. The manufacturing of the clamps, after corrections and revaluations;
6. Mechanical tensile testing with porcine ligaments conducted with the new clamps;
7. Achievement of the clamps' validation by comparison of the mechanical testing results with literature;

8. Mechanical properties characterization of the porcine knee cruciate and collateral ligaments;
9. Work on the commercial code (ABAQUS) of the knee model concerning the ligaments so as to be functional, as the FE simulation;
10. Biomechanical characterization of the FE ligaments with four constitutive models;
11. The neo-Hookean model reinforced with fibre revealed to be the most suitable quantitatively and qualitatively, among the constitutive models studied;
12. Biomechanical study, using the knee finite element with the neo-Hookean reinforced with fibres, of five mechanisms of ligaments' injury.

For the clamp design and evaluation, the SOLIDWORKS drawing and simulator was used. Relatively to the knee study with finite elements, two different commercial software programs were used: FEMAP, used to work on the knee model's geometry, and ABAQUS, used to conduct the FE simulations.

10.2 CONCLUSIONS

10.2.1 **New clamp and the mechanical conclusions**

The new approach for ligaments testing was an achievement, since the tests' results were concordant with literature. The method showed to be flawless if the following requirements are fulfilled. First, the ligament needs to be well dissected, with a good portion of bone, as displayed before in Section 7.3. Then, a bone release agent may be used in the clamp cavity, where the bone cement will be added. This step guarantees a perfect demolding of the bone cement. Finally, with a disposable needle, the bone cement is applied in order to fulfil the cavity and fix the bone. With the accomplishment of these steps, the ligaments are completely held and ready for the uniaxial tensile testing.

Overall, the mechanical tests in porcine ligaments, using the customized clamps, achieved similar material characterization to the ones mentioned in literature. Although most of the characterization presented in literature has been done in human knee ligaments, the ligament tissue is very similar to other animals' ligaments [35], [41], [44], [84]. Therefore, the mechanical properties of porcine knee ligaments can be inserted in the range of values obtained for the human, in order to have a referee.

At the same velocity (125 $mm.min^{-1}$), the posterior cruciate ligament showed to be the most rigid ligament (228.4 ± 134.2 $N.mm^{-1}$), and the lateral collateral ligament the less rigid (7.534 ± 0.0255 $N.mm^{-1}$) among the major knee ligaments. Curiously, they are both the less injured ligaments, which may explain these results. The lateral collateral is more flexible and hardly injured due to

its anatomical position, whereas, the posterior cruciate is more resistant to injury than the others.

The injuries on ligaments often result at higher strain rates. Thus, the most frequently injured ligaments, the ACL and MCL, were tested under 500 $mm.min^{-1}$. The study revealed that at higher velocity, the ultimate load of the ACL increased from 1087 ± 371.6 N at 125 $mm.min^{-1}$ to 1347 ± 245.6 N at 500 $mm.min^{-1}$. The MCL followed similar trends, but the variations were smaller: from 228.7 ± 135.0 N at 125 $mm.min^{-1}$ to 291.7 ± 208.0 N at 500 $mm.min^{-1}$.

In regards to creep and relaxation tests, the PCL demonstrated a time-dependent behaviour. The data from the conducted tests confirms the stress- and strain- dependent nonlinear viscoelastic behaviour. Overall, both studies exhibited an initial quick adaptation to the imposed test (increase of deformation in creep test, and decrease of load in the relaxation test), and then a progressively and slow variation of the ligaments' properties. Notwithstanding, more studies are required to investigate this behaviour in PCL and in the rest of the knee ligaments.

10.2.2 **Numerical conclusions**

In this thesis, four different ligament constitutive models were simulated and analysed to study the effect of each constitutive model on the stress distribution pattern and knee biomechanics. The simulation's results demonstrated that, although the material properties of different constitutive models were acquired by other authors' experimental studies, the ligament material constitutive model change has induced altered stress distribution patterns and joint kinematics.

According to previous papers, no constitutive model can be used to describe successfully all ligament material behaviours under longitudinal tension, transverse tension, and finite simple shear [117], [122], [166]. Also, the results of the constitutive models achieved on this thesis corroborate this statement.

The neo-Hookean model was tested with and without fibres' addition. Also, the polynomial hyperelastic and the HGO models were investigated. The four constitutive models were studied under the swing phase of normal walking. The polynomial revealed to be the most inaccurate, with low stress distribution patterns, and with the highest maximum stress in the PCL (83.6 MPa), found among the studies. The neo-Hookean without fibres and the HGO showed similar maximum stress values (22.32 MPa and 22.07 MPa, respectively). Finally, the neo-Hookean model with fibres demonstrated the best representation of the ligament behaviour. The stress distribution displayed (maximum of 13.83 MPa) in the fibres is longitudinal and unidirectional according to the applied tension, which is the most accurate behaviour representation. Moreover, the other constitutive models presented values near to the failure stress, which is not accurate. The neo-Hookean model with fibres was the model which achieved the lower value for the swing phase of normal walking, and, thus, was used to perform five mechanisms of injury.

The LCL and MCL damages were investigated under adduction and abduction, the ACL was investigated under two mechanisms of injury mentioned by Dr. José Carlos Noronha and finally, the PCL injury was investigated for a car crash mechanism of injury. Thus, the MCL and the LCL showed 17.95 MPa and 18.20 MPa, respectively, for failure stress near to the tibia-ligament attachment. Qualitatively, the mechanism of injuries simulated for the ACL demonstrated that the ACL tends to tear anteriorly close to the femoral attachment. Nonetheless, the maximum stress achieved in these situations was 3.44 MPa and 3.73 MPa, which is much lower than the failure stress achieved in literature. Finally, relatively to a car crash simulation, with the knee flexed 90° and with a tibial dislocation, the PCL showed a rupture in the posterior region close to the tibial attachment and in the medial portion of the ligament with 21.74 MPa of maximum stress.

Relatively to the mechanisms of injury of the MCL and LCL, there are some studies of strain distributions, for the MCL [194], under tibial torque, which reveal that, with the knee at full extension, the MCL is most highly strained near the femoral insertion. Nonetheless, these conclusions must not be directly compared, since the kinematics and kinetics imposed on the knee are not the same. Thus, future investigations regarding the influence of loads and torques are required. Furthermore, there was not found any finite element published studies of the ACL injury under the mechanisms of injuries mentioned by Dr. José Carlos Noronha. Lastly, regarding the PCL injury, qualitatively it is in accordance to literature [197], [198]; However, there is no published study with the finite element analysis.

In conclusion, these results showed that the ligaments' stress varies according to the constitutive model used. The insertion of the fibres in the ligaments demonstrated the most accurate representation among the constitutive models investigated. Also, including the mechanisms of injury, a qualitative validation of the knee model was achieved.

10.3 ORIGINAL CONTRIBUTIONS

The most notable contributions of this thesis are listed below:

1. A new approach for the bone-ligament-bone complex clamping for the mechanical tests;
2. Mechanical properties characterization of the porcine knee's ligaments;
3. Qualitative validation of the constitutive model neo-Hookean with fibres;
4. Biomechanical study of five mechanisms of injury to the cruciate and collateral ligaments.

10.4 FUTURE WORK

The overall thesis goal was to make a contribution to the investigation of the biomechanical properties of the knee ligaments. In this sense, a new approach for the ligaments' clamping was developed and the constitutive models used in ligaments were analysed by the finite element method.

Directing to the mechanical tests, there are several experimental factors that can affect the determination of biomechanical properties of ligaments. The specimen orientation and the influence of different strain rates still remain under investigation.

The influence of strain rate on injury is a debated topic. Sports-related injuries are estimated to occur at strain rates that vary from relatively slow rates to high rates [7]. Although injuries to ligaments often result at high strain rates, many experimental studies have examined the ligament properties under low-to-medium rates of strain because of the limitations of testing approaches and data collection systems. With the new clamps, the highest strain rate tested was about 20%/s for the ACL and 12%/s for the MCL. Thus, more studies at highest velocities should be performed.

To future ligament studies can be subjected to the orientation deviations in order to investigate its influence. The docking area of the clamps in the machine is easily adapted by the construction of adaptors to fit into the desired machine. Thus, a tilting device can be designed to fit into the clamps and, consequently, allow controlling the ligament orientation during the experimental tests.

Future studies are also required to investigate the creep-relaxation relation, and to try to define a standard pattern through a constitutive model. This will give a clear understanding of the ligament behaviour under transient loadings and ligament time-dependency, which are not yet completely defined.

Another suggestion for future work is that, during the uniaxial tensile tests, a microscopic analysis component should be done in parallel to investigate the ligament behaviour and to determine, for instance, the exact time of ligament failure.

Finally, since the main goal is to contribute for the advancement in ligament's reconstruction methods, for the mechanical properties' characterization of the ligament, the tests should be performed preferentially in human knee ligaments. Also, these tests should be used as a base to investigate new differentiated parameters according to each major ligament, to be then inserted in the constitutive models.

When the mechanical properties of the human knee ligaments are determined, the obtained data will be further introduced into the FE knee model to define the ligament behaviour according to the suitable constitutive model. Thus, an approach involving both experimental and computational methods is more suitable. When both methods are matched and compared the model is validated and can be used to compute the stress and strain distributions in ligament grafts,

as well as to predict *in situ* forces in the ligaments during more complex *in vivo* motions that could not be done in laboratory experiments. The mechanisms of injury analysed in this thesis are examples of the potentiality of the 3D model. However, more studies with the complete knee structure, and under different loads and moments, should be conducted in order to corroborate the results achieved in this thesis.

A future work for the knee model is to compare the models already analysed with the transversely isotropic hyperelastic material model, using a user-defined subroutine UMAT. This model is a nearly incompressible constitutive model and has been described as the most accurate representation of the ligaments [117]. Notwithstanding, this constitutive model needs more development. The ligament transverse stress-strain curves should also be measured experimentally to determine the whole material behaviours of ligaments in future studies. Moreover, the simulations performed in this thesis are free of stress. Nevertheless, the ligaments in normal conformity are pre-tensioned, therefore this condition should be explored and added to the model in the future.

11 REFERENCES

[1] F. Mo, P. J. Arnoux, D. Cesari, and C. Masson, "Investigation of the injury threshold of knee ligaments by the parametric study of car–pedestrian impact conditions," *Saf. Sci.*, vol. 62, pp. 58–67, Feb. 2014.

[2] J. a Weiss, J. C. Gardiner, B. J. Ellis, T. J. Lujan, and N. S. Phatak, "Three-dimensional finite element modeling of ligaments: technical aspects.," *Med. Eng. Phys.*, vol. 27, no. 10, pp. 845–61, Dec. 2005.

[3] A. Oh, "Understanding Exercise – Planes, Axes and Movement," 2012. [Online]. Available: http://www.todaysfitnesstrainer.com/understanding-exercise-planes-axes-movement/.

[4] C. L. VanPutte, J. Regan, A. Russo, R. R. Seeley, T. D. Stephens, and P. Tate, *Seeley's anatomy & physiology*. McGraw-Hill., 2014.

[5] E. Peña, "Estudio Biomecánico de la Articulación de la Rodilla: Aplicación al Análisis de Lesiones Meniscales y Ligamentosas y de la Cirugía Asociada," PhD Thesis, The University of Zaragoza, 2004.

[6] E. S. Grood and W. J. Suntay, "A joint coordinate system for the clinical description of three-dimensional motions Applications to the knee," *Journal of Biomechanical Engineering*, 1983.

[7] S. L.-Y. Woo, R. E. Debski, J. D. Withrow, and M. A. Janaushek, "Biomechanics of knee ligaments.," *Am. J. Sports Med.*, vol. 27, no. 4, pp. 533–543, 1999.

[8] Y. Takeda, J. W. Xerogeanes, G. A. Livesay, F. H. Fu, and S. L.-Y. Woo, "Biomechanical function of the human anterior cruciate ligament," *Arthrosc. J. Arthrosc. Relat. Surg.*, vol. 10, no. 2, pp. 140–147, Apr. 1994.

[9] J. C. Noronha, "Ligamento Cruzado Anterior." ISBN 978-989-98508-0-4., p. pp.277, 2013.

[10] K. S. Saladin and L. Miller, *Anatomy & physiology*. McGraw-Hill, 1998.

[11] M. Nordin and V. H. Frankel, "Basic Biomechanics of the Musculoskeletal System," 4º edition., Lippincott Williams & Wilkins, a Wolters Kluwer business., 2012, pp. 102–127.

[12] J. E. Gordon, *Strukturen unter Stress: mechanische Belastbarkeit in Natur und Technik*. Spektrum-d.-Wiss.-Verlag-Ges., 1989.

[13] A. Completo and F. Fonseca, *Fundamentos de Biomecânica Músculo-Esquelética e Ortopédica*. Publindústria, Edições Técnicas, 2011.

[14] S. L.-Y. Woo, R. E. Debski, J. D. Withrow, and M. A. Janaushek, "Current Concepts Biomechanics of Knee Ligaments," *Am. J. Sports Med.*, vol. 27, no. 4, pp. 533–543, 1999.

[15] S. L.-Y. Woo, M. I. Danto, K. J. Ohland, T. Q. Lee, and P. O. Newton, "The use of a laser micrometer system to determine the cross-sectional shape and area of ligaments: a

comparative study with two existing methods," *J. Biomech. Eng.*, vol. 112, no. 4, pp. 426–431, 1990.

[16] F. Iaconis, R. Steindler, and G. Marinozzi, "Measurements of cross-sectional area of collagen structures (knee ligaments) by means of an optical method," *J. Biomech.*, vol. 20, no. 10, pp. 1003–1010, 1987.

[17] R. P. Jakob and H.-U. Stäubli, *The Knee and the Cruciate Ligaments*, Springer-V. Springer-Verlag New York, Inc., 1990.

[18] D. Butler, M. Kay, and D. Stouffer, "Comparison of Material Properties in Fascicle-Bone Units from Human Patellar Tendon And Knee Ligaments," *J. Biomech.*, vol. 19, no. 6, pp. 425–432, 1986.

[19] J. P. Goldblatt and J. C. Richmond, "Anatomy and biomechanics of the knee," *Oper. Tech. Sports Med.*, vol. 19, no. 2, pp. 82–92, Jun. 2003.

[20] K. L. Moore, A. F. Dalley, and A. M. R. Agur, *Clinical Oriented Anatomy*, 7th Editio. Lippincott Williams & Wilkins, a Wolters Kluwer business, 2014.

[21] S. Standring, *Gray 's Anatomy. The Anatomical Basis of Clinical Practice.*, 40th Editi. Churchill Livingstone Elsevier Limited, 2008.

[22] D. Shier, J. Butler, and R. Lewis, *Hole's Human Anatomy & Physiology*, 11th Editi. McGraw-Hill,Higher Education, 2007.

[23] B. D. Ghosh, *Human Anatomy for Students*, 2nd Editio. Jaypee Brothers Medical Publishers (P) Ltd., 2013.

[24] T. Taylor, "Fibula Anatomy and Function," 1999. [Online]. Available: INNERBODY.COM COPYRIGHT ©.

[25] N. S. Landínez-Parra, D. A. Garzón-Alvarado, and J. C. Vanegas-Acosta, "Mechanical Behavior of Articular Cartilage," in *Injury and Skeletal Biomechanics*, 2012, pp. 197–216.

[26] D. R. Peterson and J. D. Bronzíno, *Biomechanics: Principles and Applications*. Taylor & Francis Group, LLC, 2008.

[27] F. H. Netter, *Atlas of Human Anatomy*, 6th Editio. United States of America: Saunders Elsevier, 2014.

[28] T. W. Rudy, G. A. Livesay, and F. H. Fu, "A Combined Robotic/Universal Force Sensor Approach To Determine In Situ Forces Of Knee Ligaments," *J. Biomech.*, vol. 29, no. 10, pp. 1357–1360, 1996.

[29] S. Takai, S. L.-Y. Woo, G. a Livesay, D. J. Adams, and F. H. Fu, "Determination of the in situ loads on the human anterior cruciate ligament.," *J. Orthop. Res.*, vol. 11, no. 5, pp. 686–95, Sep. 1993.

[30] D. Johnson, *ACL Made Simple*. United States of America: Springer-Verlag New York, Inc., 2004.

[31] K. Rajendran, "Mechanism of locking at the knee joint.," *J. Anat.*, vol. 143, pp. 189–194, 1985.

[32] N. Chandrashekar, H. Mansouri, J. Slauterbeck, and J. Hashemi, "Sex-based differences in the tensile properties of the human anterior cruciate ligament.," *J. Biomech.*, vol. 39, no. 16, pp. 2943–50, Jan. 2006.

[33] A. Roaas and G. B. J. Andersson, "Normal Range of Motion of the Hip , Knee and Ankle Joints in Male Subjects, 30-40 Years of Age," *Munksgaard, Copenhagen*, no. Bergstrand 1980, pp. 205–208, 1982.

[34] B. Ytterstad, "The Harstad injury prevention study: the epidemiology of sports injuries. An 8 year study.," *Br. J. Sports Med.*, vol. 30, no. 1, pp. 64–68, 1996.

[35] B. L. Proffen, M. McElfresh, B. C. Fleming, and M. M. Murray, "A comparative anatomical study of the human knee and six animal species.," *Knee*, vol. 19, no. 4, pp. 493–9, Aug. 2012.

[36] T. Watanabe, M. Ishizuki, T. Muneta, and S. a Banks, "Knee kinematics in anterior cruciate ligament-substituting arthroplasty with or without the posterior cruciate ligament.," *J. Arthroplasty*, vol. 28, no. 4, pp. 548–52, Apr. 2013.

[37] D. S. Jevsevar, "Knee Kinematics and Kinetics During Locomotor Activities of Daily Living in Subjects with Knee Arthroplasty and in Healthy Control Subjects," *Phys. Ther. i*, vol. 73, no. 4, 1993.

[38] K. N. Laubenthal, G. L. Smidt, and D. B. Kettelkamp, "A quantitative analysis of knee motion during activities of daily living.," *Phys. Ther.*, vol. 52, no. 1, pp. 34–43, 1972.

[39] D. B. Kettelkamp, R. J. Johnson, G. L. Smidt, E. Y. Chao, and M. Walker, "An electrogoniometric study of knee motion in normal gait.," *J. Bone Joint Surg. Am.*, vol. 52, no. 4, pp. 775–790, 1970.

[40] I. B. Morrison, "The Mechanics of the Knee Joint in Relation to Normal Walking," *J. Biomech.*, vol. 3, pp. 51–61, 1970.

[41] G. Osterhoff, S. Löffler, H. Steinke, C. Feja, C. Josten, and P. Hepp, "Comparative anatomical measurements of osseous structures in the ovine and human knee.," *Knee*, vol. 18, no. 2, pp. 98–103, Mar. 2011.

[42] R. BARONE, *Anatomie Comparée des Mammifères Domestiques. Tomo 1: Ostéologie.*, 3ª ed. Vigot, Paris., 1986.

[43] F. K. Fuss, "Anatomy and function of the cruciate ligaments of the domestic pig (Sus scrofa domestica): a comparison with human cruciates.," *J. Anat.*, vol. 178, pp. 11–20, Oct. 1991.

[44] J. W. Xerogeanes, R. J. Fox, Y. Takeda, H. S. Kim, Y. Ishibashi, G. J. Carlin, and S. L. Woo, "A functional comparison of animal anterior cruciate ligament models to the human anterior cruciate ligament.," *Ann. Biomed. Eng.*, vol. 26, no. 3, pp. 345–52, 1998.

[45] L. Blankevoort, R. Huiskes, and A. De Lange, "The envelope of passive knee joint motion," *J. Biomech.*, vol. 21, no. 9, pp. 705–720, 1988.

[46] M. L. Ireland, "Why Are Women More Prone Than Men to ACL Injuries?," *Lexington, Kentucky*. [Online]. Available: http://www.hughston.com/hha/a.acl.htm. [Accessed: 16-Apr-2015].

[47] E. Arus, *Biomechanics of Human Motion. Applications in the Martial Arts*. Taylor & Francis Group, LLC, 2012.

[48] T. J. Bonner, N. Newell, A. Karunaratne, A. D. Pullen, A. a Amis, A. M J Bull, and S. D. Masouros, "Strain-rate sensitivity of the lateral collateral ligament of the knee.," *J. Mech. Behav. Biomed. Mater.*, pp. 1–10, Jul. 2014.

[49] T. J. A. Mommersteeg, L. Blankevoort, R. Huiskes, J. G. M. Kooloost, and J. M. G. Kauer, "Characterization of the mechanical behavior of human knee ligaments: a numerical-experimental approach," *J. Biomech.*, vol. 29, no. 2, pp. 151–160, 1996.

[50] C. Kweon, E. S. Lederman, and A. Chhabra, "Anatomy and Biomechanics of the Cruciate Ligaments and Their Surgical Implications," in *The Multiple Ligament Injured Knee: A Practical Guide to Management*, G. C. Fanelli, Ed. New York, NY: Springer New York, 2013.

[51] S. L.-Y. Woo, S. D. Abramowitch, R. Kilger, and R. Liang, “Biomechanics of knee ligaments: injury, healing, and repair.,” *J. Biomech.*, vol. 39, no. 1, pp. 1–20, Jan. 2006.

[52] E. S. Grood, S. F. Stowers, and F. R. Noyes, “Limits of movement in the human knee. Effect of sectioning the posterior cruciate ligament and posterolateral structures.,” *J. Bone & Jt. Surg.*, vol. 70, no. 1, pp. 88–97, Jan. 1988.

[53] F. Girgis, J. Marshall, and A. Monajem, “The cruciate ligaments of the knee joint. Anatomical, functional and experimental analysis.,” *Clin Orthop Relat Res*, vol. 106, no. 216–231, p. 1975, 1975.

[54] M. Yagi, E. K. Wong, A. Kanamori, R. E. Debski, F. H. Fu, and S. L. Woo, “Biomechanical Analysis of an Anatomic Anterior Cruciate Ligament Reconstruction,” *Am. J. Sports Med.*, vol. 30, no. 5, pp. 660–666, 2002.

[55] K. F. Bowman and J. K. Sekiya, “Anatomy and Biomechanics of the Posterior Cruciate Ligament and Other Ligaments of the Knee,” *Oper. Tech. Sports Med.*, vol. 17, no. 3, pp. 126–134, Jul. 2009.

[56] B. R. Meister, S. P. Michael, R. A. Moyer, J. D. Kelly, and C. D. Schneck, “Anatomy and Kinematics of the Lateral Collateral Ligament of the Knee,” *Am. J. Sports Med.*, vol. 28, no. 6, pp. 869–878, 2000.

[57] D. Gollehon, P. Torzilli, and R. Warren, “The role of the posterolateral and cruciate ligaments in the stability of the human knee. A Biomechanical study.,” *J Bone Jt. Surg*, vol. 69A, no. 233–242, p. 1987, 1987.

[58] P. Hansen, J. Bojsen-Moller, P. Aagaard, M. Kjaer, and S. P. Magnusson, “Mechanical properties of the human patellar tendon, in vivo.,” *Clin. Biomech. (Bristol, Avon)*, vol. 21, no. 1, pp. 54–8, Jan. 2006.

[59] S. Boisgard, J. P. Levai, B. Geiger, K. Saidane, and B. Landjerit, “Study of the variations in length of the anterior cruciate ligament during flexion of the knee : use of a 3D model reconstructed from MRI sections,” *Surg. Radiol. Anat.*, vol. 21, no. 5, pp. 313–317, 1999.

[60] V. B. Duthon, C. Barea, S. Abrassart, J. H. Fasel, D. Fritschy, and J. Ménétrey, “Anatomy of the anterior cruciate ligament,” *Knee Surg. Sports Traumatol. Arthrosc.*, vol. 14, no. 3, pp. 204–13, Mar. 2006.

[61] C. D. Harner, J. W. Xerogeanes, G. A. Livesay, G. J. Carlin, B. A. Smith, T. Kusayama, S. Kashiwaguchi, and S. L.-Y. Woo, “The human posterior cruciate ligament complex: an interdisciplinary study Ligament morphology and biomechanical evaluation,” *Am. J. Sports Med.*, vol. 23, no. 6, pp. 736–745, 1995.

[62] J. C. Gali, H. C. D. S. Oliveira, B. C. B. Lisboa, B. D. Dias, F. D. G. Casimiro, and E. B. Caetano, “Inserções tibiais do ligamento cruzado posterior: anatomia topográfica e estudo morfométrico,” *Rev. Bras. Ortop.*, vol. 48, no. 3, pp. 263–267, May 2013.

[63] K. M. Quapp and J. A. Weiss, “Material characterization of human medial collateral ligament,” *J. Biomech. Eng.*, vol. 120, no. 6, pp. 757–763, 1998.

[64] W. Mesfar and a Shirazi-Adl, “Biomechanics of changes in ACL and PCL material properties or prestrains in flexion under muscle force-implications in ligament reconstruction.,” *Comput. Methods Biomech. Biomed. Engin.*, vol. 9, no. February 2015, pp. 201–209, 2006.

[65] P. Fratzl, K. Misof, I. Zizak, G. Rapp, and S. Bernstorff, “Fibrillar Structure and Mechanical Properties of Collagen,” *J. Struct. Biol.*, vol. 122, pp. 119–122, 1997.

[66] V. Ottani, M. Raspanti, and a Ruggeri, “Collagen structure and functional implications,” *Micron*, vol. 32, no. 3, pp. 251–260, Apr. 2001.

[67] R. De Vita, "Structural Constitutive Models for Knee Ligaments," University of Pittsburgh, 2005.

[68] A. H. Hsieh, R. L. Sah, and K. L. Paul Sung, "Biomechanical regulation of type I collagen gene expression in ACLs in organ culture.," *J. Orthop. Res.*, vol. 20, no. 2, pp. 325–31, Mar. 2002.

[69] R. Sopakayang and R. De Vita, "A mathematical model for creep, relaxation and strain stiffening in parallel-fibered collagenous tissues.," *Med. Eng. Phys.*, vol. 33, no. 9, pp. 1056–63, Nov. 2011.

[70] D. P. Pioletti, L. R. Rakotomanana, J. Benvenuti, and P. Leyvraz, "Viscoelastic constitutive law in large deformations : application to human knee ligaments and tendons," *J. Biomech.*, vol. 31, pp. 753–757, 1998.

[71] I. A. Kapandji, "Funktionelle Anatomie der Gelenke," *Schematisierte und kommentierte Zeichnungen zur Menschl. Biomech.*, vol. 3, 1985.

[72] R. Wung, *Superimposed four-bar linkage to follow joint flexion there are no fixed link lengths*. 2009.

[73] F. H. Fu, C. D. HARNER, D. L. JOHNSON, M. D. MILLER, and S. L.-Y. WOO, "Biomechanics of knee ligaments basic concepts and clinical application," *J. Bone Jt. Surg.*, vol. 75, no. 11, pp. 1716–1727, 1993.

[74] T. J. A. Mommersteeg, L. Blankevoort, R. Huiskes, J. G. M. Kooloos, J. M. G. Kauer, and J. C. M. Hendriks, "The effect of variable relative insertion orientation of human knee bone-ligament-bone complexes on the tensile stiffness," *J. Biomech.*, vol. 28, no. 6, pp. 745–752, 1995.

[75] D. . Pioletti, L. . Rakotomanana, and P.-F. Leyvraz, "Strain rate effect on the mechanical behavior of the anterior cruciate ligament–bone complex," *Med. Eng. Phys.*, vol. 21, no. 2, pp. 95–100, Mar. 1999.

[76] J. R. Robinson, A. M. J. Bull, and A. a Amis, "Structural properties of the medial collateral ligament complex of the human knee.," *J. Biomech.*, vol. 38, no. 5, pp. 1067–74, May 2005.

[77] B. C. Fleming, B. D. Beynnon, P. a Renstrom, R. J. Johnson, C. E. Nichols, G. D. Peura, and B. S. Uh, "The strain behavior of the anterior cruciate ligament during stair climbing: an in vivo study.," *Arthroscopy*, vol. 15, no. 2, pp. 185–91, Mar. 1999.

[78] W. Petersen and T. Zantop, "Anatomy of the anterior cruciate ligament with regard to its two bundles.," *Clin. Orthop. Relat. Res.*, vol. 454, no. 0, pp. 35–47, Jan. 2007.

[79] V. Predescu, V. Georgeanu, C. Prescura, V. Stoian, and S. Cristea, "Anterior Cruciate Ligament Reconstruction: Soft Tissue vs. Bone-Tendon-Bone," *2010 Adv. Technol. Enhancing Qual. Life*, pp. 53–57, Jul. 2010.

[80] D. Subit, C. Masson, C. Brunet, and P. Chabrand, "Microstructure of the ligament-to-bone attachment complex in the human knee joint.," *J. Mech. Behav. Biomed. Mater.*, vol. 1, no. 4, pp. 360–7, Oct. 2008.

[81] L. M. Dourte, A. F. Kuntz, and L. J. Soslowsky, "Twenty-five years of tendon and ligament research," *J. Orthop. Res.*, vol. 26, no. 10, pp. 1297–1305, 2008.

[82] S. L.-Y. Woo, C. A. Orlando, J. F. Camp, and W. H. Akeson, "Effects of postmortem storage by freezing on ligament tensile behavior.," *J. Biomech.*, vol. 19, no. 5, pp. 399–404, 1986.

[83] J. C. Kennedy, R. J. Hawkins, R. B. Willis, and K. D. Danylchuk, "Tension Studies of Human Knee Ligaments. Yield Point, Ultimate Failure and Disruption of the Cruciate and Tibial Collateral Ligaments," *J Bone Jt. Surg A*, vol. 58, no. 4, pp. 350–355, 1976.

[84] G. M. Thornton, T. D. Schwab, and T. R. Oxland, "Cyclic loading causes faster rupture and strain rate than static loading in medial collateral ligament at high stress.," *Clin. Biomech. (Bristol, Avon)*, vol. 22, no. 8, pp. 932–40, Oct. 2007.

[85] D. L. Butler, Y. Guan, M. D. Kay, J. F. Cummings, S. M. Feder, and M. S. Levy, "Location-dependent variations in the material properties of the anterior cruciate ligament," *J. Biomech.*, vol. 25, no. 5, pp. 511–518, May 1992.

[86] F. R. Noyes and E. S. Grood, "The Strength of the Anterior and Rhesus Cruciate Monkeys Ligament in Humans," *J. Bone Jt. Surg. Am*, vol. 58, pp. 1074–1082, 1976.

[87] K. Mabuchi and H. Fujie, "Use of robotics technology to measure friction in animal joints.," *Clin. Biomech. (Bristol, Avon)*, vol. 11, no. 3, pp. 121–125, Apr. 1996.

[88] F. L. Buczek, E. W. Sinsel, D. S. Gloekler, B. M. Wimer, C. M. Warren, and J. Z. Wu, "Kinematic performance of a six degree-of-freedom hand model (6DHand) for use in occupational biomechanics.," *J. Biomech.*, vol. 44, no. 9, pp. 1805–9, Jun. 2011.

[89] X. Zhang, G. Jiang, C. Wu, and S. L.-Y. Woo, "A subject-specific finite element model of the anterior cruciate ligament.," *30th Annu. Int. IEEE EMBS Conf.*, vol. 2008, no. 2, pp. 891–4, Jan. 2008.

[90] G. Li, J. Gil, A. Kanamori, and S. L.-Y. Woo, "A Validated Three-Dimensional Computational Model of a Human Knee Joint," *J. Biomech. Eng.*, vol. 121, pp. 657–662, 1999.

[91] L. Blankevoort and R. Huiskes, "Validation of a three-dimensional model of the knee," *J. Biomech.*, vol. 29, no. 7, pp. 955–961, 1996.

[92] Z. Haidong, H. Rongying, Z. Hongguang, and Z. Jun, "Effects of Bony Structure Simplification Methods on Biomechanics of Knee's Cartilage, Ligaments and Menisci in Series of Flexion Angles," *Third Int. Conf. Digit. Manuf. Autom.*, pp. 351–355, Jul. 2012.

[93] A. Vairis, M. Petousis, N. Vidakis, B. Kandyla, C. Chrisoulakis, and A.-M. Tsainis, "Evaluating the efficacy of a numerical model of a human anatomy joint," *24th EAEEIE Annu. Conf. (EAEEIE 2013)*, pp. 170–173, May 2013.

[94] J. Zelle, M. Barink, M. De Waal Malefijt, and N. Verdonschot, "Thigh-calf contact: does it affect the loading of the knee in the high-flexion range?," *J. Biomech.*, vol. 42, no. 5, pp. 587–93, Mar. 2009.

[95] J.-P. Micaleff and F. Bonne, "Biomechanics of the ligaments of the human knee and of artificial ligaments," *Sur Radiol Anat*, vol. 10, pp. 221–227, 1988.

[96] A. G. Au, A. B. Liggins, V. J. Raso, J. Carey, and a Amirfazli, "Representation of bone heterogeneity in subject-specific finite element models for knee.," *Comput. Methods Programs Biomed.*, vol. 99, no. 2, pp. 154–71, Aug. 2010.

[97] Y. C. Fung, "Biorheology of soft tissues.," *Biorheology*, vol. 10, no. 2, pp. 139–155, 1973.

[98] S. L.-Y. Woo, R. E. Debski, J. Zeminski, S. D. Abramowitch, M. S. Chan Saw Serena S, and J. A. Fenwick, "Injury and repair of ligaments and tendons," *Annu. Rev. Biomed. Eng.*, vol. 2, no. 1, pp. 83–118, 2000.

[99] M. Lee and W. Hyman, "Modeling of failure mode in knee ligaments depending on the strain rate," *BMC Musculoskelet. Disord.*, vol. 3, no. 1, pp. 1–8, 2002.

[100] E. B. Goudie, E. M. Will, and J. F. Keating, "Functional outcome following PCL and complex knee ligament reconstruction.," *Knee*, vol. 17, no. 3, pp. 230–4, Jun. 2010.

[101] R. Rossi, *Knee Ligament Injuries*. Milano: Springer Milan, 2014.

[102] R. R. Regatte, *Advanced Quantitative Imaging of Knee Joint Repair*. NYU Langone Medical Center, USA: World Scientific Publishing Co. Pte. Ltd., 2014.

[103] A. F. Cipriano and H. Liu, *Nanomaterials in Tissue Engineering*. Elsevier, 2013.

[104] J. Herndon, L. S. Matthews, and P. Johnson, "Knee Ligament Injury," *Wiserhealth*, 2014. [Online]. Available: https://mywiserhealth.com/motion/knee-ligament-injury/learn/.

[105] B. C. Twaddle, T. A. Bidwell, and J. R. Chapman, "Knee Dislocations : Where Are the Lesions ? A Prospective Evaluation of Surgical Findings in 63 Cases," *J. Orthop. Trauma*, vol. 17, no. 3, pp. 198–202, 2003.

[106] E. M. B. Da Silva, M. B. Albano, H. A. A. Alberti, F. A. Pereira Filho, M. M. Namba, J. L. V. Da Silva, and L. A. M. Da Cunha, "Lesões ligamentares do joelho: Estudo biomecânico comparativo de duas técnicas de sutura em tendões: análise in vitro em tendões de bovinos," *Rev. Bras. Ortop.*, vol. 48, no. 1, pp. 80–86, Jan. 2013.

[107] M. Milankov Ziva, R. Semnic, N. Miljković, and V. Harhaji, "Reconstruction of patellar tendon rupture after anterior cruciate ligament reconstruction: a case report.," *Knee*, vol. 15, no. 5, pp. 419–22, Oct. 2008.

[108] T. L. HAUT and R. C. HAUT, "The state of tissue hydration determines the strain-rate-sensitive stiffness of human patellar tendon.," *J. Biomech.*, vol. 30, no. 1, pp. 79–81, 1997.

[109] F. R. Noyes, D. L. Butler, E. S. Grood, R. F. Zernicke, and M. S. Hefzy, "Biomechanical analysis of human ligament grafts used in knee-ligament repairs and reconstructions," *J. Bone Jt. Surg.*, 1984.

[110] G. Milano, P. D. Mulas, F. Ziranu, L. Deriu, and C. Fabbriciani, "Comparison of femoral fixation methods for anterior cruciate ligament reconstruction with patellar tendon graft: a mechanical analysis in porcine knees.," *Knee Surg. Sports Traumatol. Arthrosc.*, vol. 15, no. 6, pp. 733–8, Jun. 2007.

[111] N. G. Weiss, L. D. Kaplan, and B. K. Graf, "Graft Selection in Surgical Reconstruction of the Multiple-Ligament-Injured Knee," *Oper. Tech. Sports Med.*, vol. 11, no. 3, pp. 218–225, 2003.

[112] H. Huang, Y. Ou, P. Li, T. Zhang, S. Chen, H. Shen, Q. Wang, and X. Zheng, "Biomechanics of single-tunnel double-bundle anterior cruciate ligament reconstruction using fixation with a unique expandable interference screw.," *Knee*, vol. 21, no. 2, pp. 471–6, Mar. 2014.

[113] H.-G. Zheng, R.-Y. Huang, Q. Xu, and H.-D. Zheng, "Effects of different double-bundle anterior cruciate ligament reconstructions on femur stress," *2011 6th IEEE Conf. Ind. Electron. Appl.*, no. c, pp. 1766–1770, Jun. 2011.

[114] S. L.-Y. Woo, C. Wu, O. Dede, F. Vercillo, and S. Noorani, "Biomechanics and anterior cruciate ligament reconstruction.," *J. Orthop. Surg. Res.*, vol. 1, no. 1, p. 2, Jan. 2006.

[115] V. I. Walters, "Design and Analysis of a Collagenous Anterior Cruciate Ligament Replacement," Faculty of the Virginia Polytechnic Institute and State University, 2011.

[116] A. Vairis, M. Petousis, N. Vidakis, G. Stefanoudakis, and B. Kandyla, "Modelling a Knee Ligament Repair Device," *Ninth Int. Symp. Distrib. Comput. Appl. to Business, Eng. Sci.*, pp. 55–60, Aug. 2010.

[117] C. Wan, Z. Hao, and S. Wen, "The effect of the variation in ACL constitutive model on joint kinematics and biomechanics under different loads: a finite element study.," *J. Biomech. Eng.*, vol. 135, no. 4, p. 041002, Apr. 2013.

[118] D. K. Moon, S. L.-Y. Woo, Y. Takakura, M. T. Gabriel, and S. D. Abramowitch, "The effects of refreezing on the viscoelastic and tensile properties of ligaments.," *J. Biomech.*, vol. 39, no. 6, pp. 1153–7, Jan. 2006.

[119] H. R. C. Screen, D. a Lee, D. L. Bader, and J. C. Shelton, "An investigation into the effects of the hierarchical structure of tendon fascicles on micromechanical properties," *Proc. Inst. Mech. Eng. Part H J. Eng. Med.*, vol. 218, no. 2, pp. 109–119, Jan. 2004.

[120] P. Lertwanich, C. a Q. Martins, Y. Kato, S. J. M. Ingham, S. Kramer, M. Linde-Rosen, P. Smolinski, and F. H. Fu, "Contribution of the meniscofemoral ligament as a restraint to the posterior tibial translation in a porcine knee.," *Knee Surg. Sports Traumatol. Arthrosc.*, vol. 18, no. 9, pp. 1277–81, Sep. 2010.

[121] V. C. Mow and R. Huiskes, *Basic orthopaedic biomechanics & mechano-biology*. Lippincott Williams & Wilkins, 2005.

[122] J. A. Weiss, J. C. Gardiner, and C. Bonifasi-lista, "Ligament material behavior is nonlinear , viscoelastic and rate-independent under shear loading," *J. Biomech.*, vol. 35, pp. 943–950, 2002.

[123] S. E. Duenwald, R. Vanderby, and R. S. Lakes, "Viscoelastic relaxation and recovery of tendon.," *Ann. Biomed. Eng.*, vol. 37, no. 6, pp. 1131–40, Jun. 2009.

[124] Y. Zhang, G. Liu, and S. Q. Xie, "Biomechanical simulation of anterior cruciate ligament strain for sports injury prevention.," *Comput. Biol. Med.*, vol. 41, no. 3, pp. 159–63, Mar. 2011.

[125] K. D. Shelbourne, S. E. Lawrance, and B. Kerr, "Patellar Tendon Rupture After Anterior Cruciate Ligament Surgery," *Oper. Tech. Sports Med.*, vol. 14, no. 1, pp. 8–14, Jan. 2006.

[126] S. L. Y. Woo, J. M. Hollis, D. J. Adams, R. M. Lyon, and S. Takai, "Tensile properties of the human femur- anterior cruciate ligament-tibia complex. The effects of specimen age and orientation," *Am. J. Sports Med.*, vol. 19, no. 3, pp. 217–225, 1991.

[127] R. S. Jones, N. S. Nawana, M. J. Pearcy, D. J. A. Learmonth, D. R. Bickerstaff, J. J. Costi, and R. S. Paterson, "Mechanical Properties of the Human Anterior Cruciate Ligament," *Clin. Biomech.*, vol. 10, no. 7, pp. 339–344, 1995.

[128] J. L. Cartner, Z. M. Hartsell, W. M. Ricci, and P. Tornetta, "Can we trust ex vivo mechanical testing of fresh--frozen cadaveric specimens? The effect of postfreezing delays.," *J. Orthop. Trauma*, vol. 25, no. 8, pp. 459–61, Aug. 2011.

[129] W.-R. Su, H.-H. Chen, and Z.-P. Luo, "Effect of cyclic stretching on the tensile properties of patellar tendon and medial collateral ligament in rat.," *Clin. Biomech. (Bristol, Avon)*, vol. 23, no. 7, pp. 911–7, Aug. 2008.

[130] A. F. Dota, M. R. Zenaide, M. K. Demange, G. L. Camanho, and A. J. Hernandez, "Study of the Mechanical Properties of the Posterior Cruciate Ligament and Patellar Tendon on Fresh Human Cadavers after Radiofrequency Shrinkage.," *Acta ortop. bras*, vol. 15, no. 3, pp. 138–142, 2007.

[131] A. E. V Kokron, F. D. E. S. Prada, M. M. Soares, A. J. Hernandez, G. L. Camanho, and T. P. Leivas, "Seria o ligamento cruzado posterior o principal estabilizador do joelho ? *," *Rev. Bras. Ortop.*, vol. 28, pp. 4–9, 1993.

[132] M. H. Sadd, *Elasticity: theory, applications, and numerics*. Academic Press, 2014.

[133] J. Bonet and R. D. Wood, *Nonlinear Continuum Mechanics for Finite Element Analysis*. Cambridge: Cambridge University Press, 2008.

[134] E. Peña, M. a. Martínez, B. Calvo, D. Palanca, and M. Doblaré, "A finite element simulation of the effect of graft stiffness and graft tensioning in ACL reconstruction," *Clin. Biomech.*, vol. 20, pp. 636–644, 2005.

[135] G. A. Holzapfel, T. C. Gasser, and R. A. Y. W. Ogden, "A New Constitutive Framework for Arterial Wall Mechanics and a Comparative Study of Material Models," *J. Elast.*, vol. 61, pp. 1–48, 2001.

[136] T. C. Gasser, R. W. Ogden, and G. a Holzapfel, "Hyperelastic modelling of arterial layers with distributed collagen fibre orientations.," *J. R. Soc. Interface*, vol. 3, no. 6, pp. 15–35, 2006.

[137] J. M. Elkins, N. J. Stroud, M. J. Rudert, Y. Tochigi, D. R. Pedersen, B. J. Ellis, J. J. Callaghan, J. a. Weiss, and T. D. Brown, "The capsule's contribution to total hip construct stability-A finite element analysis," *J. Orthop. Res.*, vol. 29, no. 11, pp. 1642–1648, 2011.

[138] J. E. Kelleher, T. Siegmund, M. Du, E. Naseri, and R. W. Chan, "The anisotropic hyperelastic biomechanical response of the vocal ligament and implications for frequency regulation: A case study.," *J. Acoust. Soc. Am.*, vol. 133, no. 3, pp. 1625–1636, 2013.

[139] P. Provenzano, R. Lakes, T. Keenan, and R. Vanderby Jr, "Nonlinear ligament viscoelasticity," *Ann. Biomed. Eng.*, vol. 29, no. 10, pp. 908–914, 2001.

[140] Y. C. Fung, "Biomechanics: material properties of living tissues," *Springer*, 1993.

[141] L. E. Defrate and G. Li, "The prediction of stress-relaxation of ligaments and tendons using the quasi-linear viscoelastic model.," *Biomech. Model. Mechanobiol.*, vol. 6, no. 4, pp. 245–51, Jul. 2007.

[142] Y.-C. Fung, "Stress-strain-history relations of soft tissues in simple elongation," *Biomech. Its Found. Object.*, vol. 7, pp. 181–208, 1972.

[143] R. C. Haut and R. W. Little, "A constitutive equation for collagen fibers," *J. Biomech.*, vol. 5, no. 5, pp. 423–430, 1972.

[144] S. L.-Y. Woo, M. A. Gomez, and W. H. Akeson, "The time and history-dependent viscoelastic properties of the canine medial collateral ligament," *J. Biomech. Eng.*, vol. 103, no. 4, pp. 293–298, 1981.

[145] G. A. Johnson, G. A. Livesay, S. L. Y. Woo, and K. R. Rajagopal, "A single integral finite strain viscoelastic model of ligaments and tendons," *J. Biomech. Eng.*, vol. 118, no. 2, pp. 221–226, 1996.

[146] J. S. Horvath, "Mathematical Modeling of the Stress-Strain-Time Behavior of Geosynthetics Using the Findley Equation : General Theory and Application to EPS-Block Geofoam," *Manhattan Coll. Res. Rep. No. CE/GE-98-3*, no. May 1998, 1998.

[147] R. C. Koeller, "A Theory Relating Creep and Relaxation for Linear Materials With Memory," *J. Appl. Mech.*, vol. 77, no. 3, p. 031008, 2010.

[148] T. J. A. Mommersteeg, R. Huiskes, L. Blankevoort, J. G. M. Kooloos, J. M. G. Kauer, and P. G. . Maathuis, "A Global verification study of a quasi-static knee model with multi-bundle ligaments," *J. Biomech.*, vol. 29, no. 12, pp. 1659–1664, 1996.

[149] J. A. Silva, "Ensaios de caracterização dos ligamentos cruzados e colaterais na articulação do joelho suíno," Porto, 2014.

[150] T. D. Schwab, C. R. Johnston, T. R. Oxland, and G. M. Thornton, "Continuum damage mechanics (CDM) modelling demonstrates that ligament fatigue damage accumulates by different mechanisms than creep damage.," *J. Biomech.*, vol. 40, no. 14, pp. 3279–84, Jan. 2007.

[151] G. K. McPherson, H. V Mendenhall, D. F. Gibbons, H. Plenk, W. Rottmann, J. B. Sanford, J. C. Kennedy, and J. H. Roth, "Experimental mechanical and histologic evaluation of the Kennedy ligament augmentation device," *Clin. Orthop. Relat. Res.*, no. 196, pp. 186–195, 1985.

[152] M. P. Prietto, J. R. Bain, S. N. Stonebrook, and R. A. Settlage, "Tensile strength of the human posterior cruciate ligament (PCL)," *Trans Orthop Res Soc*, vol. 13, no. 195, pp. 736–745, 1988.

[153] A. Race and A. a. Amis, “The mechanical properties of the two bundles of the human posterior cruciate ligament,” *J. Biomech.*, vol. 27, no. 1, pp. 13–24, Jan. 1994.

[154] D. L. Butler, M. Dressler, and H. Awad, “Functional tissue engineering: assessment of function in tendon and ligament repair,” in *Functional Tissue Engineering*, Springer, 2003, pp. 213–226.

[155] R. V. Hingorani, P. P. Provenzano, R. S. Lakes, A. Escarcega, and R. Vanderby, “Nonlinear viscoelasticity in rabbit medial collateral ligament,” *Ann. Biomed. Eng.*, vol. 32, no. 2, pp. 306–312, 2004.

[156] P. S. Trent, P. S. Walker, and B. Wolf, “Ligament length patterns, strength, and rotational axes of the knee joint,” *Clin. Orthop. Relat. Res.*, vol. 117, pp. 263–270, 1976.

[157] J. a W. Van Dommelen, B. J. Ivarsson, M. M. Jolandan, S. a Millington, M. Raut, J. R. Kerrigan, and J. R. Crandall, “Characterization of the Rate-Dependent Mechanical Properties and Failure of Human Knee Ligaments,” *SAE Tech. Pap.*, vol. No. 2005–0, 2005.

[158] G. Marinozzi, S. Pappalardo, and R. Steindler, “Human knee ligaments: mechanical tests and ultrastructural observations.,” *Ital. J. Orthop. Traumatol.*, vol. 9, no. 2, pp. 231–240, 1983.

[159] R. D. Crowninshield and M. H. Pope, “The strength and failure characteristics of rat medial collateral ligaments.,” *J. Trauma Acute Care Surg.*, vol. 16, no. 2, pp. 99–105, 1976.

[160] S. S. Quek and G. R. Liu, *Finite element method: a practical course*, 2nd ed. Butterworth-Heinemann, 2014.

[161] M. T. Junior, E. A. Fancello, C. R. de M. Roesler, and A. D. O. More, “Simulação numérica tridimensional da mecânica do joelho humano,” *Acta Ortop Bras*, vol. 17, no. 2, pp. 18–23, 2008.

[162] M. Tuna, E. Sunbuloglu, and E. Bozdag, “Finite element simulation of the behavior of the periodontal ligament: a validated nonlinear contact model.,” *J. Biomech.*, vol. 47, no. 12, pp. 2883–90, Sep. 2014.

[163] J. Zelle, P. J. C. Heesterbeek, M. De Waal Malefijt, and N. Verdonschot, “Numerical analysis of variations in posterior cruciate ligament properties and balancing techniques on total knee arthroplasty loading.,” *Med. Eng. Phys.*, vol. 32, no. 7, pp. 700–7, Sep. 2010.

[164] J. Zelle, a C. Van der Zanden, M. De Waal Malefijt, and N. Verdonschot, “Biomechanical analysis of posterior cruciate ligament retaining high-flexion total knee arthroplasty.,” *Clin. Biomech. (Bristol, Avon)*, vol. 24, no. 10, pp. 842–9, Dec. 2009.

[165] A. Erdemir, S. Sibole, C. Bennetts, B. Borotikar, S. Maas, A. J. van den Bogert, and J. A. Weiss, “Open Knee : A Three Dimensional Finite Element Representation of the Knee Joint,” *34th Annu. Meet. Am. Soc. Biomech.*, 2010.

[166] J. C. Gardiner and J. a Weiss, “Subject-specific finite element analysis of the human medial collateral ligament during valgus knee loading.,” *J. Orthop. Res.*, vol. 21, no. 6, pp. 1098–1106, 2003.

[167] E. Peña, B. Calvo, M. a Martínez, and M. Doblaré, “A three-dimensional finite element analysis of the combined behavior of ligaments and menisci in the healthy human knee joint.,” *J. Biomech.*, vol. 39, no. 9, pp. 1686–701, Jan. 2006.

[168] G. Limbert, M. Taylor, and J. Middleton, “Three-dimensional finite element modelling of the human ACL: Simulation of passive knee flexion with a stressed and stress-free ACL,” *J. Biomech.*, vol. 37, no. 11, pp. 1723–1731, 2004.

[169] M. Ozkan, N. E. Akalan, and Y. Temelli, "Interaction of ligament bundles and articular contacts for the simulation of passive knee flexion," in *Annual International Conference of the IEEE Engineering in Medicine and Biology - Proceedings*, 2007, pp. 4297–4300.

[170] T. Wang, Z. Hao, and C. Wan, "The Effect of Anterior Cruciate Ligament Injury on the Biomechanical Behavior of Human Knee Joint," *2nd Int. Conf. Biomed. Eng. Informatics*, pp. 1–5, 2009.

[171] Y. Zhong, Y. Wang, H. Wang, K. Rong, and L. Xie, "Stress changes of lateral collateral ligament at different knee flexion with or without displaced movements: a 3-dimensional finite element analysis," *Chinese J. Traumatol. English Ed.*, vol. 14, no. 2, pp. 79–83, 2011.

[172] Z. Gaolong, H. Rongying, Z. Hongguang, and G. Yunfei, "Effects of Posterior Cruciate Ligament Deficient on Biomechanics of Knee's Principal Ligaments at Different Flexion Angles," *2012 Third Int. Conf. Digit. Manuf. Autom.*, pp. 369–372, Jul. 2012.

[173] A. D. Orsi, S. Chakravarthy, H. Nayeb-hashemi, P. K. Canavan, and R. Goebel, "Investigating the Effects of Knee Joint Motion Schemes on Knee Joint Injury A Finite Element Analysis," *IEEE*, pp. 1–2, 2014.

[174] M. Veselko and I. Godler, "Biomechanical study of a computer simulated reconstruction of the anterior cruciate ligament (ACL)," *Comput. Biol. Med.*, vol. 30, no. 6, pp. 299–309, Nov. 2000.

[175] E. Peña, B. Calvo, M. a. Martinez, D. Palanca, and M. Doblaré, "Influence of the tunnel angle in ACL reconstructions on the biomechanics of the knee joint," *Clin. Biomech.*, vol. 21, pp. 508–516, 2006.

[176] C. Wan, Z. Hao, and S. Wen, "The finite element analysis of three grafts in the anterior cruciate ligament reconstruction," *2011 4th Int. Conf. Biomed. Eng. Informatics*, pp. 1338–1342, Oct. 2011.

[177] R. W. Westermann, B. R. Wolf, and J. M. Elkins, "Effect of ACL Reconstruction Graft Size on Simulated Lachman Testing: A Finite Element Analysis," *Iowa Orthop. J.*, vol. 33, pp. 70–77, 2013.

[178] L. Bogdan, N. Faur, R. J. Natal, and M. Parente, "Nitinol Artificial Anterior Cruciate Ligament : A Finite Element Study," *E-Health and Bioengineering Conference (EHB). IEEE*, 2013.

[179] J. Okrajni, M. Plaza, and S. Ziemba, "Validation of computer models of an artificial hip joint," *Arch. Mater. Sci. Eng.*, vol. 28, no. 5, pp. 305–308, 2007.

[180] K. L. Moffat, W.-H. S. Sun, N. O. Chahine, P. E. Pena, S. B. Doty, C. T. Hung, G. a Ateshian, and H. H. Lu, "Characterization of the mechanical properties and mineral distribution of the anterior cruciate ligament-to-bone insertion site.," *Conf. Proc. ... Annu. Int. Conf. IEEE Eng. Med. Biol. Soc. IEEE Eng. Med. Biol. Soc. Annu. Conf.*, vol. 1, pp. 2366–9, Jan. 2006.

[181] M. Kub, "Stress strain analysis of knee joint," *Eng. Mech.*, vol. 16, no. 5, pp. 315–322, 2009.

[182] M. Abdi and A. Karimi, "Stress distribution analysis in healthy and pathologic knee joint : A finite element study," *Int. J. Adv. Biol. Sci. Eng.*, vol. 1, no. 1, pp. 1–16, 2014.

[183] J. M. Carneiro, "Estudo Biomecânico da Articulação do Joelho," Universidade do Porto, 2010.

[184] F. R. Berry, *Angle Variation Patterns of Normal Hip, Knee, and Ankle in Different Operations*. Prosthetic Devices Research Project, Institute of Engineering Research, University of California, 1952.

[185] I. P. Herman, *Physics of the human body*. Springer Science & Business Media., 2007.

[186] K. Shamaei and A. M. Dollar, "On the mechanics of the knee during the stance phase of the gait.," *IEEE Int. Conf. Rehabil. Robot.*, vol. 2011, p. 5975478, Jan. 2011.

[187] A. Chincisan, H. Choi, L. Assassi, S. Lynch, C. Hurschler, and N. Magnenat-Thalmann, "Subject-specific assessment of loading variation in the knee ligaments with a view to preoperative planning," in *IEEE BHI*, 2014, pp. 640–643.

[188] S. G. Kulkarni, X.-L. Gao, S. E. Horner, R. F. Mortlock, and J. Q. Zheng, "A transversely isotropic visco-hyperelastic constitutive model for soft tissues," *Math. Mech. Solids*, no. June, p. Accepted in May 2014, 2014.

[189] J. E. Bischoff, E. Siggelkow, D. Sieber, M. Kersh, H. Ploeg, and M. Münchinger, "Advanced material modeling in a virtual biomechanical knee," in *Abaqus Users' Conference*, 2008, pp. 1–15.

[190] C.-H. Lee, G.-S. Huang, K.-H. Chao, S.-S. Wu, and Q. Chen, "Differential pretensions of a flexor tendon graft for anterior cruciate ligament reconstruction: a biomechanical comparison in a porcine knee model.," *Arthroscopy*, vol. 21, no. 5, pp. 540–6, May 2005.

[191] S. Hirokawa, K. Yamamoto, and T. Kawada, "Circumferential measurement and analysis of strain distribution in the human ACL using a photoelastic coating method," *J. Biomech.*, vol. 34, no. 9, pp. 1135–1143, 2001.

[192] B. D. Beynnon and B. C. Fleming, "Anterior cruciate ligament strain in-vivo: A review of previous work," *J. Biomech.*, vol. 31, no. 6, pp. 519–525, Jun. 1998.

[193] S. Hirokawa and R. Tsuruno, "Three-dimensional deformation and stress distribution in an analytical/computational model of the anterior cruciate ligament," *J. Biomech.*, vol. 33, no. 9, pp. 1069–1077, 2000.

[194] J. C. Gardiner, J. a Weiss, and T. D. Rosenberg, "Strain in the human medial collateral ligament during valgus loading of the knee.," *Clin. Orthop. Relat. Res.*, no. 391, pp. 266–274, 2001.

[195] M. Bendjaballah, a Shirazi-Adl, and D. Zukor, "Finite element analysis of human knee joint in varus-valgus," *Clin. Biomech.*, vol. 12, no. 3, pp. 139–148, 1997.

[196] R. S. Behnke, *Kinetic Anatomy With Web Resource*. Human Kinetics, 2012.

[197] P. Landreau, "PCL injury diagnosis and treatment options," *Aspetar, Sport. Med. J.*, pp. 246–254, 2015.

[198] M. S. Schulz, K. Russe, A. Weiler, H. J. Eichhorn, and M. J. Strobel, "Epidemiology of posterior cruciate ligament injuries.," *Arch. Orthop. Trauma Surg.*, vol. 123, no. 4, pp. 186–191, 2003.

[199] L. E. Claes, A. Beyer, W. Krischke, and R. Schmid, "Biomechanical properties of collateral and cruciate ligaments," in *Biomechanics of Human Knee Ligaments, Proc. European Society of Biomechanics*, 1987, p. 22.

[200] A. M. J. Bull, "Measurement and computer simulation of knee kinematics," Imperial College London (University of London), 1999.

[201] M. Mylle, S. Claes, P. Verdonk, and J. Bellemans, "A novel core biopsy technique for anterior cruciate ligament preserves ligament structural integrity: a porcine study.," *Arthroscopy*, vol. 30, no. 1, pp. 80–5, Jan. 2014.

APPENDIX

Annex I	Clamp's drawings
Annex II	Ligament mechanical properties resume
Annex III	Porcine ligament anatomical measurements
Annex IV	FE Ligament anatomical measurements
Annex V	Bone cement PALAMED ® Data sheet
Annex VI	FREKOTE ® Data Sheet
Annex VII	Mechanical testing with plaster
Annex VIII	1st Doctoral Congress in Engineering

Annex I - Clamp's drawings

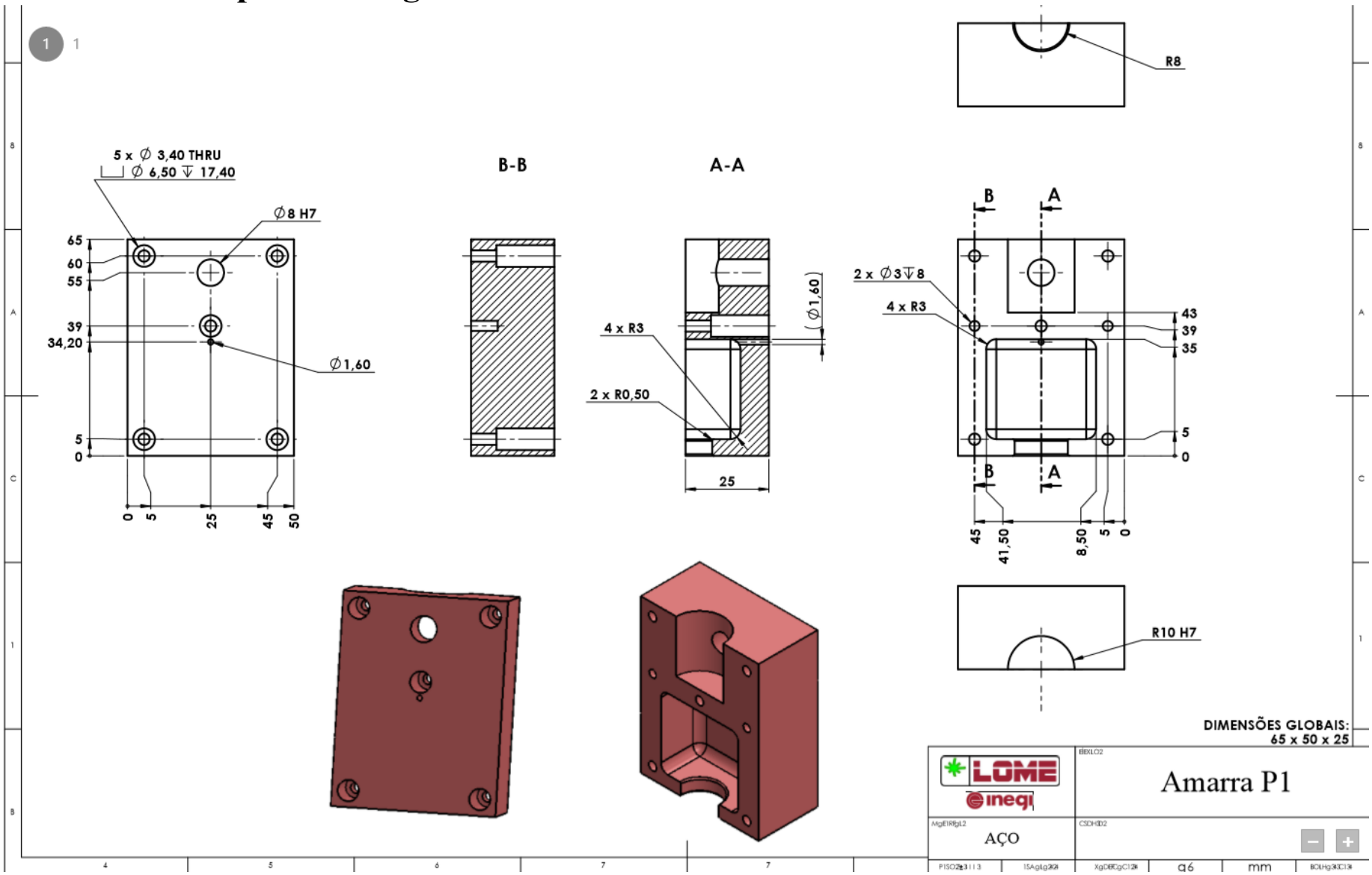

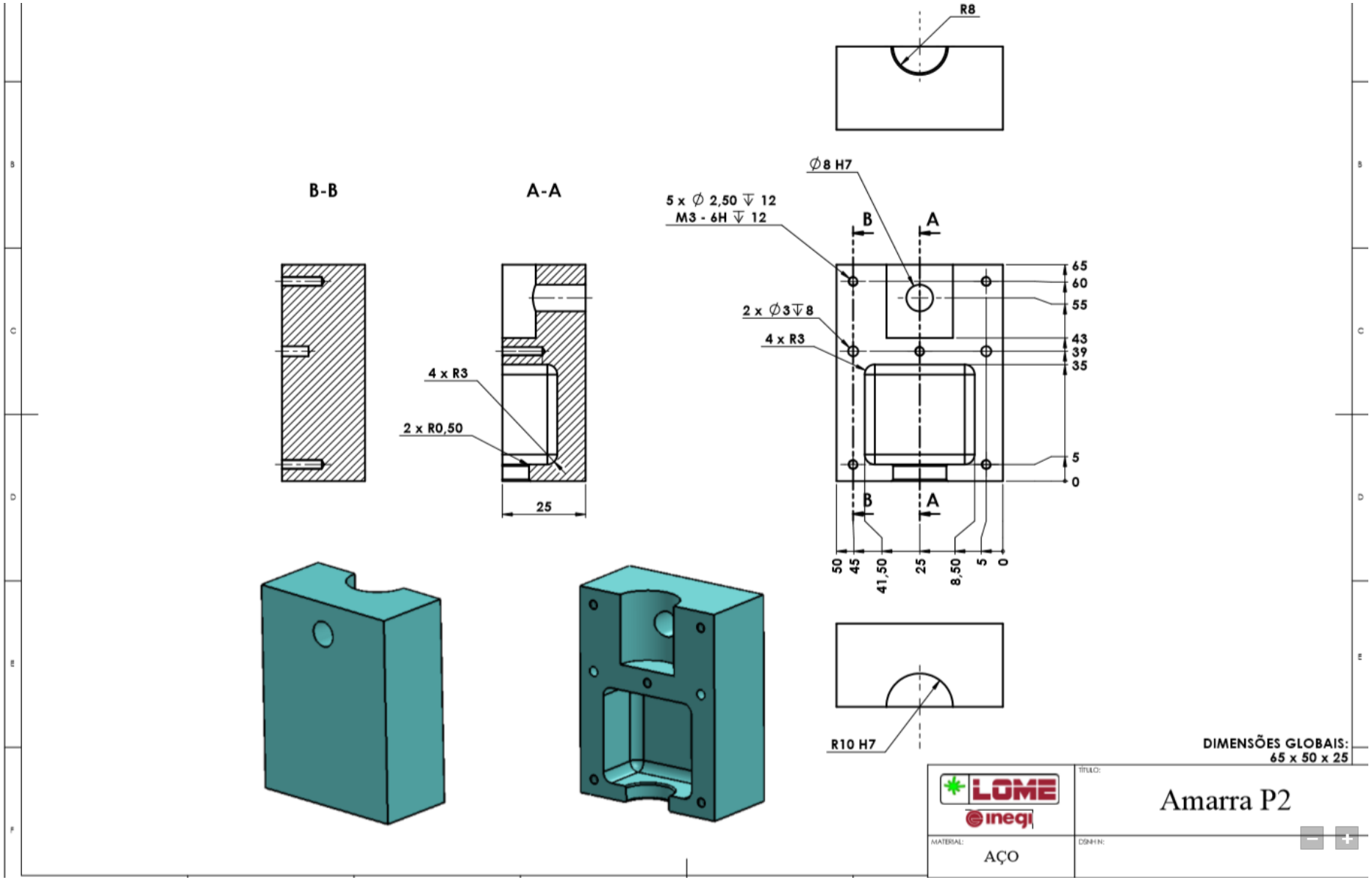
R8
B-B
A-A
∅8 H7
5 x ∅ 2,50 ↧ 12
M3 - 6H ↧ 12
B
A
2 x ∅3↧8
4 x R3
4 x R3
2 x R0,50
25
65
60
55
43
39
35
5
0
50
45
41,50
25
8,50
5
0
R10 H7
DIMENSÕES GLOBAIS:
65 x 50 x 25
LOME
inegi
TITULO:
Amarra P2
MATERIAL:
AÇO
DENHIN:

Annex II - Ligament mechanical properties resume

***Table 0-1** – Overall state of art table with ligament mechanical properties under uniaxial tensile tests.*

	Bundle	*Reference*	*Specie*	*N° of Specimens*	*Age*	*Young's modulus (MPa)*	*Ultimate Load (N)*	*Ultimate Stress (MPa)*	*Ultimate Strain (%)*	*Stiffness (N. mm^{-1})*	*Pre-condition*	*Strain rate/ velocity*
ACL	(-)	Chandrashekar et al. (2006) [32]	Human	17	17-50	128 ± 35	1526 ±658	24.36 ± 9.38	0.28 ± 0.07	308 ± 89	20 cycles between 25 - 150 N at 0.25 Hz	100%/s
	(-)	Butler et al. (1986) [18]	Human	3	21,30,30	309,7 ± 29.5	--------	34,3 ± 3,96	13,4 ± 1,75	--------	--------	100%/s
	(-)	Noyes et Grood et al. (1976) [86]	Human	20	48-86	65,3 ± 24,0	734 ±266	13,3 ± 5,0	48,5 ± 11,9	129 ± 39	--------	1/s
	(-)		Human	6	16-26	111 ± 26	1730 ± 660	37,8 ± 9,3	60,25 ±6,78	182 ± 56	--------	1/s
	(-)		Rhesus Monkey	25	--------	186 ± 26	830 ± 0.11	66.1 ± 8.4	60 ± 6.3	194 ± 28	--------	0.66/s
	(-)	Woo et al. (1991) [126]	Human	9	22-35	--------	2169 ± 157	--------	--------	242 ± 28	10 cycles between 0-2 mm at 20 mm.min^{-1}	200 mm.min^{-1}
	(-)		Human	9	40-50	--------	1503 ± 83	--------	--------	220 ± 24		
	(-)		Human	9	60-97	--------	658 ± 129	--------	--------	180 ± 25		
	(-)	Trent et al. (1976) [156]	Human	10	29-55	--------	--------	--------	--------	141 ± 99	5 cycles of 150 N	500 mm.min^{-1}
	(-)	Mommersteeg et al. (1995) [74]	Human	3	63-81 Av. 69	--------	--------	--------	8.6 ± 1.1	201 ± 102	--------	57%/s ± 7.4
	AM	Butler et al. (1992) [85]	Human	7	21-30 (Av.26)	283.1 ± 114.4	--------	45.7 ± 19.5	19.1 ± 2.8	--------	--------	100%/s
	AL		Human	7	21-30 (Av.26)	285.9 ± 140.6	--------	30.6 ± 11.0	16.1 ± 3.9	--------	--------	100%/s
	PB		Human	7	21-30 (Av.26)	154.9 ± 119.5	--------	15.4 ± 9.5	15.2 ± 5.2	--------	--------	100%/s
	(-)	Kennedy et al. (1976) [83]	Human	10	--------	--------	472.4 ± 27.4	--------	30.8 ± 2.3	--------	--------	125 mm.min^{-1}
	(-)		Human	10	--------	--------	625.2 ± 22.5	--------	35.8 ± 2.8	--------	--------	500 mm.min^{-1}

	Bundle	*Reference*	*Specimen*	*Nº of Specimens*	*Age*	*Young's modulus (MPa)*	*Ultimate Load (N)*	*Ultimate Stress (MPa)*	*Ultimate Strain (%)*	*Stiffness (N. mm^{-1})*	*Pre-condition*	*Strain rate/ velocity*
PCL	PM	Harner et al. (1995) [61]	Human	5	48-77 (Av. 64)	294 ± 115	419 ± 128	--------	--------	57 ± 22	10 cycles between 0 - 2 mm at 20 mm.min^{-1}	200 mm.min^{-1}
	AL		Human	5	48-77 (Av. 64)	150 ± 69	1120 ± 362	--------	--------	120± 37		
	(-)	Trent et al. (1976) [156]	Human	6	29-55	--------	--------	--------	--------	180 ± 58	5 cycles of 150 N	500 mm.min^{-1}
	(-)	Marinozzi et al. (1983) [158]	Human	5	55-90	--------	855 ± 225	--------	20 ± 5	145 ±66	--------	--------
	(-)	Prietto et al. (1988) [152]	Human	4	22.5 ± 3	109 ±50	1627 ± 491	26.8± 9.1	28.5 ± 9.1	204 ± 49	--------	--------
	(-)	Butler et al. (1986) [18]	Human	3	21,30,30	384,7 ± 71.07	--------	38,5 ± 4,74	15,9 ± 2,40	--------	--------	100%/s
	PM	Race et Amis (1994) [153]	Human	7	74 ± 14	145 ± 69	258±83	24.4 ± 10.0	19.5 ± 5.4	77 ± 32	--------	1000 mm.min^{-1} (~50%/s)
	AL		Human	7	75 ± 14	248 ±119	1620 ± 500	35.9 ±15.2	18.0 ± 5.3	347 ± 140	--------	
	(-)	Mommersteeg et al. (1995) [74]	Human	4	63-81 Av. 69	--------	--------	--------	7.7 ± 0.67	258 ± 62	--------	53.3 ± 6.1 %/s
	(-)	Kennedy et al. (1976) [83]	Human	10	--------	--------	921.2 ± 47.0	--------	28.3 ± 1.9	--------	--------	125 mm.min^{-1}
	(-)		Human	10	--------	--------	1951.54 ± 79.38	--------	24.2 ± 2.1	--------	--------	500 mm.min^{-1}

	Reference	Specimen	Nº of Specimens	Age	Young's modulus (MPa)	Ultimate Load (N)	Ultimate Stress (MPa)	Ultimate Strain (%)	Stiffness (N. mm^{-1})	Pre-condition	Strain rate / velocity
MCL	Quapp et Weiss (1998) [63]	Human	10	62 ± 18	332.2 ± 58.3	467 ± 33.32	38.6 ± 4.8	17.1 ± 1.5	--------	10 cycles of 0.5 mm at 10 mm.min^{-1}	10 mm.min^{-1}
	Trent et al. (1976) [156]	Human	4	29-55	--------	516	--------	--------	72 ± 17	5 cycles of 150 N	500 mm.min^{-1}
	Claes et al. (1987) [199]	Human	10	--------	--------	--------	--------	--------	94 ± 21	--------	--------
	Mommersteeg et al. (1995) [74]	Human	2	63-81 Av. 69	--------	--------	--------	6.8 ± 0.5	134 ± 1	--------	71%/s ± 3.3
	Robinson et al. (2005) [76]	Human	8	72-89		534 (supMCL), 194 (deep MCL), 425 (Posteromedia capsule)		Extension (mm): 10.2 ± 1.1; 7.1 ± 1.1; 12.0 ± 3.0	80 ± 8; 42 ± 14; 56 ± 20	10 cycles between 1-40 N at 10 mm.min^{-1}	1000 mm.min^{-1}
	Marinozzi et al. (1983) [158]	Human	5	55-90	--------	465 ± 190	--------	--------	60 ± 22	--------	100 mm.min^{-1}
	Bull et al. (1998) [200]	Human	2	59, 74	--------	--------	--------	--------	44.3	--------	200 mm.min^{-1} (~ 50%/s)
	Thornton et al. (2007) [84]	Rabbit	47	--------	--------	--------	97.7 ± 12.6	--------	--------	30 cycles from 1N to 5% of UTS	20 mm.min^{-1}
	Kennedy (1976) [83]	Human	10	--------	--------	467.5± 33.3	--------	23.0 ± 2.4	--------	--------	125 mm.min^{-1}
		Human	10	--------	--------	664.4 ± 74.48	--------	24.3 ± 1.3	--------	--------	500 mm.min^{-1}

	Reference	*Specimen*	*Nº of Specimens*	*Age*	*Young's modulus (MPa)*	*Ultimate Load (N)*	*Ultimate Stress (MPa)*	*Ultimate Strain (%)*	*Stiffness (N. mm^{-1})*	*Pre-condition*	*Strain rate / velocity*
LCL	Butler et al. (1986) [18]	Human	3	21,30,30	372 ± 33,9	--------	36,5 ± 6,16	13,23 ± 3,13	--------	--------	100%/s
	Trent et al. (1976) [156]	Human	4-6	29-55	--------	--------	--------	--------	61 ± 43	5 cycles of 150 N	500 mm.min^{-1}
	Claes et al. (1987) [201]	Human	10	--------	--------	--------	--------	--------	47 ± 13	--------	--------
	Mommersteeg et al. (1995) [74]	Human	3	63-81 Av. 69	--------	--------	--------	6.7 ± 0.1	114 ± 29	--------	62 %/s ± 6.6
	Bonner et al. (2014) [48]	Porcine	7	--------	288	--------	39.9	17	--------	1-10 N at 10 mm.min-1	0.01/s
		Porcine	7	--------	364	--------	56.5	18	--------	1-10 N at 10 mm.min-1	0.1/s
		Porcine	7	--------	656	--------	72.8	15	--------	1-10 N at 10 mm.min-1	1/s
		Porcine	7	--------	763	--------	75.9	11	--------	1-10 N at 10 mm.min-1	10/s
		Porcine	12	--------	906	--------	77.4	9	--------	1-10 N at 10 mm.min-1	100/s

Annex III - Porcine ligament anatomical measurements

Table 0-2- *Porcine ACL measurements after the mechanical tests.*

ACL ID	Length (mm)	Proximal width (mm)	Medial width (mm)	Distal width (mm)	Thickness (mm)	Cross-sectional area (mm^2)
1	49,53	11,36	7,45	8,75	4,37	31,53
2	50,82	6,32	7,38	7,06	3,80	20,65
3	49,68	8,27	9,95	11,56	4,39	34,23
4	45,43	9,90	9,70	8,53	2,16	15,91
5	54,11	8,42	8,03	9,04	4,64	30,96
6	45,96	9,13	9,22	8,42	3,72	26,07
7	45,06	8,67	9,01	9,15	4,01	28,17
8	51,80	13,00	11,00	14,00	5,80	57,70
9	54,10	10,00	12,00	13,00	5,60	51,31
10	54,90	9,00	10,90	11,20	5,50	44,78
11	53,20	15,50	14,50	13,40	5,90	67,04
12	45,91	9,96	9,60	11,35	5,18	41,92
Mean	50,04	9,96	9,90	10,46	4,59	37,52
±SD	3,70	2,41	2,02	2,26	1,09	15,38

Table 0-3- *Porcine PCL measurements after the mechanical tests.*

PCL ID	Length (mm)	Proximal width (mm)	Medial width (mm)	Distal width (mm)	Thickness (mm)	Cross-sectional area (mm^2)
1	65,19	9,31	7,88	11,27	4,08	30,40
2	56,85	10,26	9,58	11,58	4,57	37,59
3	41,79	8,55	9,19	11,51	4,31	33,00
4	41,25	6,95	10,40	6,90	3,60	22,86
5	51,55	7,30	9,05	6,75	3,33	20,14
6	34,65	7,20	9,70	9,23	3,90	26,68
7	56,35	9,25	11,95	10,65	4,10	34,19
8	36,90	14,00	13,00	16,00	4,50	50,66
9	64,80	16,00	16,00	17,00	4,50	57,73
10	76,40	19,00	11,30	12,10	4,40	48,84
11	77,80	24,50	14,30	13,20	4,60	62,62
12	50,35	10,20	8,95	11,20	3,55	28,21
Mean	54,49	11,88	10,94	11,45	4,12	37,74
±SD	14,52	5,47	2,45	3,07	0,44	13,96

Table 0-4- *Porcine MCL measurements after the mechanical tests.*

MCL ID	Length (mm)	Proximal width (mm)	Medial width (mm)	Distal width (mm)	Thickness (mm)	Cross-sectional area (mm^2)
1	65,50	14,00	11,00	16,00	2,50	26,83
2	65,80	15,00	19,00	17,00	2,60	34,71
3	73,90	11,10	9,00	11,10	2,30	18,79
4	78,64	11,33	10,02	12,79	2,94	26,28
5	65,93	13,03	9,15	10,16	2,80	23,71
6	67,05	8,72	6,98	15,38	2,50	20,34
7	90,61	18,64	16,98	13,51	4,33	42,68
8	66,93	10.52	11,24	13,56	2,81	27,70
9	74,99	7,89	9,11	7,63	2,01	19,81
10	69,36	15,45	19,77	16,43	4,16	41,01
11	79,82	5,69	6,28	9,19	2,91	28,69
12	87,10	18,10	13,60	17,50	2,50	32,20
Mean	73,80	12,46	11,84	13,35	2,86	26,12
±SD	8,68	4,00	4,53	3,26	0,70	5,84

Table 0-5- *Porcine LCL measurements after the mechanical tests.*

LCL ID	Length (mm)	Proximal width (mm)	Medial width (mm)	Distal width (mm)	Thickness (mm)	Cross-sectional area (mm^2)
1	80,60	10,00	6,00	10,00	2,90	19,74
2	99,66	21,37	9,64	9,55	2,60	27,61
3	83,35	14,45	10,09	10,25	2,05	18,67
4	101,20	15,00	7,00	12,00	3,10	27,59
5	103,90	12,00	15,40	21,10	2,80	35,55
Mean	93,74	14,56	9,63	12,58	2,69	25,83
±SD	10,89	4,30	3,66	4,85	0,40	6,88

Annex IV - FEM Ligament anatomical measurements

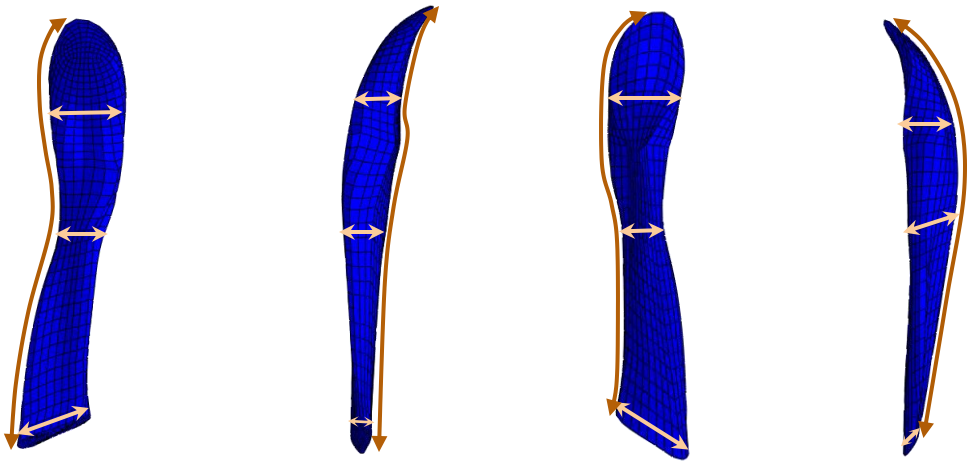

(a) **(b)** **(c)** **(d)**

Figure 0-1*-Anterior cruciate ligament.* ***(a)*** *Anterior view,* ***(b)*** *medial view,* ***(c)*** *posterior view and* ***(d)*** *lateral view.*

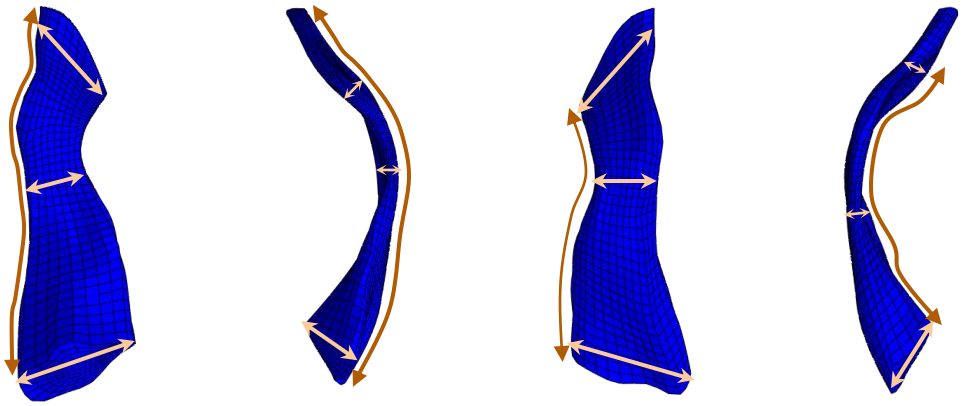

(a) **(b)** **(c)** **(d)**

Figure 0-2*- Posterior cruciate ligament.* ***(a)*** *Anterior view,* ***(b)*** *medial view****, (c)*** *posterior view and* ***(d)*** *lateral view.*

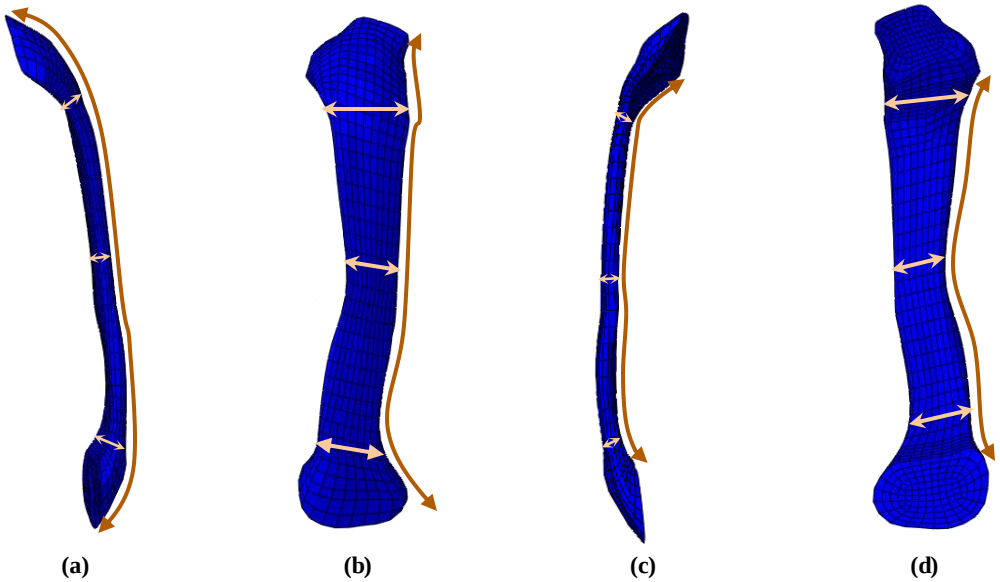

(a) **(b)** **(c)** **(d)**

Figure 0-3 *–Medial collateral ligament.* ***(a)*** *Anterior view****, (b)*** *medial view,* ***(c)*** *posterior view and* ***(d)*** *lateral view.*

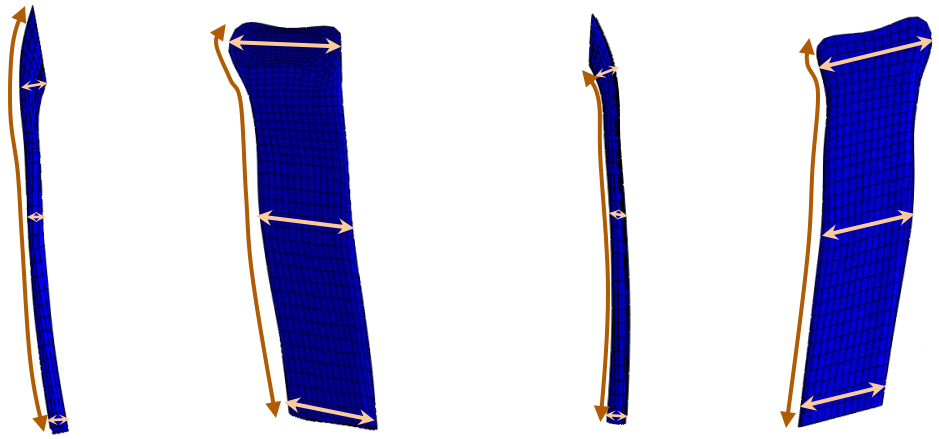

Figure 0-4 *- Lateral collateral ligament.* ***(a)*** *Anterior view,* ***(b)*** *medial view,* ***(c)*** *posterior view and* ***(d)*** *lateral view.*

Table 0-6*-Ligament measurements. Length, width and width (mm) and elliptical cross-sectional area (mm^2). P – Proximally, MS-Mid-substance, D-Distally and M - Mean ± SD*

Ligaments	Length (mm)	Thickness (mm)	Width (mm)	Cross-sectional Area (mm^2)
ACL	38.78	P: 3.36 MS:2.29 D: 1.86 M: 2.50 ± 0.77	P: 6.84 MS:4.93 D: 7.73 M: 6.5 ± 1.43	P: 18.05 MS:8.87 D: 11.29 M: 12.73 ± 4.76
PCL	32.59	P: 6.69 MS:1.55 D: 1.92 M: 3.39 ± 2.87	P: 12.55 MS:6.49 D: 12.69 M: 10.58 ± 3.54	P: 65.94 MS:7.90 D: 19.14 M: 28.17 ±30.78
MCL	63.87	P: 3.17 MS:2.05 D: 3.67 M: 2.96 ± 0.83	P: 13.20 MS:6.13 D: 10.29 M: 9.67 ± 3.55	P: 32.86 MS:9.87 D: 29.66 M: 24.13 ± 12.45
LCL	30.05	P: 3.39 MS:0.90 D: 1.16 M: 1.82 ± 1.37	P: 9.52 MS:7.52 D: 6.54 M: 7.86 ± 1.53	P: 25.35 MS:5.32 D: 5.21 M: 11.38 ±14.52

Annex V – Bone Cement PALAMED ® Data Sheet

PALAMED®

EN

Properties – Composition
PALAMED® is a radiopaque, quick-setting bone cement and exhibits low initial viscosity. It is obtained by mixing a polymer powder component with a liquid monomer component. Zirconium oxide has been added to the cement powder as an X-ray contrast medium. The sterile-filtrated monomer component is supplied in an amber glass ampoule and comes in a sterile blister pack.
The polymer powder component is supplied in a double sterile packaging. The inner polyethylene sachet which contains the powder component is wrapped in an additional polyethylene sachet; both sachets were sterilized with ethylene oxide. The polyethylene sachets are contained in a non-sterile protective aluminium packaging.
Chlorophyll (Type E141) has been used to obtain the green colour of **PALAMED®** in order to ensure clear visibility of the cement at the operating site. After mixing, a plastic dough is obtained which is filled into the bone as an anchoring medium. The cement which then hardens in the bone allows stable fixation of the endoprostheses. The stress forces resulting from motions are transferred via the cement coating widely onto the bone.

Intended use
PALAMED® is a radiopaque cement-like substance which allows the implantation and fixation of prostheses in the bone.

Indications
PALAMED® is indicated for the fixation of prostheses in the bone in partial and total arthroplastic surgery of the hip, knee or other joints.

Contraindications
PALAMED® must not be used during pregnancy or nursing. In cases of known hypersensitivity to the constituents of the bone cement **PALAMED®** must not be used..

Warning information – Side effects
PALAMED® has not been evaluated with regard to spinal surgery. In some cases, the use of this cement beyond the listed indications in spine surgery resulted in serious, life-threatening complications. Cases of pulmonary embolism, respiratory and cardiac insufficiency and death have been reported.

Composition	**PALAMED® 1x40** **PALAMED® 2x40**
	1 sachet of 44 g powder contains:
Poly (methyl acrylate, methyl methacrylate)	38.3 g
Zirconium dioxide	5.3 g
Benzoyl peroxide	0.4 g
	1 ampoule of 20 ml liquid contains:
Methyl methacrylate	18.4 g
N,N-Dimethyl-p-toluidine	0.4 g
Other constituents:	In the powder: colourant E141 In the liquid: colourant E141, hydroquinone

Prior to using **PALAMED®** the surgeon should be familiar with its properties, handling and application during arthroplastic surgery. It is also recommended for surgeons to practice mixing, handling and application of **PALAMED®** prior to the use. Precise knowledge is also required, if mixing systems and syringes are used for the application of the cement. The monomer liquid is highly volatile and flammable; accordingly, suitable precautionary measures should be taken for the use in the operating room. The monomer is also a powerful lipid solvent and should not come into direct contact with the body. When working with the monomer or the cement, gloves must be worn to ensure adequate protection against the penetration of the monomer (methyl methacrylate) into the skin. PVP (three-layer polyethylene, ethylene-vinyl alcohol-copolymer, polyethylene) and Viton/Butyl gloves have proven to provide good protection over an extended period. Wearing two pairs of gloves has also proved to offer adequate protection.
The use of latex or polystyrene-butadiene gloves, however, must be avoided. Please request the confirmation of your glove supplier whether the respective gloves are suitable for the use with **PALAMED®**.
The monomer vapors may irritate the respiratory tract and the eyes and possibly damage the liver. Skin irritations have been reported, which must be attributed to the contact with the monomer. Manufacturers of soft contact lenses recommend the removal of the lenses in the presence of harmful or irritating vapors. Since contact lenses are permeable to liquids and gases, they should not be worn in the operating room if methyl methacrylate is used.

Precautionary measures
Blood pressure, pulse and breathing must be carefully monitored during and immediately after implanting the bone cement. Any significant change of these vital signs must be immediately responded to with adequate measures.
If **PALAMED®** is used for a total hip endoprosthesis, the proximal part of the medullary (bone marrow) canal of the femur and the acetabulum need to be thoroughly cleaned, aspirated and dried.
To reduce the considerable increase in pressure in the intraosseous area during the implantation of the prosthesis, it is recommended to use suction drainage. If pulmonary, cardiovascular complications arise, monitoring and – in some cases – even increasing the blood volume may be required. In case of acute respiratory insufficiency, anaesthesiological measures should be taken.

Undesired effects
Frequently, a temporary drop in blood pressure immediately after the implantation of the bone cement and the endoprosthesis has been observed. Rare cases of hypotension, including anaphylactic shock, followed by cardiac arrest and sudden death have been reported.
The following, additional undesired effects of the use of methyl methacrylate bone cement have been observed:
Thrombophlebitis, superficial wound infection, deep wound infection, pulmonary embolism, haemorrhage and haematoma, trochanter bursitis, loosening or displacement of the prosthesis, trochanter detachment.
Other side effects observed: heterotopic bone regeneration, myocardial infarction, temporary cardiac arrhythmia, cerebrovascular accident.

Interactions
Not known for **PALAMED®**.

Incompatibilities
Aqueous (e.g containing antibiotics solutions) must not be added to the bone cement since they considerably impair the mechanical properties of the cement.

Dosing and preparation
A single dose is prepared by mixing the entire content of a powder sachet with one ampoule. The quantity to be used depends on the respective surgical operation and the technique employed. Before the beginning of the operation, at least one additional dose of **PALAMED®** should be readily available. Each dose is prepared separately.
The following is required to prepare the bone cement:
Sterile working surface, porcelain or stainless steel bowls, sterile mixing spoons or porcelain or stainless steel spatulas or a sterile vacuum mixing system.
The protective aluminium packaging, the outer non-sterile polyethylene sachet and the blister pack of the ampoules should be opened by an assistant in a way to maintain sterility. The sterile polyethylene

sachet and the ampoule are placed under aseptic conditions on a sterile table. Sterile conditions must be ensured when opening the polyethylene sachet and the ampoule.

Application
Two different methods can be used for mixing:
Manual mixing
Mixing under vacuum

Manual mixing
The liquid is poured into a bowl and the powder is added. Then the mixture is stirred carefully for 30 sec.
If the dough-like mass no longer sticks to the rubber gloves, it can be processed. The application time depends on the material and room temperature. If the required consistency is obtained, the cement can be applied. To ensure adequate fixation, the prosthesis should be implanted and stabilized within the given time until the bone cement has hardened completely. Surplus cement must be removed as long as it is still soft. If additional cement is needed during the operation, another sachet of powder can be mixed with one ampoule of liquid as described above. The kneadable mass which is obtained must be applied to the previously applied cement before it hardens. It is always required to mix the entire content of a sachet with the entire content of an ampoule.

Mixing under vacuum
To obtain a bone cement with reduced porosity, the components are mixed under vacuum. For this purpose an airtight closed system and rapid build-up of sufficient vacuum in the mixing equipment are required (absolute pressure: approx. 200 mbar). The stirring times for mixing under vacuum and mixing without vacuum are identical (30 sec). For details of the mixing method refer to the instructions of the mixing system used.

Cranial defects
When treating large cranial defects, after careful preparation of the osseous defect, the dura mater is covered with moist cotton wool or cellulose and a thin plastic or aluminium foil is placed on top for additional protection. The stirred paste is filled into the prepared osseous defect and is contoured onto the bone edges to obtain a desired thickness of 4–5 mm. As the cement is curing, rinsing with physiological salt solution is carried out in order to withdraw the polymerization heat. Then the almost cured graft is removed, the margins are corrected and perforations are prepared; this way it s ensured that the epidural fluid can drain and connective tissue can form later on. Once the cotton wool resp. the cellulose and the foil have been removed, the graft is fixed at three or four points using non-resorbable suture material.

Storage
Do not store above 25 °C.

Shelf life/Sterility
The expiration date is printed on the folded box, the protective aluminium packaging and the inner sachet. **PALAMED®** must not be used after the expiration date. The contents of unused but opened or damaged packs must be discarded and must not be resterilized. **PALAMED®** has been sterilized with ethylene oxide gas and must not be resterilized. The polymer powder must not be used if it exhibits yellow discoloration.

EN

Manual processing

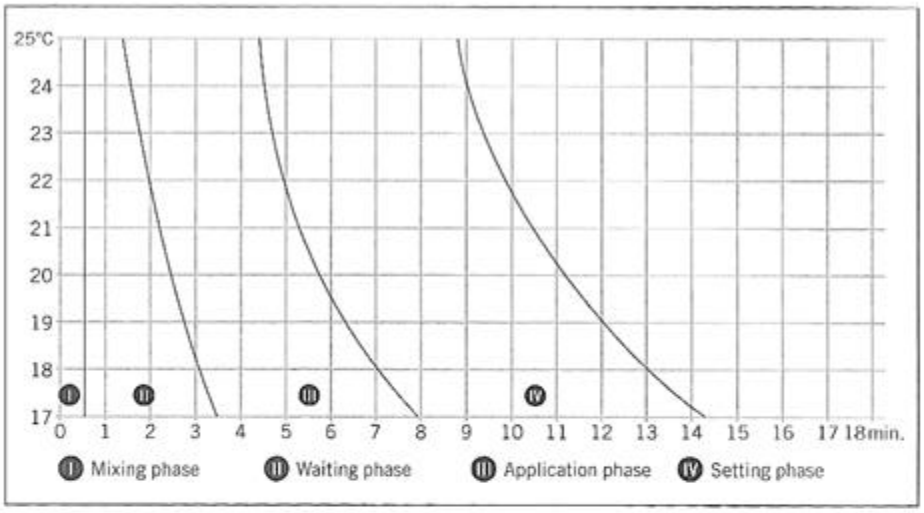

Processing with the vacuum mixing system

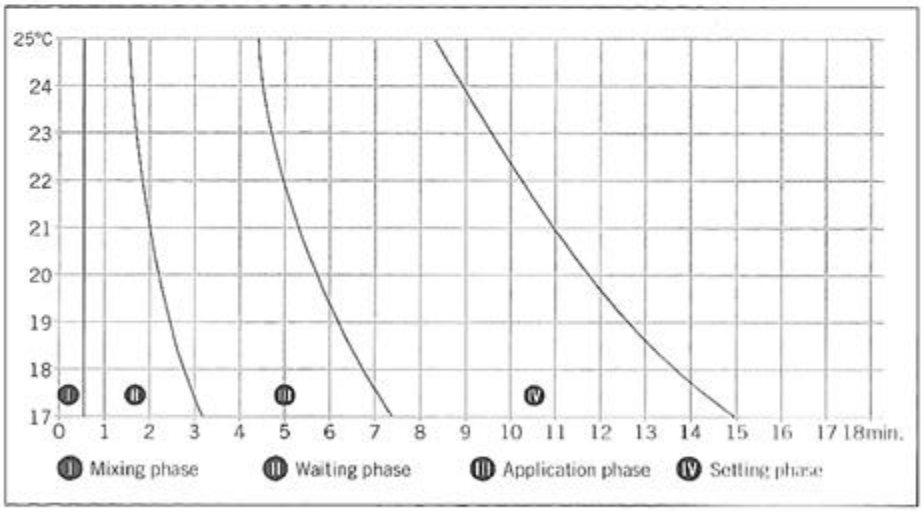

Manufacturer
Heraeus Medical GmbH
Philipp-Reis-Straße 8/13
61273 Wehrheim/Ts.
Germany

Revision status 05/2007

CE 0123

Heraeus

Annex VI – FREKOTE ® Data Sheet

Technical Data Sheet

FREKOTE®

700-NC™

October 2009

PRODUCT DESCRIPTION

700-NC™ provides the following product characteristics:

Technology	Mold Release
Appearance	Clear, colorless[LMS]
Chemical Type	Solvent Based Polymer
Odor	Solvent
Cure	Room temperature cure
Cured Thermal Stability	≤400 °C
Application	Release Coatings
Application Temperature	13 to 135 °C
Specific Benefit	• No chlorinated solvents • High gloss finish • High slip • No contaminating transfer • No mold build-up

700-NC™ offers excellent release properties for the most demanding applications and is a great all-purpose release agent. 700-NC™ releases epoxies, polyester resins, thermoplastics, rubber compounds and most other molded polymers.

TYPICAL PROPERTIES OF UNCURED MATERIAL

Specific Gravity @ 25 °C 0.755 to 0.764[LMS]

Flash Point - See MSDS

GENERAL INFORMATION

This product is not recommended for use in pure oxygen and/or oxygen rich systems and should not be selected as a sealant for chlorine or other strong oxidizing materials

For safe handling information on this product, consult the Material Safety Data Sheet (MSDS).

Mold Preparation

Cleaning:

Mold surfaces must be thoroughly cleaned and dried. All traces of prior release must be removed. This may be accomplished by using Frekote® PMC or other suitable cleaner. Frekote® 915WB™ or light abrasives can be used for heavy build-up.

Sealing New/Repaired Molds:

Occasionally, green or freshly repaired molds are rushed into service prior to complete cure causing an increased amount of free styrene on the mold surface. Fresh or "production line" repairs, new fiberglass and epoxy molds should be cured per manufacturer's instructions, usually a minimum of 2 -3 weeks at 22°C before starting full-scale production. Fully cured previously unused molds should be sealed before use. This can be accomplished by applying one to two coats of an appropriate Frekote® mold sealer, following the directions for use instructions. Allow full cure of the appropriate Frekote® mold sealer before you apply the first coat of 700-NC™ as outlined in the directions of use.

Directions for use:

1. 700-NC™ can be applied to mold surfaces at room temperature up to 135°C by spraying, brushing or wiping with a clean lint-free, cloth. When spraying ensure a dry air source is used or use an airless spray system. Always use in a well ventilated area.
2. Wipe or spray on a smooth, thin, continuous, wet film. Avoid wiping or spraying over the same area that was just coated until the solvent has evaporated. If spraying, hold nozzle 20 to 30cm from mold surface. It is suggested that small areas be coated, working progressively from one side of the mold to the other.
3. Initially, apply 2 to 3 base coats allowing 5 to 10 minutes between coats for solvent evaporation .
4. Allow the final coat to cure for 15 to 20 minutes at 22°C.
5. Maximum releases will be obtained as the mold surface becomes conditioned to 700-NC™. Performance can be enhanced by re-coating once, after the first few initial pulls.
6. When any release difficulty is experienced, the area in question can be "touched-up" by re-coating the entire mold surface or just those areas where release difficulty is occurring.
7. **NOTE**: 700-NC™ is moisture sensitive, keep container tightly closed when not in use. The product should always be used in a well ventilated area.
8. **Precaution:** Users of closed mold systems(rotomolding) must be certain that solvent evaporation is complete and that all solvent vapors have been ventilated from the mold cavity prior to closing the mold. An oil-free compressed air source can be used to assist in evaporation of solvents and ventilation of the mold cavity.

Mold Touch up

Touch up coats should only be applied to areas where poor release is noticed and should be applied using the same method as base coats. This will reduce the possibility of release agent or polymer build-up. The frequency of touch ups will depend on the polymer type, mold configuration, and abrasion parameters.

Loctite Material Specification[LMS]

LMS dated May 10, 2006. Test reports for each batch are available for the indicated properties. LMS test reports include selected QC test parameters considered appropriate to specifications for customer use. Additionally, comprehensive controls are in place to assure product quality and consistency. Special customer specification requirements may be coordinated through Henkel Quality.

Henkel

Storage
The product is classified as flammable and must be stored in an appropriate manner in compliance with relevant regulations. Do not store near oxidizing agents or combustible materials. Store product in the unopened container in a dry location. Storage information may also be indicated on the product container labelling.
Optimal Storage: 8 °C to 21 °C. Storage below 8 °C or greater than 28 °C can adversely affect product properties.
Material removed from containers may be contaminated during use. Do not return product to the original container. Henkel cannot assume responsibility for product which has been contaminated or stored under conditions other than those previously indicated. If additional information is required, please contact your local Technical Service Center or Customer Service Representive.

Conversions
(°C x 1.8) + 32 = °F
kV/mm x 25.4 = V/mil
mm / 25.4 = inches
µm / 25.4 = mil
N x 0.225 = lb
N/mm x 5.71 = lb/in
N/mm^2 x 145 = psi
MPa x 145 = psi
N·m x 8.851 = lb·in
N·m x 0.738 = lb·ft
N·mm x 0.142 = oz-in
mPa·s = cP

Note
The data contained herein are furnished for information only and are believed to be reliable. We cannot assume responsibility for the results obtained by others over whose methods we have no control. It is the user's responsibility to determine suitability for the user's purpose of any production methods mentioned herein and to adopt such precautions as may be advisable for the protection of property and of persons against any hazards that may be involved in the handling and use thereof. In light of the foregoing, **Henkel Corporation specifically disclaims all warranties expressed or implied, including warranties of merchantability or fitness for a particular purpose, arising from sale or use of Henkel Corporation's products. Henkel Corporation specifically disclaims any liability for consequential or incidental damages of any kind, including lost profits.** The discussion herein of various processes or compositions is not to be interpreted as representation that they are free from domination of patents owned by others or as a license under any Henkel Corporation patents that may cover such processes or compositions. We recommend that each prospective user test his proposed application before repetitive use, using this data as a guide. This product may be covered by one or more United States or foreign patents or patent applications.

Trademark usage
Except as otherwise noted, all trademarks in this document are trademarks of Henkel Corporation in the U.S. and elsewhere. ® denotes a trademark registered in the U.S. Patent and Trademark Office.

Reference 0.0

Annex VII – Mechanical testing with plaster

A second option to test the ligaments, but less effective is the use of plaster. The plaster used was bought from a common bricolage shop, with fast dry property. The plaster revealed to make reaction with the clamp. Then, aluminium foil was used to cover the compartment from the clamp, in order to facilitate the plaster removal (**Figure 0-5**).

Figure 0-5- *Clamps coated with aluminium foil.*

The plaster was added with a spoon, because it presented a lower viscosity than the bone cement used before. The opening of the clamps was equally easy as with the bone cement, when the bone was uniformly wrapped by the plaster **Figure 0-6**. Nonetheless, the plaster revealed to be more aggressive to the bone, changing their properties.

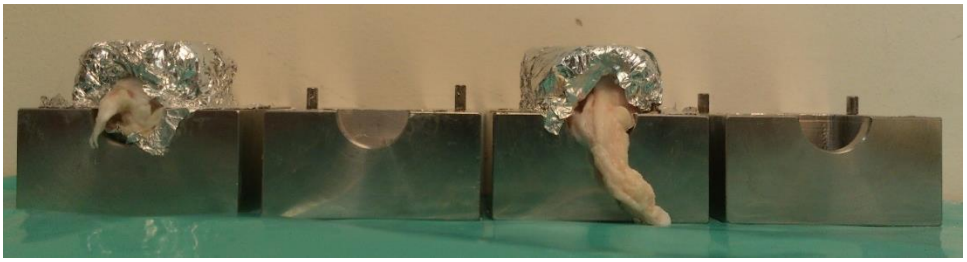

Figure 0-6- *Result after uniaxial tensile tests with porcine knee ligaments. Bone wrapped with plaster inside the clamps.*

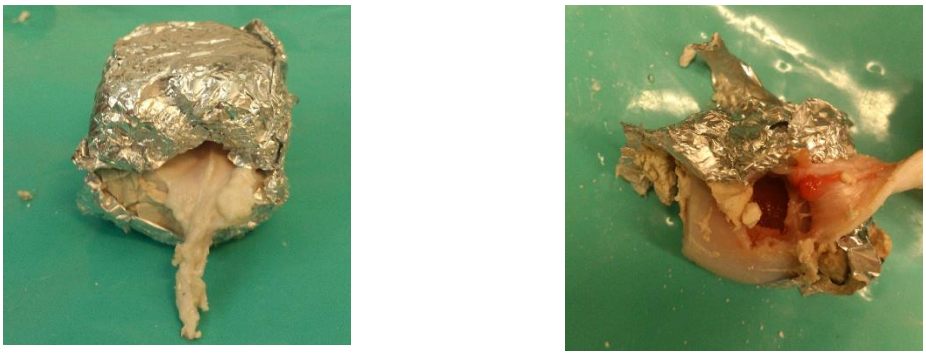

(a) **(b)**

Figure 0-7- (a) *Plaster and bone block removed from the clamp successfully with an MCL ruptured in the mid-substance.* ***(b)*** *Unusual rupture of the ligament in the bone insertion.*

The plaster properties are not well described, neither the data sheet was available. Concluding, this option should be thoroughly investigated.

DCE

DOCTORAL CONGRESS IN ENGINEERING

11-12 JUNE 2015 · FEUP · PORTO · PORTUGAL

CERTIFICATE

Joana Arantes Silva

attended DCE'2015 | Doctoral Congress in Engineering, held 11th and 12th of June, 2015 in Porto, Portugal and presented at the Symposium on Biomedical Engineering, the oral communication entitled 'Biomechanical Characterization of Human Knee Ligaments: New Approach for Finite Element Analysis'.

U.PORTO
FEUP FACULDADE DE ENGENHARIA UNIVERSIDADE DO PORTO

Prof. Paulo J. V. Garcia
(President of DCE'2015 Organizing Committee)

DCE

DOCTORAL CONGRESS IN ENGINEERING

11-12 JUNE 2015 · FEUP · PORTO · PORTUGAL

CERTIFICATE

Joana Arantes Silva

attended DCE'2015 | Doctoral Congress in Engineering, held 11th and 12th of June, 2015 in Porto, Portugal and presented at the "Biomedical Eng. Symposium" the Oral entitled

Methods used in Clamping Soft Tissues Specimen: Review and New Approach.

U.PORTO
FEUP FACULDADE DE ENGENHARIA
UNIVERSIDADE DO PORTO

Prof. Paulo J. V. Garcia
(President of DCE'2015 Organizing Committee)